

CONTRIBUTION TO THE METHODS OF MEASURING  
STRESSES BELOW THE SURFACE



By

RECEP ALI SAFOGLU

S.B., Massachusetts Institute of Technology, 1943

Submitted in Partial Fulfillment of the  
Requirements for the Degree of  
DOCTOR OF SCIENCE  
from the  
Massachusetts Institute of Technology  
1947

Signature of Author  
Department of Metallurgy  
February 1947

Signature redacted

Signature of Professor  
in Charge of Research

Signature redacted

Signature of Chairman of  
Department Committee on  
Graduate Students

Signature redacted

TABLE OF CONTENTS

	<u>PAGE</u>
List of Figures	i
List of Tables	v
Acknowledgment	
I Introduction	1
II Abstract	8

PART IRESIDUAL STRESSES IN A PATCH WELDED DISK

III Introduction	11
IV Review of Literature on the Patch Welded Disk	12
V The Patch Welded Disk	13
A. Preparation of Specimen	13
B. Procedure	17
C. Steps in Procedure	17
VI Patch Welded into a Large Plate	22
A. Preparation of Specimen	22
VII Results and Discussion	30
VIII Conclusion	40
IX Appendix on the Disk	43
Data and Calculations in Measurement of Triaxial Residual Stresses in Patch Welded Circular Disk.	

PART IIMEASUREMENT OF STRESSES BELOW THE SURFACE BY RECESSING

X	Introduction	104
XI	The Theory of Recessing	106
XII	A Long and Narrow Recess	110
	A. The Bending Device	110
	B. Specimen I and Its Preparation	112
	1. The Layout of Gages	113
	2. Recessing	113
	3. The Bending Experiment	115
	4. Successive Recesses	116
	5. Results Obtained from Specimen I in Bending	116
	C. Use of Strain Gage in the Recess	118
	D. Preparation and Testing of Specimen II	120
	E. Preparation and Testing of Specimen III	121
	F. Preparation and Testing of Specimen IV	127
	1. The Effect of the Cross Recess	132
	G. Discussion of Results on the Long and Narrow Recess	133
	H. Conclusions on the Long and Narrow Recess	137
XIII	The Circular Recess	139
	A. The Choice of Specimen V and Its Preparation	139
	B. Testing of Specimen V in Tension and in Bending	142
	C. Results of Experiments in Tension and in Bending	144

	<u>PAGE</u>
D. The Shape of a Circular Hole in an Infinite Plate Under the Uniform Biaxial Stresses	153
E. Discussion of Results in Bending and in Tension	156
F. Application of the Recessing Data to the Theory of Recessing	157
G. Conclusion	159

### PART III

#### APPLICATION OF THE RECESSING METHOD TO MEASURE STRESSES

##### THROUGH THE THICKNESS IN A PLATE BENT BEYOND THE

##### ELASTIC LIMIT

XIV Residual Stresses in a One Inch Thick Bent Plate	164
A. Investigation	164
B. Preparation of the Specimen	165
C. Measurement of Residual Stresses in the Bent Plate by X-rays	165
XV Effect of the Slots on the Measured Apparent Stresses in a Recess	171
A. Machining of Slots and Results of the Tests	173
XVI Discussion of Results	174
A. Relaxations Caused by the Slots	174
B. Stresses Measured in the Recess	174
C. Calculation of True Stress from the Apparent Stresses Measured in Recesses	177
D. Conclusion	177



	<u>PAGE</u>
XVII Recommendations for Further Work	182a
XVIII Bibliography	183
XIX Biographical Note	185

LIST OF FIGURES

<u>FIGURE NUMBER</u>		<u>PAGE NUMBER</u>
1.	Deformation and residual stresses in a mild steel plate heated at the center and cooled in air.	14
2.	Residual stresses along the radius of patch welded disk.	14
3.	Cross-section of the disk and the order of welding.	16
4.	Layout of gages in the welded disk.	18
5.	Average stresses along the radius of the disk.	19
6.-9.	Distribution of residual stresses across the thickness of the disk.	23-26
10.	Stress in the thickness direction in the disk.	28
11.	The one and one-half inch thick steel plate with the patch at the center.	29
12.	Full size detail of the weld joint at the center of the plate.	29
13.	Layout of strain gages on the plate.	31
14.	Average radial and tangential stresses in plate.	32
15.	Distribution of tangential stresses across the thickness of the patch welded plate.	33
16.	Average radial and tangential stresses in the disk and in the plate.	36
17.	Cross-section of the welded disk showing the bridge between the patch and the weld.	38

<u>FIGURE NUMBER</u>		<u>PAGE NUMBER</u>
18.	Radial strains along the radius of the disk.	55
19-26.	Strain relaxed in blocks on top and bottom in splitting and successive slicing from mid-section toward both faces.	59-66
27.	The radial and cumulative strains relaxed in splitting and slicing of radial blocks Nos. 11 to 16.	89
28-30.	Relaxed radial stresses due to slicing of blocks 11 to 16 at different fractions of thickness.	90-92
31-34.	Successive graphical differentiation of radial and tangential stresses in the disk.	95-98
35-37.	Successive graphical integration for determi- nation of stress in thickness direction.	98-103
38.	Recessing of specimen.	107
39.	The bending device.	107
40.	A picture of the bending device.	111
41.	The layout of strain gages on specimen I.	114
42.	Cross-section of recesses	114
43.	The layout of gages and recesses on specimen II.	122
44.	Application of load in bending specimen II.	122
45.	Location of gages and recesses on specimen III.	122
46.	A picture of the Riehle Universal Testing Machine for bending.	126
47.	A picture of the Riehle Universal Testing Machine for bending.	128

<u>FIGURE NUMBER</u>		<u>PAGE NUMBER</u>
48.	Layout of gages and recesses on specimen IV.	130
49.	Recess Nos. 2 and 3 on specimen IV.	130
50.	Stresses in bending in specimen I.	135
51.	Increase in stress versus the length of recess.	136
52.	Increase in stress versus the length of recess.	136a
53.	The stress in recess compared with stress in the specimen III.	140
54.	Specimen V.	141
55.	Layout of gages and recesses in specimen V.	141
56.	The bending test of specimen V.	141
57.	Picture of specimen V in the tensile testing machine.	143
58.	Stress measured at the bottom of recesses and the true stress pattern in specimen V.	154
59.	Stresses measured at the bottom of recesses of specimen V in tension.	166
60.	Stress measured in one-half inch diameter recess in tension and bending and the corrected stresses.	170
61.	Deformation of a circular hole in a plate.	172
62.	The bent plate and the layout of gages.	172
63.	The bending of the plate.	172
64.	A picture of the hand drill and the Variac transformer	175

<u>FIGURE NUMBER</u>		<u>PAGE NUMBER</u>
65.	A picture of the bent plate under the x-ray camera.	180
66.	The gage to measure the depth of the layer removed in surface preparation for x-rays.	181
67.	Recesses and slots in the bent plate.	181
68.	The cross-section of a recess and slot.	181
69.	Residual stresses through the thickness of one inch thick bent plate.	181a
70.	Residual stresses through the thickness of one inch thick plate measured by the block method.	181b



LIST OF TABLES

<u>Table Number</u>		<u>Page Number</u>
1	Welding data of the specimen	15
2	Shrinkage in welding	15
3	Average radial and tangential stresses in psi in the disk.	21
4-13	Relaxation in cutting the blocks free from the disk and in splitting and slicing of blocks.	44-53
14	Strain relaxed in cutting blocks 11 to 16 free from the disk.	54
15	Strain relaxed in cutting the blocks free from the disk.	57
16-36	Tabulation of data taken from curves, Figures 19 to 26, for the computation of stress relieved in splitting and slicing of blocks.	67-87
37	Calculation of stress in the direction of thickness.	99-101
38	Relaxations recorded in Strain gages in bending of Specimen I in the bending device.	117
39	Strains recorded by gages of Specimen I in bending for four recesses of different depths.	119
40	Stress measured at the bottom of the recess as a function of the length of recess.	123
41	Results of the tensile test of Specimen III.	125

<u>Table Number</u>		<u>Page Number</u>
42	Stresses in psi at the bottom of the recesses and at the corresponding layers in the specimen.	127
43	Results of testing Specimen IV in tension.	129
44	The results of testing Specimen IV in tension after the cross recesses are machined.	133
45	Strain in recesses obtained in bending tests of Specimen V.	146
46	Stress in recesses in psi obtained in bending Specimen V.	147
47a, b	Strain in recesses obtained in the tensile test of Specimen V.	149-150
48	Average strain in recesses taken from Tables 47a and b obtained in the tensile tests of Specimen V.	151
49	Stress in psi in recesses obtained in the tensile test of Specimen V.	152
50	Strain in micro inches per inch recorded by gages No. 25 and the deviation of these readings compared with the average of gages Nos. 24 and 26.	155
51	The figures for constants a and k for the recesses of one-half inch and three-fourths inch diameters determined experimentally.	158
52	The values of the terms appearing in equation (14) to calculate true stresses in recessing.	160

<u>Table Number</u>		<u>Page Number</u>
53	Stresses introduced to Specimen V in bending and stresses computed from the measurement in recesses.	161
54	The values of the terms appearing in equation (14) and true stresses computed from the data obtained in the one-half inch diameter recess in tension.	162
55	The data recorded in bending of the specimen.	167
56.	Stresses measured at the surface of the bent plate.	168
57	Stresses measured in recesses in the longitudinal and transverse direction in psi.	173
58	Relaxation recorded in the recess with the machining of the slots in the longitudinal and transverse directions.	176
59	Calculation of true stresses in the longitudinal direction from the apparent stress measured in the recess.	178
60	Calculation of stress in the transverse direction of the bent plate from the apparent stresses measured in the recess.	179

ACKNOWLEDGMENTS

The writer wishes to take this opportunity to express his sincere appreciation:

To Professor John T. Norton for his patient and understanding supervision.

To Professor Daniel Rosenthal for his invaluable friendly advice and for the equation of the theory of recessing.

To the University Research Committee of the Welding Research Council for sponsoring the research program in this thesis.

To Mr. Roman Carl for splitting and slicing the blocks.

To Messrs. A. B. English, R. J. Bowley and C. W. Christian-  
sen of the Machine Tool Laboratory for their help and kind permission in the use of the equipment in the said laboratory.

To Professors I. H. Cowdrey, H. Majors, Jr., F. J. Mehringer and W. S. Bailey for their permission, suggestions and help in the use of the equipment in the testing laboratory.

To Mr. Kenneth Bohr for the data in Figure 70.

To the members of the Metallurgy Department for their help and cooperation in the use of the equipment in their laboratories.



## I INTRODUCTION

It was reported in 1944 that 432 out of 2993 welded merchant ships had serious fractures<sup>(1)\*</sup>. It was suspected that stresses set up in welding were the main cause of these failures. Considerable amounts of research have been undertaken to evaluate the residual stresses and their effect on the failure of metals<sup>(2)</sup>. It has been found that the effect of the biaxial stresses on the failure of metal is not pronounced<sup>(3),(4),(5)</sup>, but the same statement cannot be made about the triaxial stresses. In order to evaluate the effect of the stresses experimentally, they first have to be measured. As yet, no method exists of measuring stresses below the surface in a specimen of any shape.

In this thesis, it is proposed (a) to determine the triaxial stress pattern in a circular patch weld, (b) and to develop the method of recessing as a contribution to the methods of measuring stresses below the surface. These methods will be discussed below.

\* \* \*

Under a load, metals change their dimensions. They expand in tension and contract in compression. If the change in dimension is below the elastic limit of metal, the amount of load per square unit length is called the elastic stress.

After different steps in the production of metals parts, such as forging, rolling, cutting, welding, heat treatment, et cetera,

---

\*Numbers in paranthesis refer to the bibliography at the end of the paper.



although there is no external load on the part, nevertheless non-uniform changes in dimension in different sections of the part, i.e., the heterogeneity of plastic flow, create compressive and tensile stresses, which balance each other. These stresses are called residual stresses, as distinguished from stresses caused by an external load.

Since stress is the first step to failure and distortion of the metal parts, such as failure under load, fatigue failure, cracking and warping in hardening or machining, et cetera, its importance in bettering production methods, efficient designing and economical use of material has been recognized since the 1880's.

Stress is always accompanied by change in dimension of a metal part, or change in dimension is always caused by a stress. The ratio of elastic stress "S" to change in dimension per unit length, called strain "e", is constant for every metal. This constant is called the modulus of elasticity or the Young's modulus E of that metal. This ratio  $S/e = E$  or  $S = Ee$  is used in converting the measured strain into stress.

If the specimen had a uniform cross-section and carried a known load, it would be very easy to divide the load by the cross-sectional area and determine the stress. But, in most cases, stress is not uniform, or the load is not known; and the local strain must be measured in order to measure the local stress.

In a specimen of uniform cross-section, if the existence of longitudinal stresses only is accepted, the specimen could be cut into

many longitudinal strips, change in length measured for each strip, and the stress calculated by the equation  $S = Ee$ .

This was done to measure stresses in a railhead(6),(7). Another method, used by J. E. Howard(8) and E. Heyn(9), consists of machining off concentric layers from a round rod or tube and measuring in the remaining part the longitudinal relaxations caused by the removal of successive layers,  $f_1', f_2', \dots, f_n'$ . Stress existing at the nth layer,  $S_n$ , before machining, is(9):

$$S_n = \frac{E}{l} \cdot \frac{f_n'' d_n - f_{n-1}'' d_{n-1}}{f_n'} , \quad \text{where}$$

$l$  = length of specimen,  $f_n''$  = sectional area of remaining part of the specimen after turning off the nth layer,  $f_n'$  = sectional area of the nth layer, and  $d_n$  = change in the original length  $l$  of the specimen.

These two methods measure only uniaxial stresses. They assume that:

- (a) there is no transverse stress
- (b) the specimen is of uniform cross-section
- (c) machining or cutting does not introduce new strains to the specimen.

These assumptions limit the application of these methods and question the reliability of the results obtained, especially the assumption that there is only uniaxial stress and no transverse stress. In one case, stress measured with the triaxial method, discussed below, revealed more than three times the stress measured with uniaxial method of measuring stresses(6).

A triaxial method of measuring strains was developed by Sachs in 1927<sup>(10)</sup>: "...which permits the determination of the entire stress distribution in circular rods, large solid cylinders, and thick walled tubes having a uniform stress distribution in the circumferential direction."<sup>(11)</sup>. The Sachs' method consists of measuring the longitudinal and radial relaxations on the outside surface of the cylinder, which are caused by boring through the center of the cylinder and by removing, in steps, concentric layers from the inner toward the outer surface. If (a) is the longitudinal and (b) the circumferential unit strain; after an area F from the center of the specimen is removed, longitudinal (s), tangential (t), and radial (r) stresses are computed by the following equations<sup>(11)</sup>.

$$s = \frac{E}{1-\nu^2} \left[ (F_b - F) \frac{dV}{dF} - V \right]$$

$$t = \frac{E}{1-\nu^2} \left[ (F_b - F) \frac{d\theta}{dF} - \frac{F_b + F}{2F} \cdot \theta \right]$$

$$r = \frac{E}{1-\nu^2} \cdot \frac{F_b - F}{2F} \cdot \theta$$

where  $F_b$  = cross-sectional area of the original specimen,  $\theta = b + \nu a$ ,  $\nu$  = Poisson's ratio,  $E$  = modulus of elasticity,  $V = a + \nu b$ .

This method has been very successfully and extensively used for specimens with rotational symmetry and uniform stress in the longitudinal direction.

In the case of rectangular plates and bars, successive layers are removed from one face, and the amount of strain in each layer is determined by the deflection of the bar.



D. Rosenthal and J. T. Norton developed a method of measuring triaxial stresses in plates<sup>(12)</sup>. This method also employs the principle of relaxation, which is carried out in two steps: (a) wire strain gages are attached on both sides of the plate; and the rectangular block, containing these gages is cut loose from the plate. The block is narrow enough so that transverse stress remaining in it can be ignored. It is long enough (twice the thickness of the plate) to have only a linear relaxation through the thickness of the block. Thus, cutting of the block relaxes only the average stress at that point. (b) The second part of relaxation consists of splitting the block into two parts and slicing each part from the mid-section toward the outer surfaces. After each step, relaxations on the wire strain gages are recorded; and, from this data, stress distributed through the thickness of the block is computed<sup>(12)</sup>.

This stress through the thickness is superimposed on the average stress, and the result is the actual stress through the thickness at that point of the plate. By careful arrangement of blocks in the same specimen or in similar specimens, and by correlation of the data of different blocks, stress distribution through the thickness and in any direction of the plate can be measured. Then, stress in the third direction is computed by making use of the equations of equilibrium. An application of this method to a circular welded disk is included in this thesis, and a complete discussion of the method and calculations will be found in the text and in the appendix.

The block method of measuring stresses is very useful, especially in measuring stress distribution in weldment of thick plates

and any other plate. However, it has a few disadvantages:

(a) It is a destructive method. It cannot be applied to a specimen under load.

(b) As the thickness of the specimen increases, its length increases also. This greater length increases the distance between the blocks and decreases the number of blocks that can be obtained from one specimen.

(c) It does not account for the steep gradient of stresses.

(d) It can be applied to plates only.

Frommer and Lloyd<sup>(13)</sup> machined off successive circular layers from the surface of the specimen and measured stresses at the bottom of the recess with X-rays. Although they recognized that stresses thus measured are not the same as stresses existing at that layer before the recessing operation, they did not offer any correction.

It was thought that measuring stresses through the thickness by recessing could be a very useful tool and was worth investigating thoroughly and systematically. The development of the recessing method of measuring stresses through the thickness or at any desired depth of a part is the main subject of this thesis. The advantages of the recessing method over the others are as follows:

(a) Recessing can be applied to a specimen of any size or shape. Thus it is very general in application.

(b) It is only semi-destructive. The hole can easily be plugged.

(c) It can be applied to a specimen under load.



(d) Stress can be measured at a desired depth. There is no need to go all the way through the specimen.

(e) Stress is measured directly at any desired depth and corrected for the recessing operation, which is an advantage over the other methods where stresses are computed.

(f) Steep gradient of stress is easily determined.

## II ABSTRACT

In this thesis it is proposed (Part I) to determine the tri-axial stress pattern in a one and one-half inch thick disk, at the center of which is welded another disk of three inches diameter; (Part II) to develop the recessing method of measuring stresses below the surface, and (Part III) to apply the recessing method to measure stresses through the thickness in a one inch thick plate bent to one percent <sup>plastic</sup> deformation at the surface.

In Part I a mild steel disk of about nine inches diameter and one and one-half inches thickness is taken, and circular grooves are machined on both sides of the disk one and one-half inches away from the center, leaving only a bridge at the mid-section of the plate connecting the three inch diameter disk at the center to the main disk. These machined grooves are then filled up by welding. The block method is used to determine the triaxial stress pattern caused by the weldment. The maximum stress of **12,000** psi is computed in the direction of the thickness at the location one-half inch from the center of the disk is a low figure compared with maximum stresses in the radial and tangential directions, 28,000 and 35,000 psi respectively.

In the preparation of the disk, its radius shrunk, indicating the lack of maximum restraint on the weld. For a maximum restraint, a three inch diameter disk is welded at the center of a two foot square plate in the same manner as in the disk. The radial and tangential stresses in the plate run up to 44,000 and 48,000 psi respectively; but the indications are that stress in the direction

of the thickness is still lower than that found in the disk.

The conclusion drawn from the measurement on the disk and on the plate is that plug welds in a one and one-half inch thick plate introduces radial and tangential stresses equal to the yield stress of the material; but the stress in the third direction, and, therefore, the triaxiality of the stress pattern, is low.

In Part II long and narrow and circular recesses of varying length, depth, and diameter are machined in mild steel flats of different sizes. In order to produce a known pattern of stress through the thickness, the specimens are subjected to a pure bending or tension; and the stresses are measured at the bottom of the recesses either by x-rays or by electrical resistance strain gages. Stresses thus measured in the recesses are compared with stresses introduced at that layer, and the correction laws are found.

For a long and narrow recess, it is observed that, if only a uniaxial stress is present in the specimen and if the recess is about three-sixteenths of an inch wide and long enough to permit the x-rays reflected from the recess to come out, when taking the oblique picture, the notch effect of the recess is less than the probable error in the measurement of stresses by the x-ray method. However, when biaxial stresses are known to exist, the effect of the stress perpendicular to the recess, on the stress measured in the longitudinal direction of the recess, is so high that a long and narrow recess cannot be used.

Circular recessing proved to be the solution of the recessing problem in measuring stresses that show a multiaxial pattern. A

theory is developed to correct stresses measured in the circular recesses that gives very satisfactory results. The diameter of the recess used is either one-half inch or three-fourths of an inch. Stresses measured in the recesses are corrected by the equation of the recessing theory independent of the pattern of stress (either multiaxial or uniaxial).

In Part III measurement of stresses below the surface by the circular recessing method is applied to determine the residual stress pattern in a steel plate bent to one percent plastic deformation at the surface. The results obtained, as compared with the preliminary result from the determination of stresses in a similar plate by the use of the block method, show close agreement among stresses in the longitudinal direction of the plate.



PART I

RESIDUAL STRESSES IN A PATCH WELDED DISK

III INTRODUCTION

The block method of measuring stresses, developed by D. Rosenthal and J. T. Norton, was used by them to investigate tri-axial residual stressed in a one-inch thick straight butt welded plate<sup>(12)</sup>. Maximum stress in the thickness direction was found to be about 3,000 psi. This low stress can be explained by the equilibrium equation and the geometry of the specimen. If S indicates stress and x, y, z directions along the weld, perpendicular to the weld and through the thickness, respectively, the equilibrium equation is<sup>(12)</sup>:

$$\frac{d^2S_z}{dz^2} = \frac{d^2S_x}{dX^2} + \frac{d^2S_y}{dY^2} + 2 \frac{dT_{xy}}{dxdy} \quad (1)$$

Along the axis of the weld, variation of  $S_x$  is small; therefore, the first term on the right hand side of the equation is negligible. Because of the symmetry, small in itself,  $T_{xy}$  is zero along the axis of x and y. Therefore, only one term on the right hand side of the equation remains, showing why the stress in the third direction is low.

To have a more pronounced triaxial stress distribution, a circular weld, having more restraint than a linear weld and a thicker plate than the one used by D. Rosenthal and J. T. Norton, were used, in order to produce a higher stress in direction of the thickness. The specimen chosen for this purpose was a patch welded circular disk, Figure 3a. The preparation of this disk is explained in the following pages.



#### IV REVIEW OF LITERATURE ON THE PATCH WELDED DISK

Measurement of triaxial stress, or stress in the third direction, requires measurement of stresses in two perpendicular directions through the thickness of the specimen. This type of investigation is not found in the literature on the subject, although patch welded disks have been used to determine the influence of the type of electrode, composition, method of welding, peening, reheating, et cetera on the residual stresses produced.

Siebel and Pfender<sup>(14)</sup> (1933-34) welded a patch 2-3/4 inches by 3-1/8 inches in the center of a mild steel plate, 16 inches by 18 inches by 1.18 inches in size, and used the subdivision method to measure stresses. The stress distribution was found to be the same as in a plate heated in the center to 400° C and cooled in the air, Figure 1.

Bühler and Lohmann<sup>(14)</sup> (1934) had disks 9.8 inches and 19.6 inches in diameter, and patches 5.9 inches in diameter. The thickness of the plate was 0.79 inch. They used various kinds of steel and electrodes, and various techniques and treatments to discover their effects on the stress distribution. The Sachs method of measuring stresses was employed.

Bierett and Gruning<sup>(14)</sup> (1934) determined the residual stresses in the oxyacetylene butt welded circular disks. Patches 8 inches in diameter were welded in the center of an 80 inch square plate. The effects of peening and reheating were studied in three specimens, Figure 2.

Bollenrath<sup>(14)</sup> (1935) used the Mathar method to study stresses in a 24 inch square steel plate, in which was welded a 6 inch square steel plate.

Gerold and Müller-Stock used disks 0.79 inch thick and 19.6 inches in diameter. The patches used were 1.9 inches, 5.9 inches, 9.9 inches, and 13.9 inches in diameter. The Sachs method was used to determine the stress distribution.

## V THE PATCH WELDED DISK

### A. Preparation of Specimen

The specimen is a mild steel disk 8.9 inches in diameter and 1.5 inches thick. It was machined at the center and plugged with a disk 3 inches in diameter, of same material and thickness by welding, Figure 3a. It is proposed to find the triaxial stress distribution along the radius and through the thickness. Specimen was prepared by the Lukenweld Research and Development Department. The check analysis of the steel was as follows:

<u>C</u>	<u>Mn</u>	<u>P</u>	<u>S</u>	<u>Cu</u>	<u>Si</u>	<u>Ni</u>
0.16	0.40	0.032	0.026	0.27	0.20	0.10

Standard practice was followed in welding. The sequence of welding is shown diagrammatically in Figure 3b. Welding and shrinkage data may be found in Tables 1 and 2.

The average shrinkage of 0.0153 inches in a disk 8.9 inches in diameter, observed in Table 2, is considerable. Because of the small size of the disk, considerable relaxation has taken place, thus lowering the restraint on the weld.

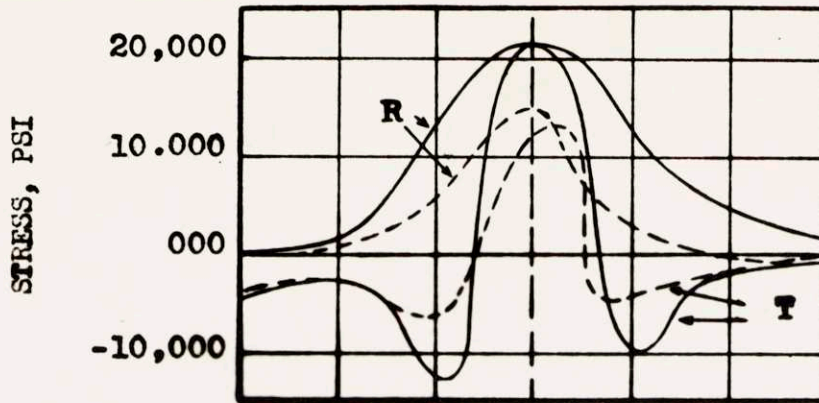


**Fig. 1 - Deformation and Residual Stresses in a Mild Steel Plate which has been Heated in the Center to About 400 C by Means of a Torch and Cooled in Air**

———— Upper face of plate (torch side)  
- - - - - Lower face of plate  
R = Radial stresses  
T = Tangential stresses

Siebel and Pfender<sup>(9)</sup>

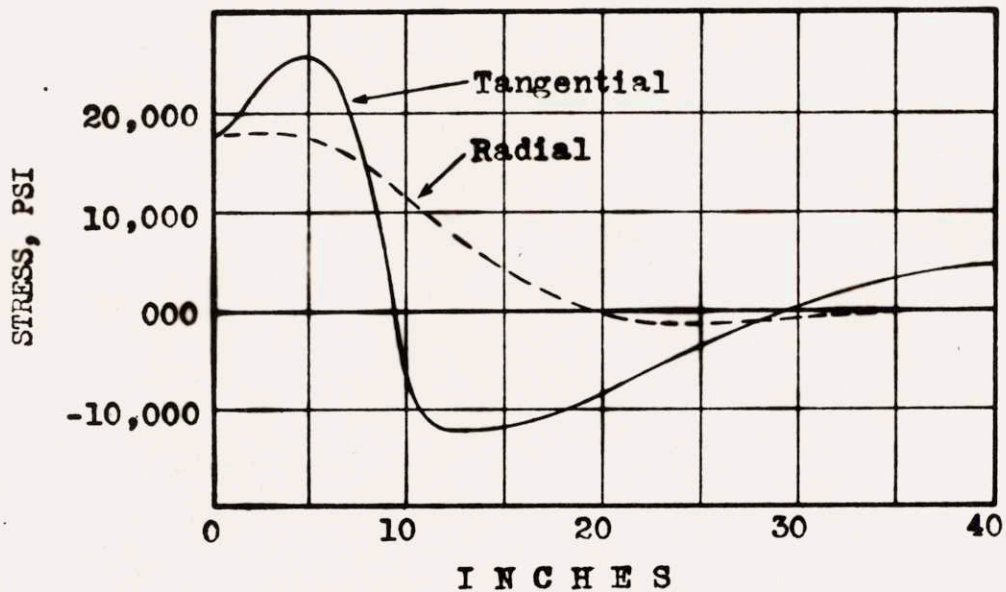


**Fig. 2 - Average Residual Stresses along the Radius of Patch Welded Disk  
0.39 inch thick plate, not peened and not reheated.**

Bierett and Gruning<sup>2(9)</sup>



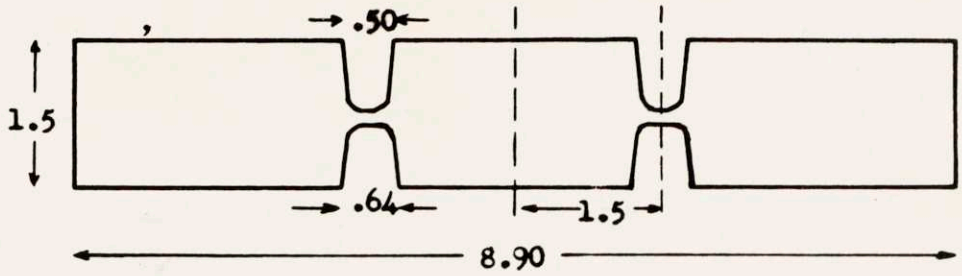
Table 1Welding Data of the Specimen

<u>Bead No.</u>	<u>Welding Rod</u>		<u>Amperes</u>
1	3/32 inch Murex Type	FHP	150
2,3,4,6	3/32 inch Murex Type	FHP	165
5	3/16 inch Murex Type	FHP	235
7,8,9,10,11,12	3/16 inch Murex Type	FHP	240
13,14	3/16 inch Murex Type	FHP	225
15,16,17,18	3/16 inch Murex Type	FHP	190

Table 2Shrinkage in Welding

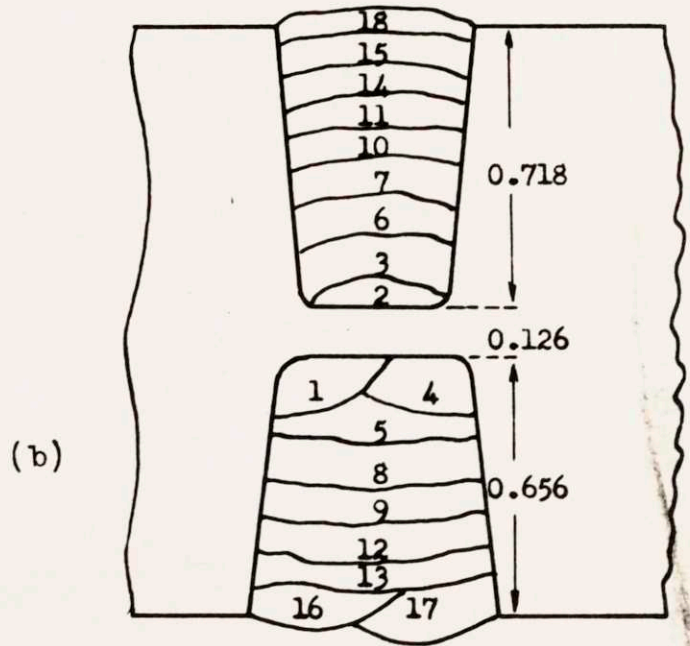
(d is the diameter of the disk in inches 45° apart)

<u>Before Welding</u>	<u>After Welding</u>	<u>Shrinkage</u>
$d_1 = 8.901$	$d_1 = 8.885$	0.016
$d_2 = 8.901$	$d_2 = 8.886$	0.015
$d_3 = 8.901$	$d_3 = 8.887$	0.014
$d_4 = 8.901$	$d_4 = 8.885$	0.016



Cross Section of the Disk to be Welded

(a)



The Order of Welding Beads

Fig. 3 - Actual Dimentions of the Disk in Inches and the Order of the Welding Beads.



## B. Procedure

The method used to measure the residual triaxial stresses in the patch welded circular disk described above is that developed by D. Rosenthal and J. T. Norton<sup>(12)</sup>. In this method, electrical strain gages are cemented on both sides of a plate, directly opposite each other; and a block containing these gages is cut free from the plate. This block is then split and each half sliced toward the outside faces. Before each step, strain gage readings are taken. From the relaxations in cutting, splitting, and slicing the block, the stress distribution through the thickness of the plate is computed.

## C. Steps in Procedure

1. The polished faces of the patch welded disk are roughened with emery paper, No. 1, as recommended by the electrical strain gage manufacturer.

2. Two sets of blocks are outlined on the disk, one set for radial stresses and the other for tangential stresses, Figure 4. Blocks are one-half inch wide and two and one-quarter inches long (one and one-half times the thickness).

3. SR-4 strain gages of type A-1 are cemented on both sides of each block. After being dried at room temperature, the disk is left in a furnace for three hours at 70-85° C, and the gages are then covered with petrosene wax while the disk is still hot. Petrosene protects gages against moisture and damage in handling. Gages were numbered 1, 2, 3 ..... 16 on the upper face and 101, 102, 103.. ...116 on the lower surface. Numbers with indices indicate duplicate blocks.

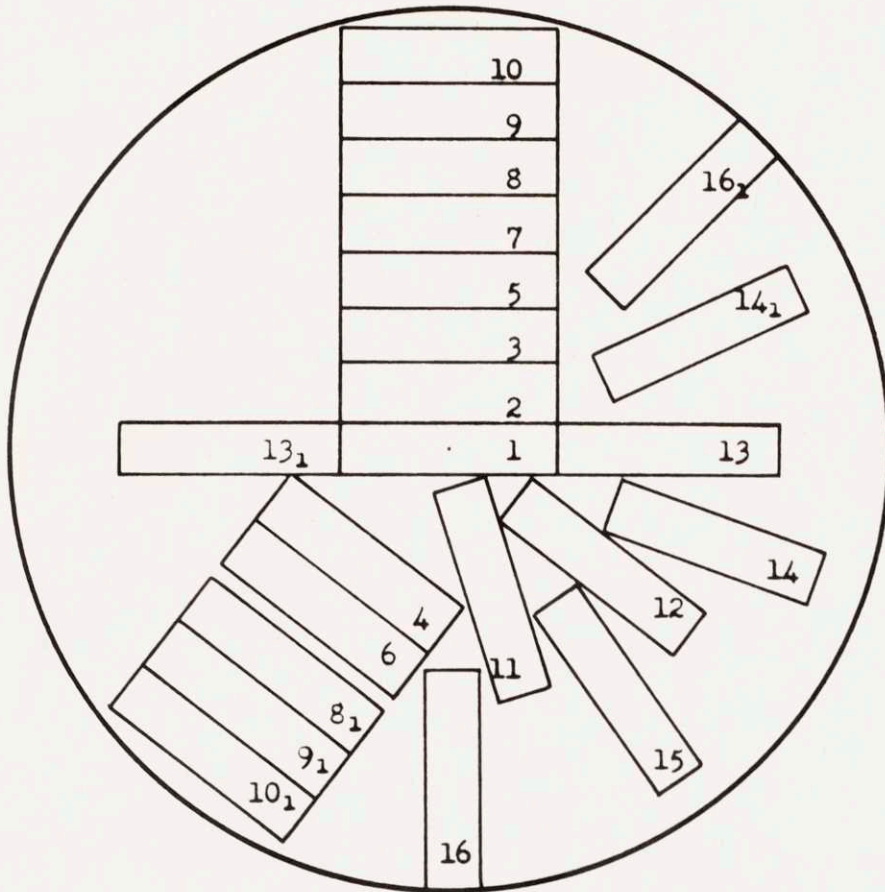


Fig. 4 - Layout of Gages in the Welded Disk. Figure is showing the actual Blocks cut free from the Disk. Numbers with Indices indicate duplicate Blocks.

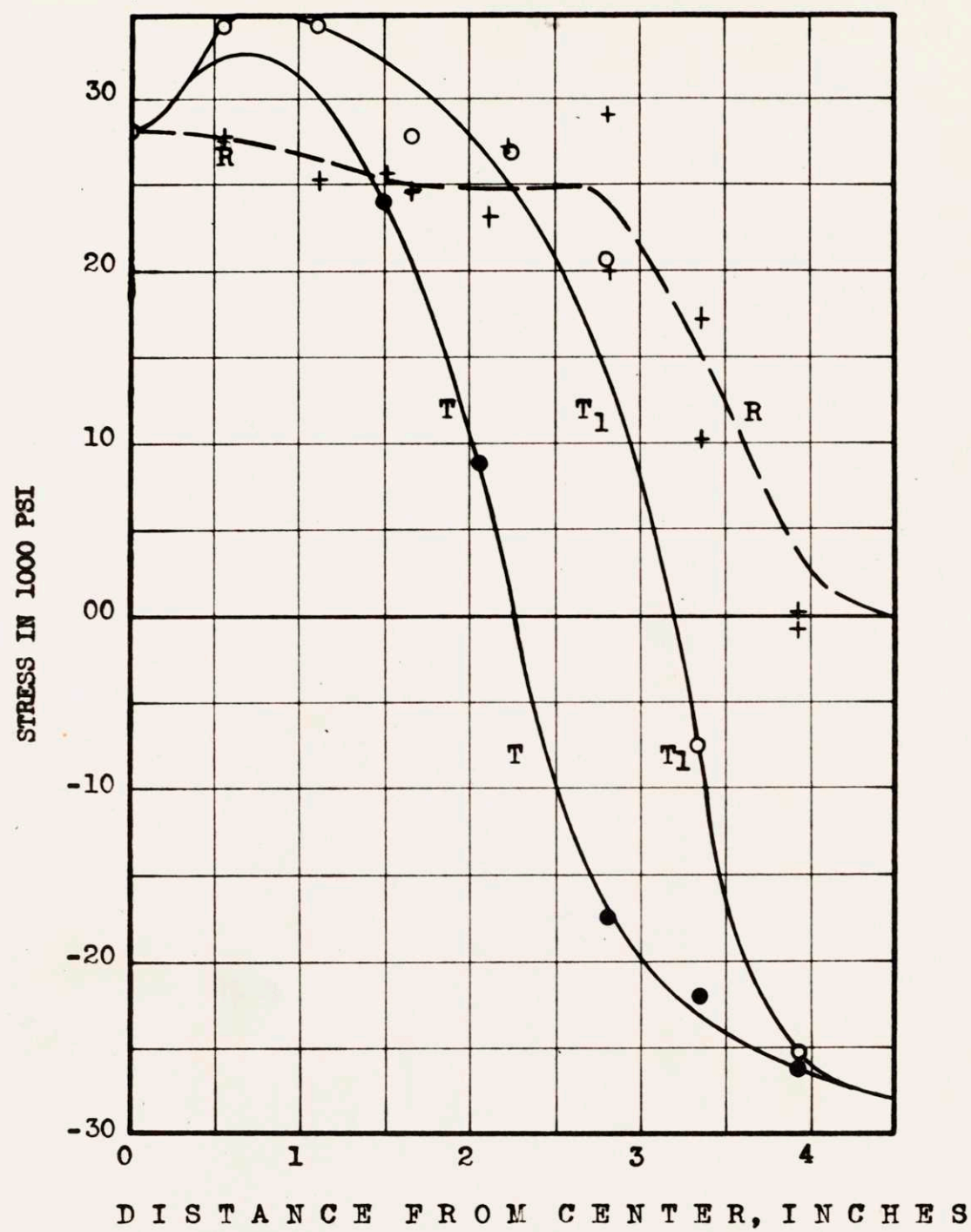


Fig. 5 - Average Stresses Along the Radius of the Disk.

R : Radial stress  
T, T<sub>1</sub> : Tangential Stress

4. The first strain gage readings are then taken. All lead connections are made by soldering throughout the experiment.

5. Blocks are cut with a band saw  $1/2$  inch wide and with 24 teeth per inch. Care is taken to prevent overheating in sawing. It has previously been found that the cutting operation does not introduce stresses of its own(12).

Relaxation from the cutting of the block gives average stresses for each block. Data recorded are in Appendix I. It will be observed from distribution of blocks, Figure 4, that blocks in the tangential direction are not at the same distance from the center as blocks in the radial direction. In order to get the stresses, both in tangential and radial directions, strains recorded in the radial direction are interpolated for blocks of the tangential direction. Table 3 shows the average radial and tangential stresses in psi,  $s_r$  and  $s_t$ , respectively, for the top and bottom sides of the disk, and also their averages, Figure 5. These data will be discussed below.

6. After gage readings of individual blocks are taken, the blocks are split in half and sliced from mid-section toward the faces. Before each step, the gage reading is taken. Recorded data and calculations are in Appendix I.

The stress through thickness of the block, after it is cut loose from the disk, is calculated from the data obtained in splitting and slicing of the blocks.



Table 3

Average Radial and Tangential Stresses in psi in the Disk

(S<sub>r</sub> is the radial stress and S<sub>t</sub> the tangential stress)

<u>Block</u>	<u>Inches from the Center</u>	<u>Top</u>		<u>Bottom</u>		<u>Averages</u>	
		<u>S<sub>t</sub></u>	<u>S<sub>r</sub></u>	<u>S<sub>t</sub></u>	<u>S<sub>r</sub></u>	<u>S<sub>t</sub></u>	<u>S<sub>r</sub></u>
1	0	+28,000	+28,000	+28,050	+28,050	+28,000	+28,000
2	0.56	+34,900	+29,500	+33,960	+26,170	+34,430	+27,830
3	1.125	+42,300	+30,200	+26,320	+20,500	+34,310	+25,350
4	1.53	+26,300	+30,730	+21,640	+20,550	+23,970	+25,640
5	1.687	+36,620	+28,330	+18,500	+21,000	+27,560	+24,650
6	2.09	+ 6,450	+23,960	+11,440	+22,240	+ 8,945	+23,100
7	2.25	+28,090	+28,600	+25,925	+28,150	+27,000	+28,370
8	2.81	+20,800	+29,920	+20,300	+28,220	+20,550	+29,070
8,	2.81	-16,900	+21,930	-18,800	+18,100	-17,850	+20,000
9	3.37	- 3,830	+14,080	-11,060	+20,740	- 7,445	+17,400
9,	3.37	-21,740	+11,380	-22,240	+ 9,465	-22,000	+10,420
10	3.937	-26,431	+ 778	-24,400	- 537	-25,400	+ 120
10,	3.937	-27,960	- 660	-25,130	- 120	-26,500	- 390

This remaining stress is superimposed on the average stress in order to obtain the true stress at any layer of the disk. Calculations are shown in the Appendix. Average and true stresses in blocks Nos. 1 to 8, both in radial and tangential directions, are shown in Figures 6-9.

7. From the true stresses in radial and tangential directions through the thickness of the disk, stress in the third direction has been calculated in the Appendix on the disk and is shown in Figure 10.

## VI PATCH WELDED INTO A LARGE PLATE

A shrinkage of 0.0153 inch is observed in the radius of the disk in welding, Table 2. Therefore, it can be seen that the restraint is limited by the small size of the disk. To investigate the effect of maximum restraint, a patch similar to the first was welded at the center of a large plate.

### A. Preparation of Specimen\*

Specimen is a square, 24 inches per side, of medium carbon steel plate, grade M, Navy specification 48S5 (INT). A patch is welded at the center of the plate, similar to that on the disk, Figures 11 and 12.

1. Plate is flame cut to size and machined for welding grooves, Figures 11 and 12.

---

\*Many thanks are due to Mr. L. W. Pote at the Materials Laboratory of the Charlestown Navy Yard for valuable suggestions and preparation of this specimen.

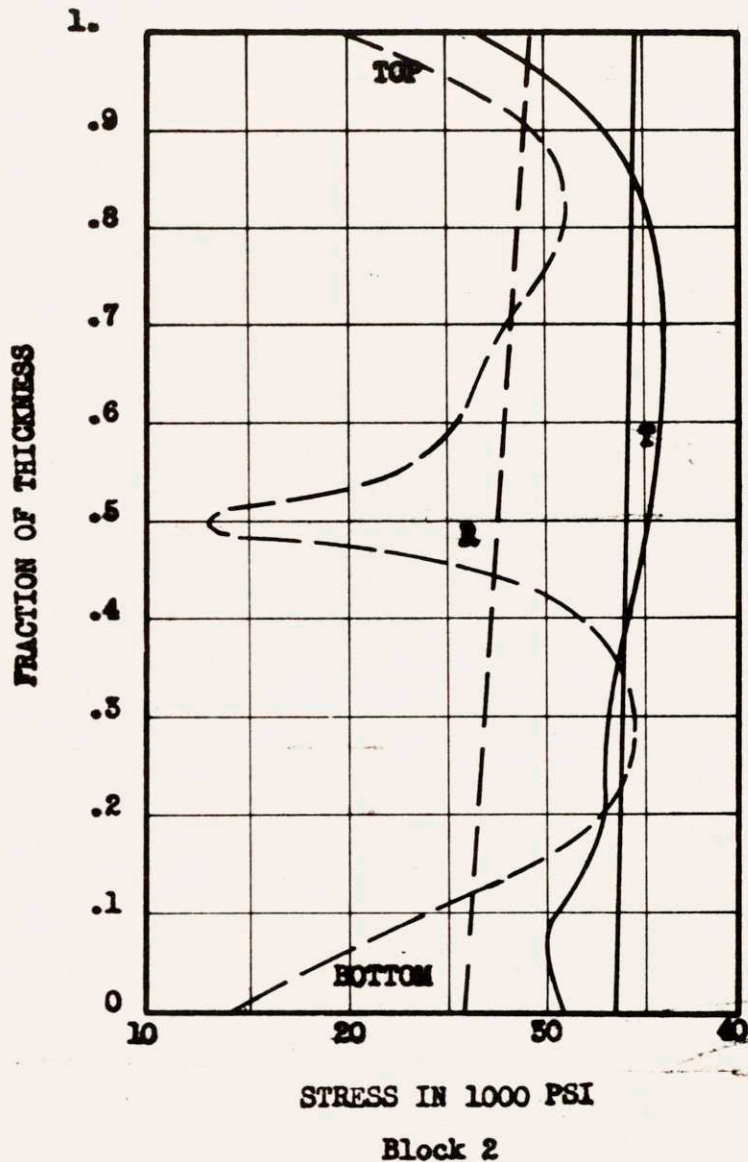
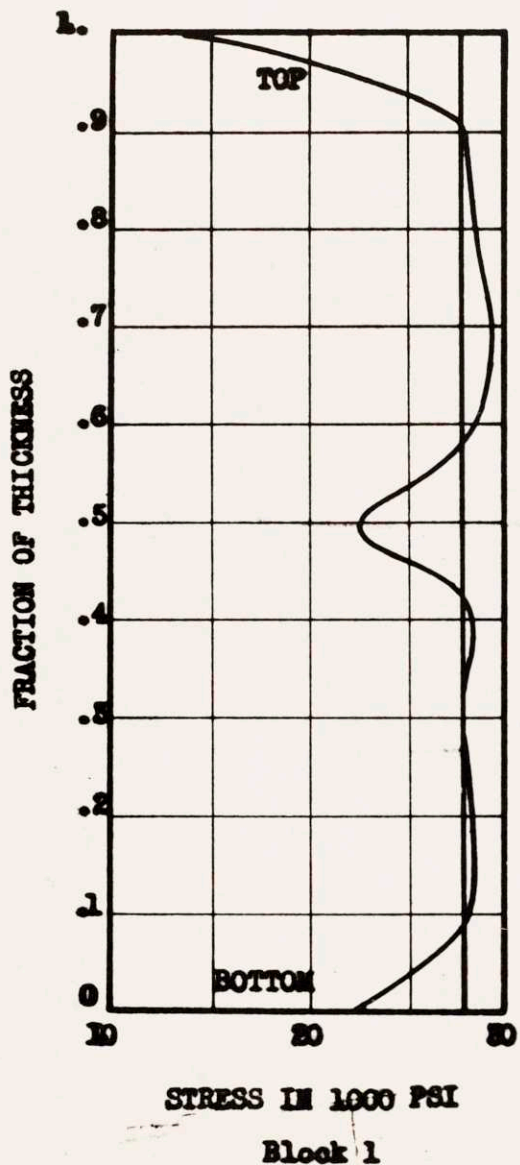


Figure 6. - Distribution of Residual Stress Across the Thickness of the Circular Patch Welded Disk.

Straight lines - average stress; Curves - actual stress; Broken lines - radial stress; Continuous lines - tang. stress.



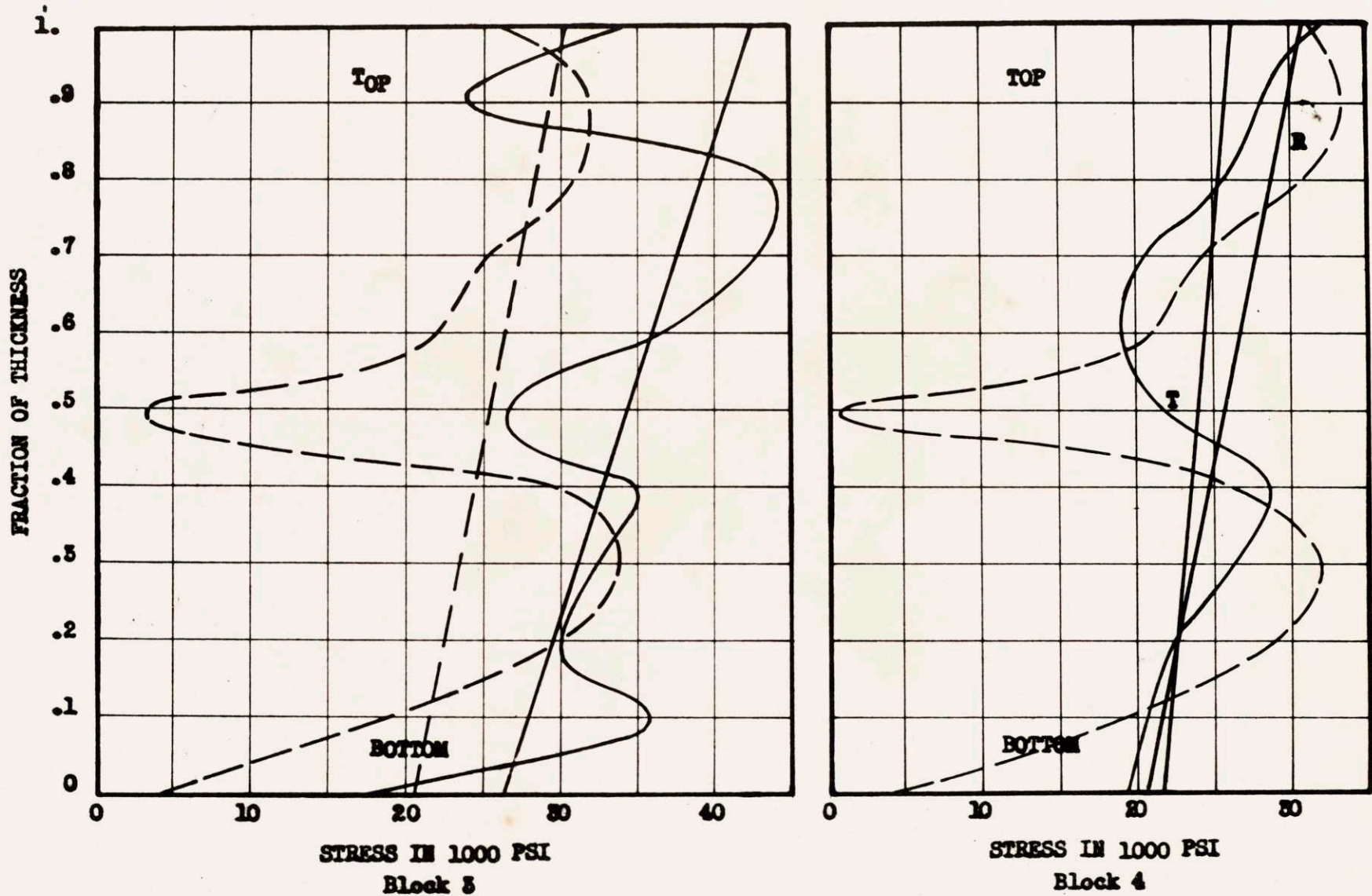


Figure 7 - Distribution of Residual Stress Across the Thickness of the Circular Patch Welded Disk.

Straight lines - average stress; Curves - actual stress; Broken lines - radial stress; Continuous lines - tang. stress.



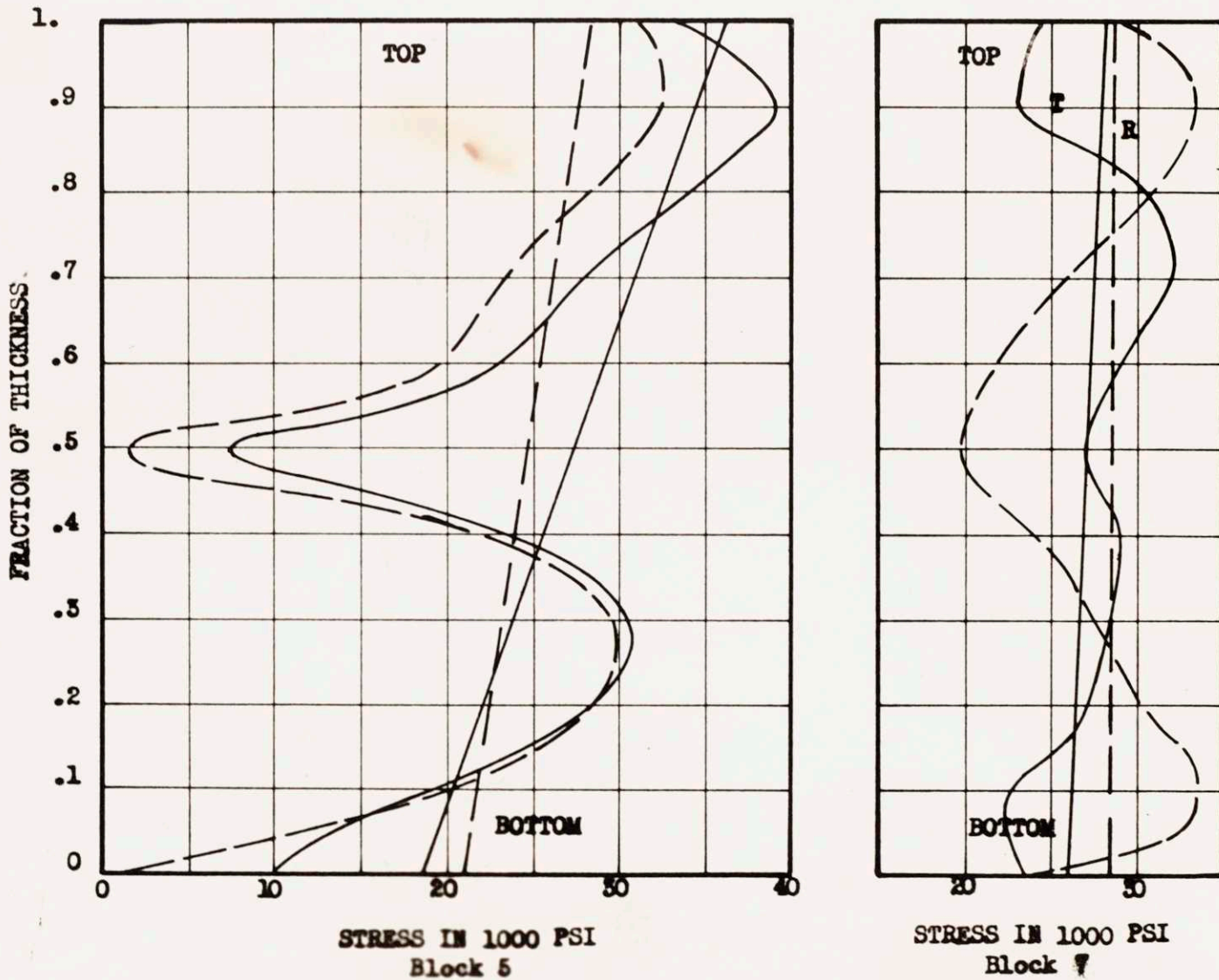


Figure 8 - Distribution of Residual Stress Across the Thickness of the Circular Patch Welded Disk.

Straight lines - average stress; Curves - actual stress; Broken lines — radial stress; Continuous lines - tang. stress.

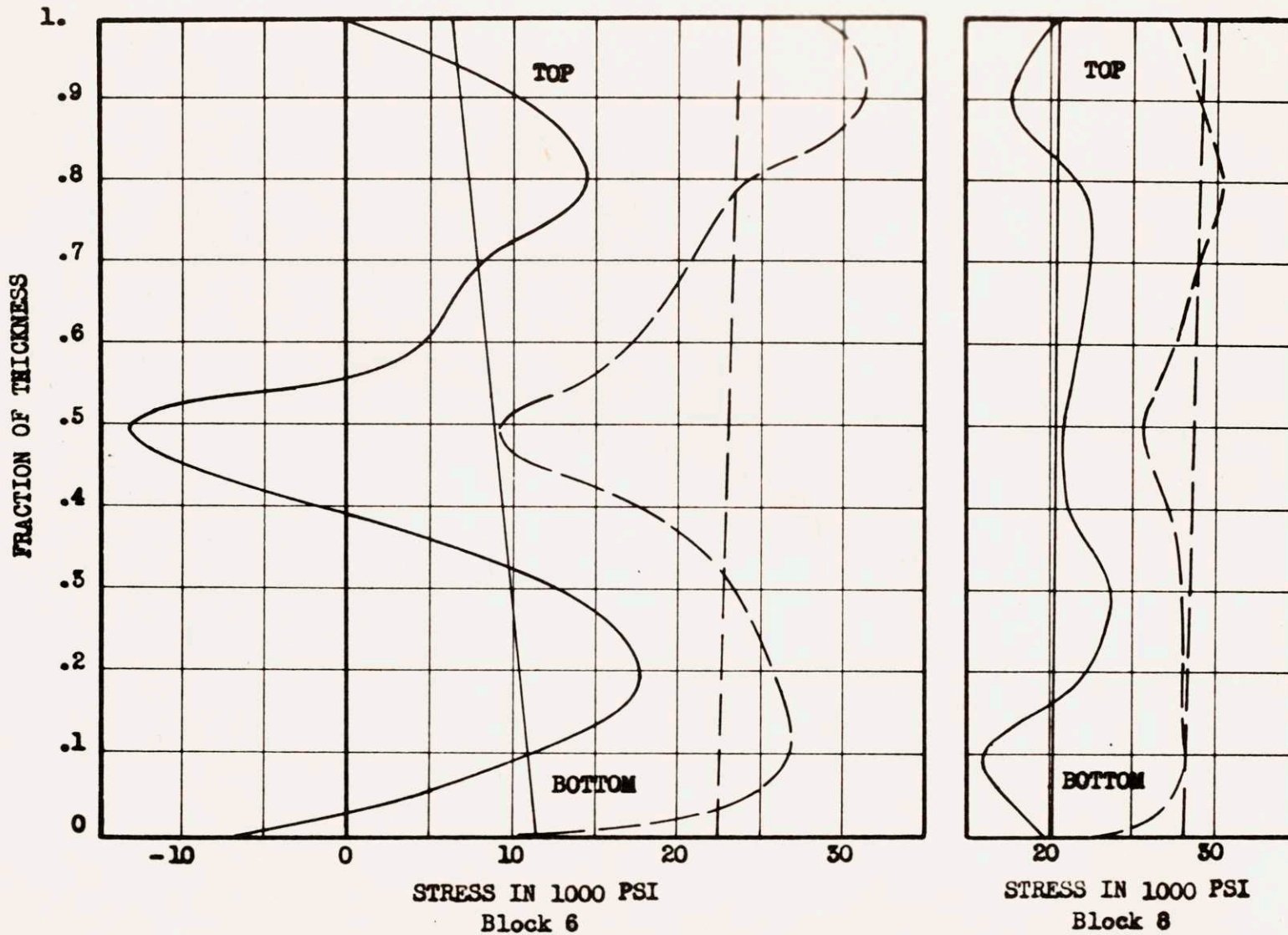


Figure 9 - Distribution of Residual Stress Across the Thickness of the Circular Patch Welded Disk.

Straight lines - average stress; Curves - actual stress; Broken lines ----- radial stress; Continuous lines - tang. stress.

2. Plate is stress relieved as follows:

	<u>Specified</u>	<u>Actual</u>
Heat at	50° F, per hr.	50° F, per hr.
Hold at	1150° F, 2 hrs. max.	1150° F, 5 hrs.
Cool at	20° F, per hr.	14° F, per hr.

3. Patch is welded to the plate.

(a) Plate is preheated at 200° F.

(b) After the second bead plate is turned, the back is chipped to the sound weld metal by using a round-nosed tool and pneumatic gun.

<u>Bead</u>	<u>E6010, RACO Welding Electrode</u>	<u>Amperes</u>	<u>Volts, DC Reversed Pole</u>	<u>Explanation</u>
1	5/32 inches	120	26-28	blocked in 1 inch in- crements
2	3/16 inches	160	28	continuous
3 to 8	3/16 inches	180	28	continuous

The excess metal of the weld on the top and bottom of the plate is machined off with a planer, ground with a hand grinder, and polished with emery paper, No. 1. Electric resistance strain gages of AX-5 type, i.e., cross gages that measure strains in two perpendicular directions, are cemented symmetrically on both sides of the plate, as shown in Figure 13. Thus, at each point, strains are measured in radial and tangential directions. The plate is then cut to the size of the disk and relaxations recorded for each point. The disk is then cut into individual blocks and the total relaxation



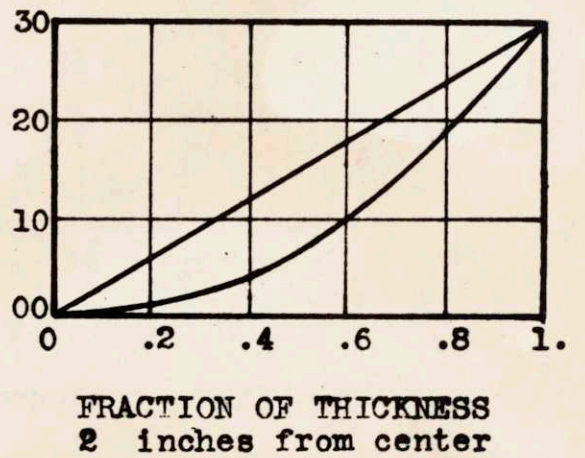
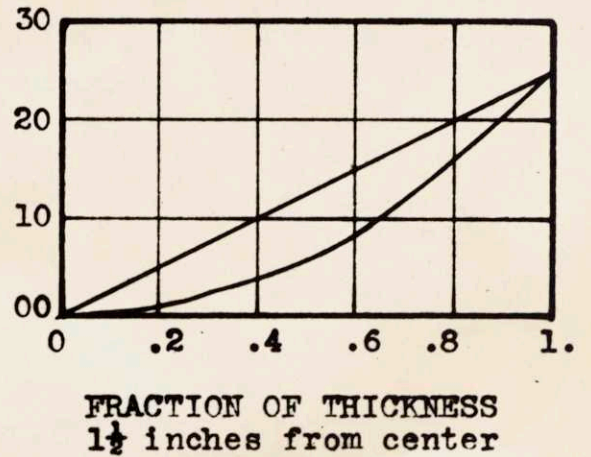
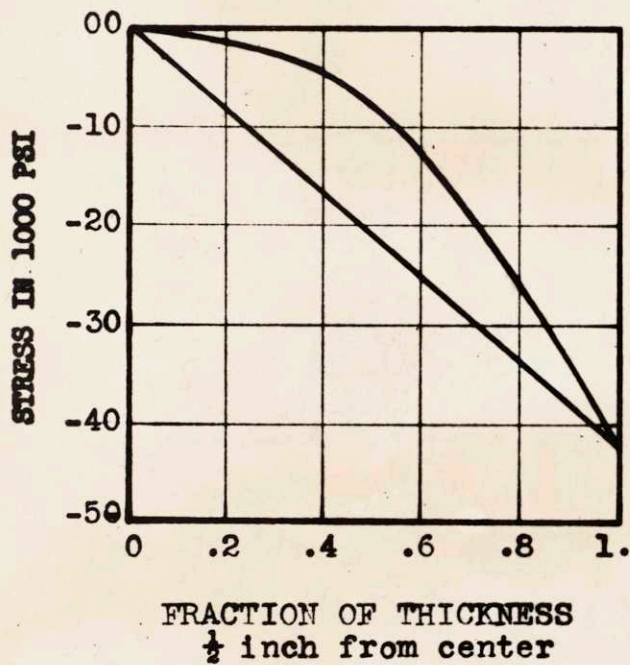
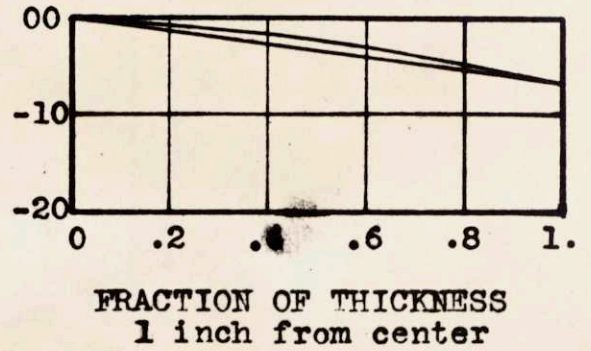
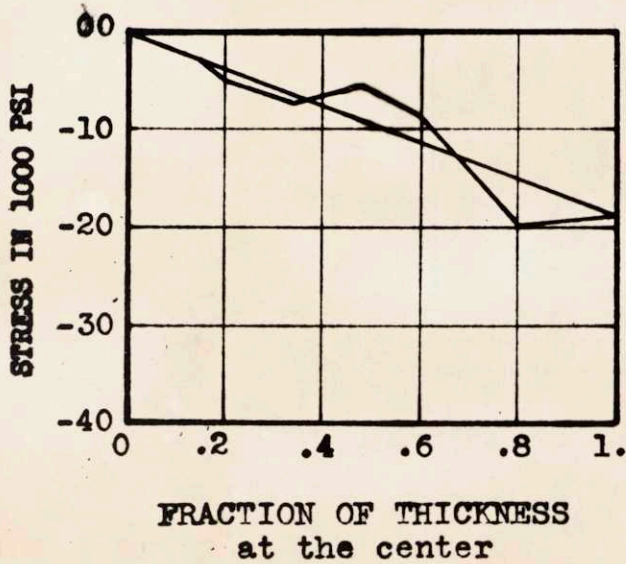


Fig. 10 - Stress in Thickness Direction in the Patch Welded Disk at a Distance of 0,  $\frac{1}{2}$ , 1,  $1\frac{1}{2}$  and 2 inches from the Center of the Disk.

Stress is measured from the straight line connecting the two ends of the curve to the curve.



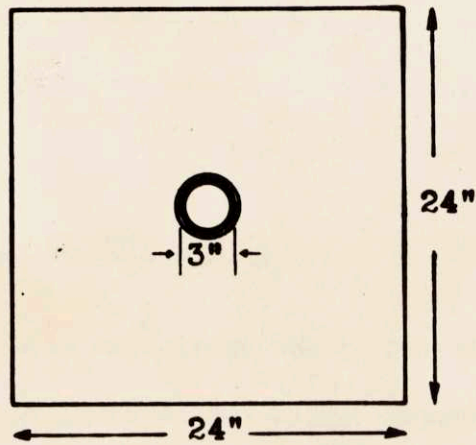


Fig. 11 - The  $1\frac{1}{2}$  inch Thick Steel Plate with the Patch at the Center

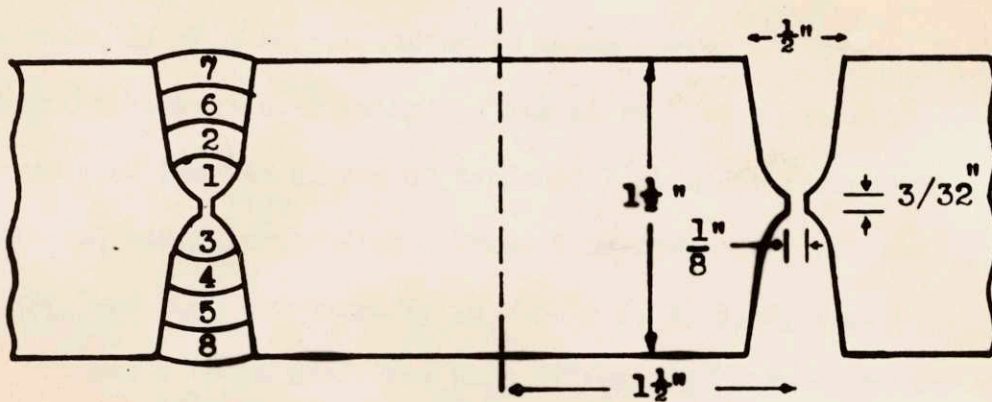
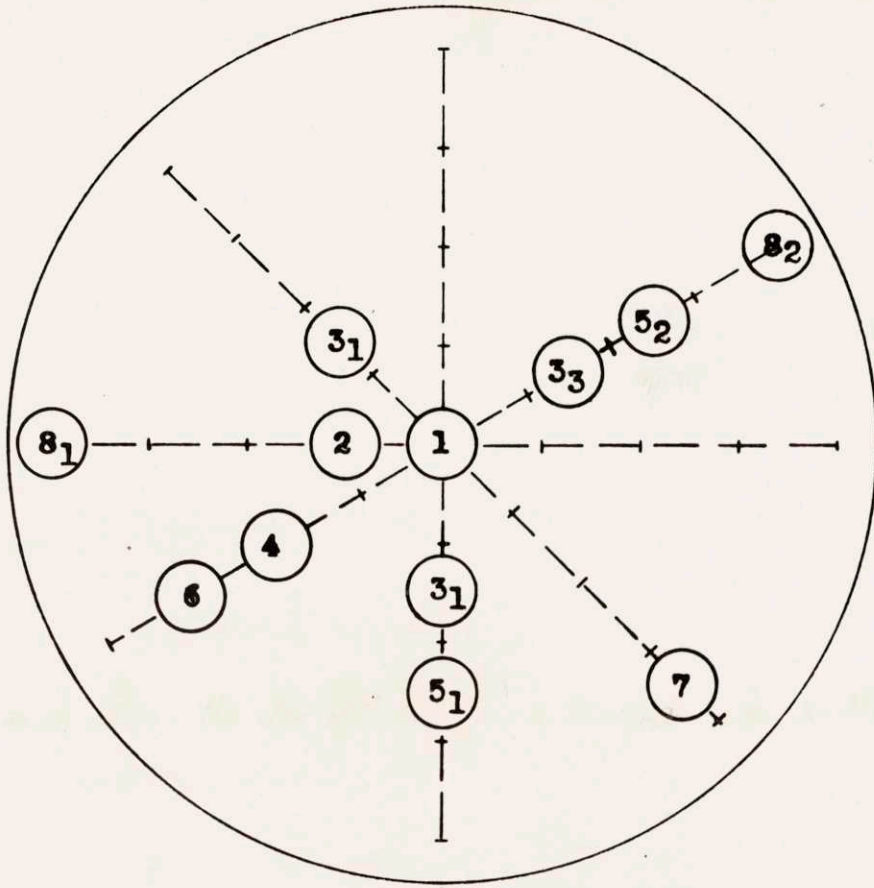



Fig. 12 - Full Size Detail of Weld Joint at the Center of the Plate with Dimensions and the Order of Weld Beads.



Scale,  $\frac{1}{2}$  

**Fig. 13 - Layout of Strain gages on the Plate.**  
This **Figure Shows the Central Part of the 2 Feet Square Plate.**

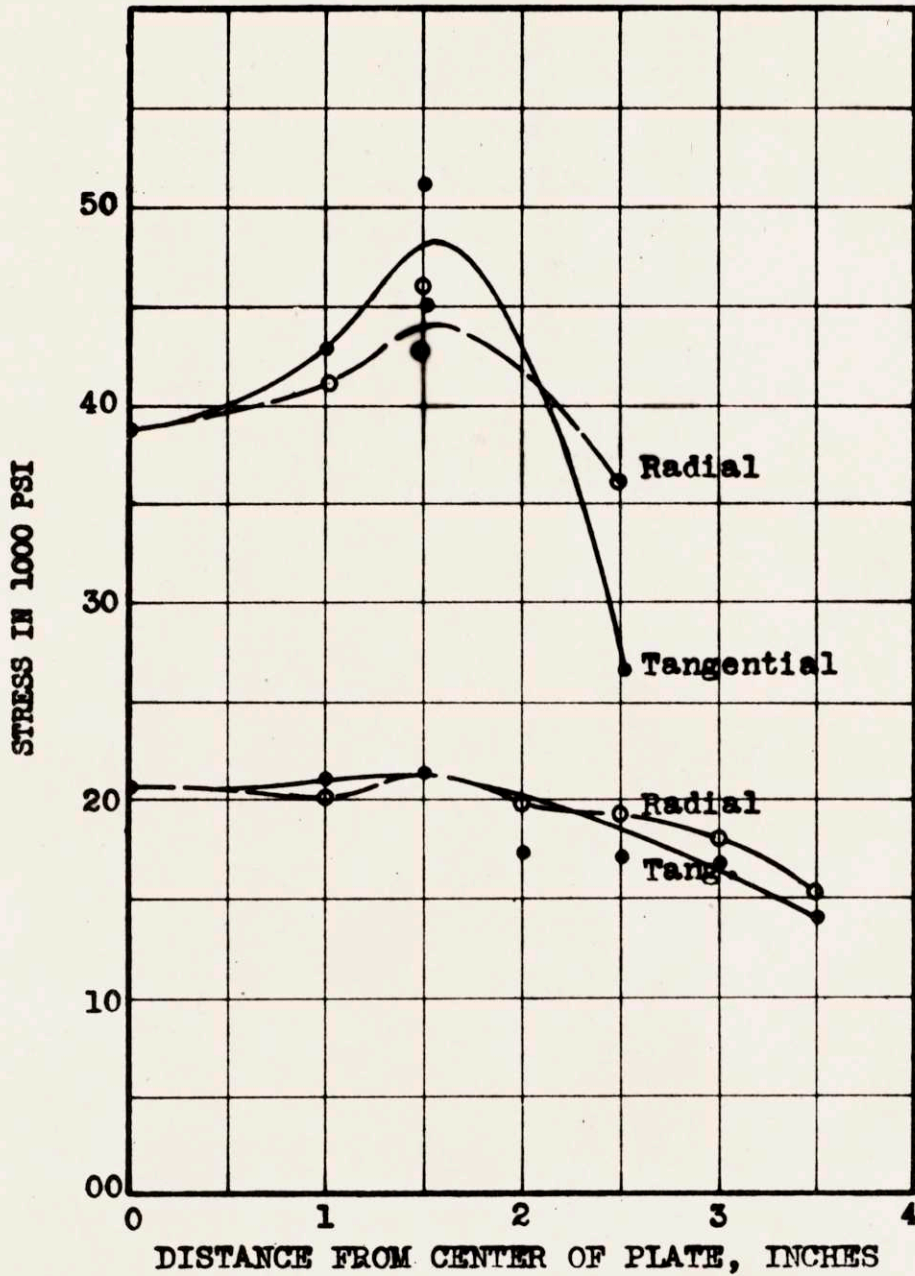


Fig. 14 - Average Radial and Tangential Stresses in Plate.

Lower Curves are the Result of Relaxation in cutting the Plate to the Size of the Disk ( 9 inches in diameter) and the upper Curves that of Total Relaxation.

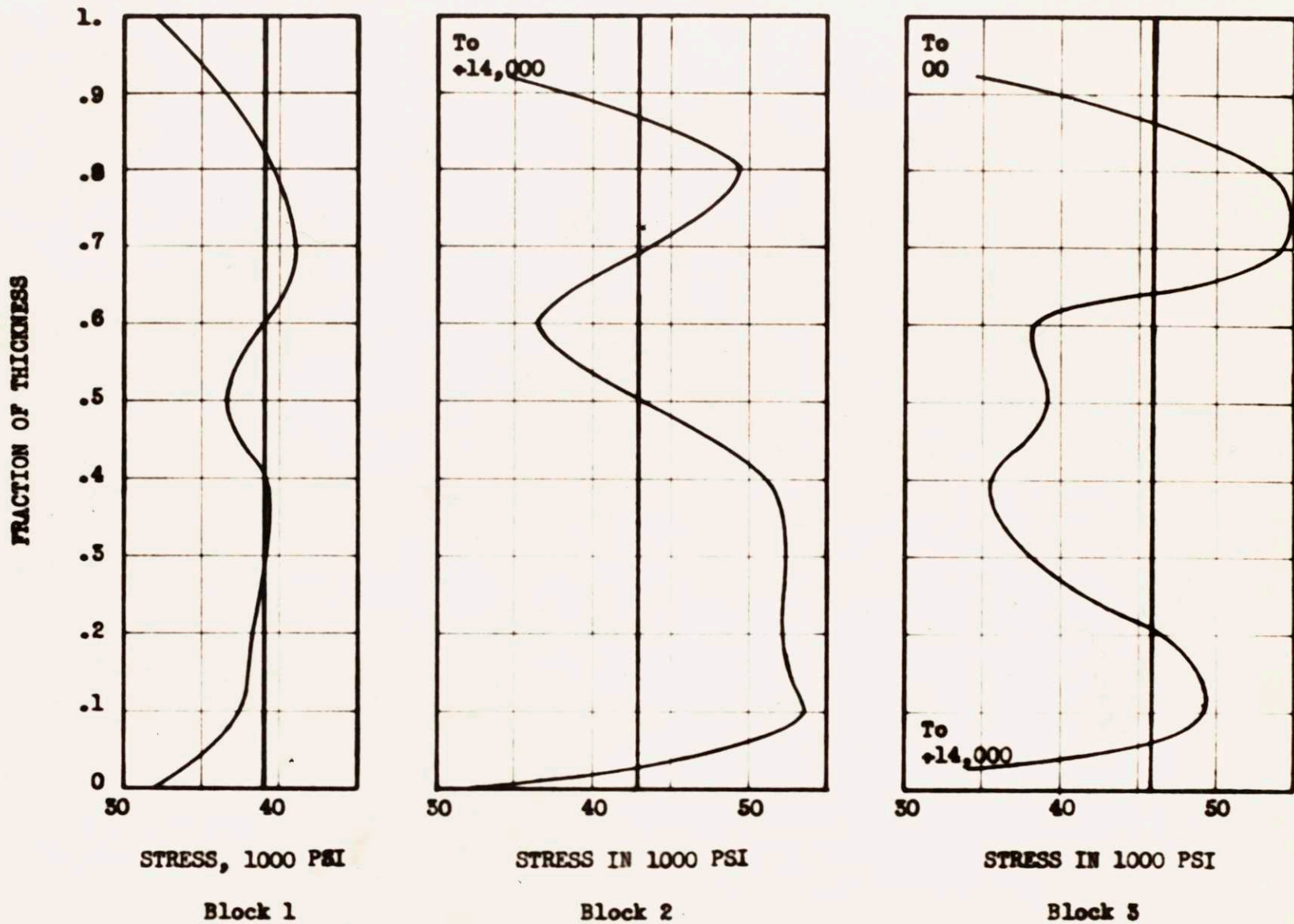


Figure 15. - Distribution of tangential stresses across the thickness of the patch welded plate.

Straight lines - average stress  
 Curves - actual stress



In the case of the plate, the strain gages were distributed more at random, and scattering was eliminated by taking the average of all the points.

As seen by the shrinkage of the disk in welding, Table 2, the restraint on the weld was not at its maximum, but the restraint on the plate was at its maximum because of its large size. By cutting the plate to the size of the disk, a relaxation corresponding to about 20,000 psi occurred within the radius of three inches from the center of the plate, Figure 14, both in radial and tangential directions. For purposes of comparison with the average total radial and tangential stresses of the plate, these 20,000 psi were added to the average radial and tangential stresses of the disk. This addition was indicated by the assumption that, if the disk had a diameter comparable to the plate, 20,000 psi would be added to the stresses found. The results are plotted in Figure 16. The discrepancy of about twenty percent in stresses at and near the center between the disk and the plate is normal, considering the differences in material and preparation of the two specimens. In machining the specimens, the patch was cut off from the plate, but not from the disk, Figures 3 and 12. In welding, heavier beads were put on the plate than on the disk, Figures 3 and 12. In the disk, a hump was found in the tangential stress between the weld and the center, rather than at either. Similar results were obtained by Bierett and Gruning<sup>(14)</sup>, Figure 2. In both cases, radial stress did not show a hump but stayed constant near the center of the specimen. In the plate, the hump occurred at the weld, both in radial and tangential directions.

The true stress distribution through the thickness, shown in Figures 6-9, for different blocks in radial and tangential directions, indicates that, in the base metal, i.e., in blocks 1, 7, 8, the variation in stress through the thickness is negligible. This conclusion is in agreement with the work done by D. Rosenthal and J. T. Norton<sup>(16)</sup>. In blocks 3, 4, and 5, which are 1.12, 1.53, and 1.68 inches from the center, respectively, tangential stress at the midsection of the disk is below 5,000 psi, a very low figure in comparison with the average stress of about 25,000 psi in this part of the disk. It is to be observed that, Figures 3a and 3b, the patch welded to the disk was partly attached to the disk when welding was begun. A cross-section of a duplicate specimen was cut and etched, Figure 17; and it was observed that the section connecting the patch to the disk was not molten in welding and, therefore, was at a lower temperature than other layers in the section. In differential cooling of the metal, the part that cools first is in compression, and the rest is in tension. This rule suggests that the stress in the midsection of the plate should be low compared with the rest of the weld, and such proved to be the case.

From the plate, three blocks were cut out and then split and sliced for stress distribution through the thickness, Figure 15. At the center of the plate, stress is almost uniform through the thickness of the plate. In blocks 2 and 3, one inch and one and one-half inches, respectively, away from the center, the pattern is very unlike corresponding blocks at the disk. In the plate, the sharp drop in stress half-way through the thickness is not observed. The difference can be taken as proof that the sharp drop

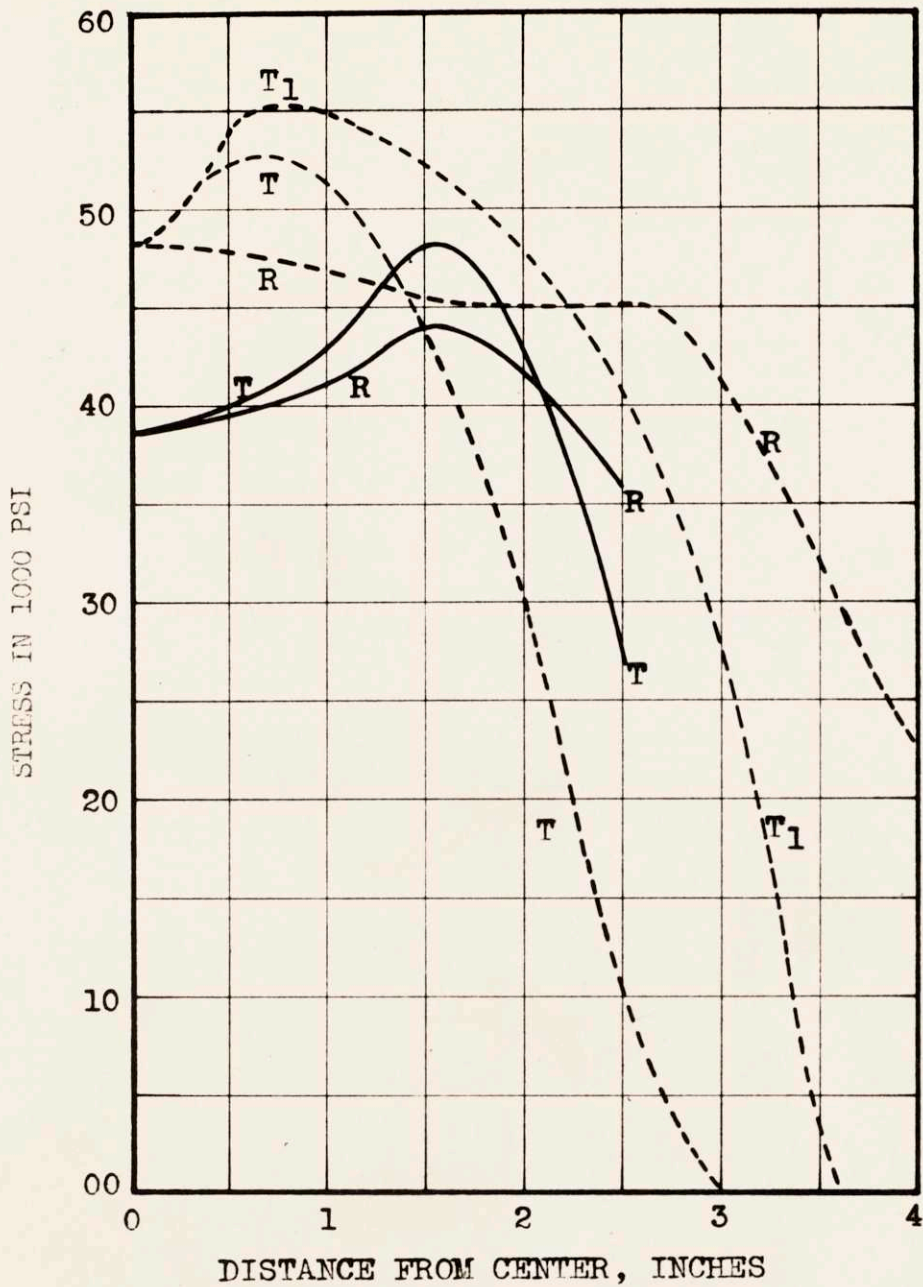


Fig. 16 - Average Radial and Tangential Stresses in the Disk, plus Stress (20,000 psi) due to Partial Relaxation in Cutting the 24 Inches Square Plate to the Size of the Disk (dotted lines), and Average Total Radial and Tangential Stresses in the Plate (solid lines)

R : Radial Stress  
T : Tangential Stress



in stress half-way through the thickness in the disk is caused by the layer connecting the patch to the disk before welding, which is not found in the plate, Figures 3 and 12. If in the plate, very low stresses on both faces in five percent of the thickness are ignored, variations from the average stress are within 16 percent. The low stresses on the faces of the plate are most likely caused by the very rough machining of the excess weld material in the planer and by the rapid cooling of the outer layer. Indeed, at the center of the plate, where there was no machining operation, or such a temperature gradient as in the weld, these low stresses were not observed.

Stress distributions in the direction of the thickness are calculated (Appendix I) at the center of the disk and for the locations  $1/2$ , 1,  $1-1/2$ , and 2 inches away from the center, Figure 10. Except at the center of the disk, where the sign of stress in the third direction changes from compression to tension, the curve showing the stress distribution in the third direction is a parabola, being zero at the top and bottom faces and maximum at the center. It is difficult to evaluate the accuracy of the stresses measured in the third direction. They are caused, not by the amount of stress in the radial and tangential directions, but by their variations along the radius of the disk. In some locations, the slope of these curves is hard to determine because of the scatter. In taking the second derivative of these curves by the graphical method (see Appendix I), the results obtained are affected.



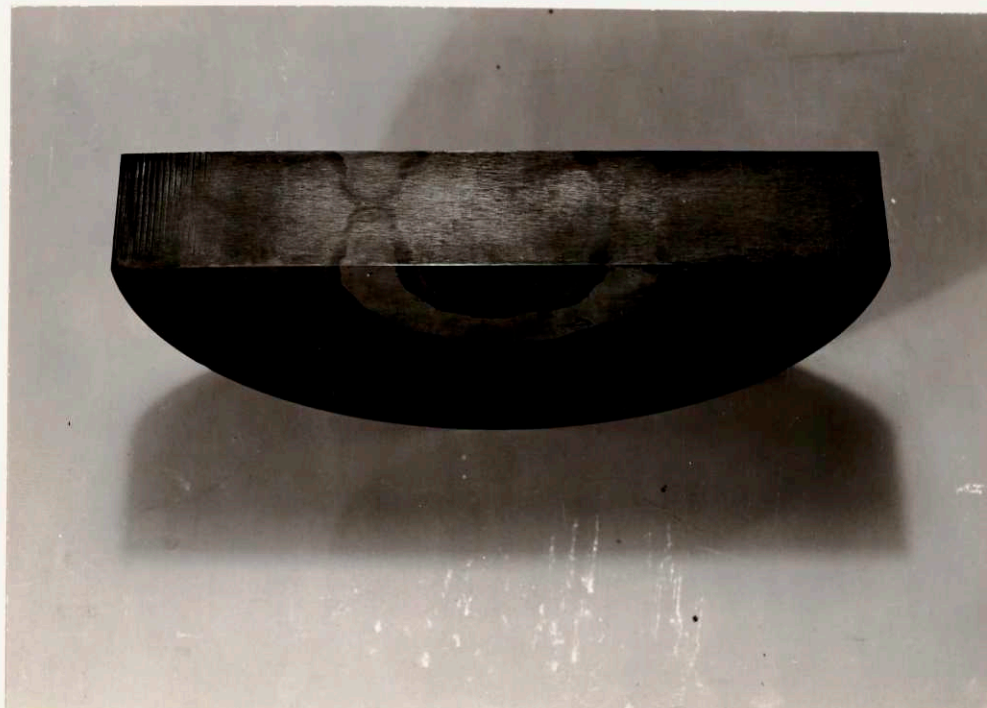


Figure 17. Cross-section of the Welded Disk  
Showing the Bridge Between the Patch and the  
Disk.

At the center of the disk, stresses measured vary between plus or minus 3,000 psi, which is within the probable error. The maximum stress of 12,000 psi in the third direction is found half an inch away from the center at the midsection of the plate. One inch away from the center, this maximum drops down to 2,000 psi; and, one inch and one-half away from the center (which is also the center of the weld bead) and two inches away from the center, it drops down to -6,000 and -7,000 psi, respectively. The maximum triaxial stress ratio  $T_r$ , defined by the equation

$$T_r = \frac{s_1 + s_2 + s_3}{3s_1}$$

where  $s_1$   $s_2$   $s_3$  are the principal stresses, is 0.73<sup>(17)</sup>. According to this definition, the triaxial stress ratio of a simple tension,  $s_2 = s_3 = 0$  is 0.33, that of biaxial tension,  $s_1 = s_2$ ,  $s_3 = 0$ , is 0.66, and that of a hydrostatic tension,  $s_1 = s_2 = s_3$ , is 1. Compared with these figures, the maximum triaxiality of 0.73 found in the disk is comparatively low.

### VIII CONCLUSION

As has been shown in the results and discussion, the average radial and tangential stresses in the disk, Figure 5, are low because of the limited restraint of the small size disk. In the large plate, stresses are much higher because of the maximum restraint on the weld, Figure 14.

The disk is of mild steel one and one-half inch thick and about nine inches in diameter with a three inch diameter patch welded at the center. The size of the plate is two foot square and contains a patch welded at the center, similar to the disk.

When stresses from the partial relaxation in cutting the plate to the size of the disk are added to the average radial and tangential stresses in the disk, Figure 16, the difference between the two sets of stresses and their average is less than 12 percent. Differences in composition of the material and preparation of the plate and the disk may account for this variation. Another difference between the two sets of stresses is that, in the plate, the peak of average stress, when the restraint on the weld is increased, is removed further away from the center of the specimen than in the disk; and the change in the average stress along the radius of the plate is less marked than that of the disk. As a first approximation, this difference in degree of change along the radius suggests lower stress in the third direction in the plate than in the disk. It must also be observed that while, in the plate, Figure 16, the slope of radial and tangential stresses

always have the same sign, in equations 3 and 4\*, used for calculations of stress in the third direction, the derivatives of radial and tangential stresses have different signs, resulting in even lower stress in the third direction in the large plate than in the disk.

The true radial and tangential stress distributions through the thickness of the specimens, Figures 6-9 and Figure 15, show unusually low points half-way through the thickness at the welding zone of the disk. As explained in the discussion of results, these sharp drops are most probably caused by the 0.126 inch thick bridge that connects the circular patch with the disk previous to welding, Figure 3b. The patch welded to the large plate is not connected to the specimen; and, therefore, a similar drop is not observed in the stress distribution through the thickness, Figure 15. If the sharp drop half-way through the thickness in the disk is omitted, the variation in stress through the thickness in the plate and in the disk is below 16 percent of the average in the welding zone. Outside of the welding zone, the stress through the thickness is almost uniform.

---

\*The equations 3 and 4 appearing in the Appendix are as follows:

For any point along the radius

$$\frac{d^2S_z}{dZ^2} = \frac{d^2S_r}{dr^2} + \frac{2}{r} \frac{dS_r}{dr} - \frac{1}{r} \frac{dS_t}{dr} \quad (3)$$

and for the center of the disk

$$\frac{d^2S_z}{dZ^2} = \frac{3}{2} \frac{d^2S_r}{dr^2} - \frac{d^2S_t}{dr^2} \quad (4)$$



The expected high degree of triaxiality is not found in the patch welded disk. This may be due partly to the insufficient thickness of the plate and partly to the large size of the blocks that furnishes the average stress along its length, but not the steep variations of stresses. As explained previously, even lower triaxiality is expected in the large plate.

Increasing the thickness of the plate beyond 1.5 inches reduces the effectiveness of the block method in detecting these steep stress gradients. In the first place, in developing the block method of measuring triaxial stresses<sup>(12)</sup>, one assumption is that, after splitting the block, there is no stress in the direction of the thickness in the two parts obtained. This assumption, however, is not necessarily valid for a thick plate. In the second place, increased thickness increases the length of the block, and steep gradients of stresses are not detected.

Another difficulty in measuring triaxial stresses arises from the fact that there is no method of producing a known triaxial stress pattern which would help to develop a method to measure them. Therefore, a new method of measuring stresses below the surface is needed, which would be able to measure stresses through the thickness of a specimen of any size and shape and, at the same time, detect the steep gradient of stresses.

The measurement of stresses below the surface by the recessing method may be the answer to this problem. Therefore, in the second part of this thesis, the problem of recessing will be taken up.

IX APPENDIX ON THE DISK

DATA AND CALCULATIONS IN MEASUREMENT OF TRIAXIAL RESIDUAL  
STRESSES IN PATCH WELDED CIRCULAR DISK

The following tables contain all the operations performed on the disk and the corresponding relaxations recorded after the electrical strain gages were attached to it. Before each operation, such as cutting of the block, splitting, et cetera, gage readings were taken, and relaxation for each step and cumulative relaxation for splitting and slicing are shown in the respective columns for top and bottom gages of each block.

From the Tables 4 to 13, the relaxations in cutting the blocks free from the disk will be considered. These are the average relaxations through the thickness. The average radial and tangential stresses in the disk are obtained from these relaxations in cutting off the blocks.

Relaxations in splitting the blocks and in slicing cannot change these averages. They will be used to calculate remaining stresses in each layer considered; and these, in turn, will be added to the average stresses to find the true stress distribution through the thickness of the disk at definite points along the radius in radial and tangential directions.

Radial strains in blocks 11 to 16 are plotted versus the distance from the center along the radius, and corresponding values for blocks 1 to 10 are interpolated in order to have radial and tangential strains for the same points, that is, for blocks 1 to 10, Table 14, Figure 18.

4  
 Table - Relaxations in Cutting the Blocks Free from the Disk and  
 in splitting and slicing of Blocks

B L O C K 1						
			TOP GAGE		BOTTOM GAGE	
Steps	Operations	Remaining thickness in inches	Relaxation, micro inches per inch	Cumulative relaxation in splitting and slicing	Relaxation micro inches per inch	Cumulative relaxation in splitting and slicing
1	cutting of block	1.5				
			+724		+681	
2	splitting of block	1.5				
			-6	- 6	+ 2	+ 2
3	slicing	.72				
			- 32	- 38	- 13	-11
4	slicing	.59				
			- 16	- 54	- 5	-16
5	slicing	.45				
			- 22	- 76	- 29	-45
6	slicing	.31				
			- 74	-150	- 34	-79
		.175				
B L O C K 2						
1	cutting of block	1.5				
			+873		+926	
2	splitting of block	1.5				
			- 70	- 70	- 30	-30
3	slicing	.72				
			- 38	-108	+ 6	-24
4	slicing	.59				
			- 29	-137	+ 2	-22
5	slicing	.45				
			- 16	-153	- 18	-40
6	slicing	.31				
			- 43	-196	- 26	-66
		.175				



5

Table - Relaxations in Cutting the Blocks Free from the Disk and in splitting and slicing of Blocks

BLOCK 3						
			TOP GAGE		BOTTOM GAGE	
Steps	Operations	Remaining thickness in inches	Relaxation, micro inches per inch	Cumulative relaxation in splitting and slicing	Relaxation micro inches per inch	Cumulative relaxation in splitting and slicing
1	cutting of block	1.5				
			+1028		+739	
2	splitting of block	1.5				
			- 80	- 80	- 70	- 70
3	slicing	.72				
			- 94	-174	- 22	- 42
4	slicing	.59				
			- 86	-260	- 8	-100
5	slicing	.45				
			- 31	-291	- 18	-118
6	slicing	.31				
			- 2	-293	- 54	-172
		.175				
BLOCK 4						
1	cutting of block	1.5				
			+ 557		+620	
2	splitting of block	1.5				
			+ 112	+112	- 72	- 72
3	slicing	.72				
			+ 12	+124	- 31	-103
4	slicing	.59				
			- 10	+114	+ 12	- 91
5	slicing	.45				
			- 2	+112	+ 13	- 78
6	slicing	.31				
			+ 59	+171	- 20	- 98
		.175				



6

Table - Relaxations in Cutting the Blocks Free from the Disk and in splitting and slicing of Blocks

B L O C K 5						
			TOP GAGE		BOTTOM GAGE	
Steps	Operations	Remaining thickness in inches	Relaxation, micro inches per inch	Cumulative relaxation in splitting and slicing	Relaxation micro inches per inch	Cumulative relaxation in splitting and slicing
1	cutting of block	1.5				
			+780			
2	splitting of block	1.5				
			-172	-172	-150	-150
3	slicing	.72				
			- 85	-257	-130	-280
4	slicing	.59				
			- 23	-280	- 61	-341
5	slicing	.45				
			+ 6	-274	- 3	-344
6	slicing	.31				
			+ 22	-252	- 9	-353
		.175				
B L O C K 6						
1	cutting of block	1.5				
			-164		+122	
2	splitting of block	1.5				
			+367	+367	+280	+280
3	slicing	.72				
			- 77	+290	- 98	+182
4	slicing	.59				
			- 77	+213	-120	+ 62
5	slicing	.45				
			- 42	+171	- 92	- 30
6	slicing	.31				
			+ 7	+178	- 88	-118
		.175				

7  
 Table - Relaxations in Cutting the Blocks Free from the Disk and  
 in splitting and slicing of Blocks

B L O C K 7						
			TOP GAGE		BOTTOM GAGE	
Steps	Operations	Remaining thickness in inches	Relaxation, micro inches per inch	Cumulative relaxation in splitting and slicing	Relaxation micro inches per inch	Cumulative relaxation in splitting and slicing
1	cutting of block	1.5				
			+514		+511	
2	splitting of block	1.5				
			-120	-120	-108	-108
3	slicing	.72				
			- 53	-173	- 25	-133
4	slicing	.59				
			- 61	-234	- 25	-158
5	slicing	.45				
			- 40	-274	- 22	-180
6	slicing	.31				
			+ 16	-258	+ 2	-178
		.175				
B L O C K 8						
1	cutting of block	1.5				
			+368		+408	
2	splitting of block	1.5				
			- 99	- 99	-107	-107
3	slicing	.72				
			- 24	-123	- 42	-149
4	slicing	.59				
			- 29	-152	- 35	-184
5	slicing	.45				
			- 6	-158	- 10	-194
6	slicing	.31				
			+ 28	-130	+ 30	-164
		.175				

8

Table - Relaxations in Cutting the Blocks Free from the Disk and in splitting and slicing of Blocks

B L O C K 8 <sub>1</sub>						
			TOP GAGE		BOTTOM GAGE	
Steps	Operations	Remaining thickness in inches	Relaxation, micro inches per inch	Cumulative relaxation in splitting and slicing	Relaxation micro inches per inch	Cumulative relaxation in splitting and slicing
1	cutting of block	1.5				
			-752		-752	
2	splitting of block	1.5				
			+124	+124	+118	+118
3	slicing	.72	+ 8	+132	+ 4	+122
4	slicing	.59	- 3	+129	0	+122
		.45				
5	slicing	.31	+ 22	+151	+ 20	+142
6	slicing	.175	+ 46	+197	+ 34	+176
B L O C K 9						
1	cutting of block	1.5				
			-335		-471	
2	splitting of block	1.5				
			- 70	- 70	- 66	- 66
3	slicing	.72	- 10	- 80	- 10	- 76
4	slicing	.59	- 12	- 92	- 5	- 81
		.45				
5	slicing	.31	+ 8	- 84	+ 15	- 66
6	slicing	.175	+ 32	- 52	+ 44	- 22



9

Table - Relaxations in Cutting the Blocks Free from the Disk and in splitting and slicing of Blocks

BLOCK 9 <sub>1</sub>						
			TOP GAGE		BOTTOM GAGE	
Steps	Operations	Remaining thickness in inches	Relaxation, micro inches per inch	Cumulative relaxation in splitting and slicing	Relaxation micro inches per inch	Cumulative relaxation in splitting and slicing
1	cutting of block	1.5				
			-826		-820	
2	splitting of block	1.5				
			+ 64	+ 64	+ 74	+ 74
3	slicing	.72				
			- 4	+ 60	- 2	+ 72
4	slicing	.59				
			0	+ 60	+ 5	+ 77
5	slicing	.45				
			+ 10	+ 70	+ 21	+ 98
6	slicing	.31				
			+ 41	+111	+ 35	+133
		.175				
BLOCK 10						
1	cutting of block	1.5				
			-859		-798	
2	splitting of block	1.5				
			+110	+110	+ 91	+ 91
3	slicing	.72				
			+ 8	+118	+ 2	+ 93
4	slicing	.59				
			+ 8	+126	- 2	+ 91
5	slicing	.45				
			+ 20	+146	+ 8	+ 99
6	slicing	.31				
			+ 46	+192	+ 35	+134
		.175				



10

Table - Relaxations in Cutting the Blocks Free from the Disk and in splitting and slicing of Blocks

B L O C K 10 <sub>1</sub>						
			TOP GAGE		BOTTOM GAGE	
Steps	Operations	Remaining thickness in inches	Relaxation, micro inches per inch	Cumulative relaxation in splitting and slicing	Relaxation micro inches per inch	Cumulative relaxation in splitting and slicing
1	cutting of block	1.5				
			-909		-816	
2	splitting of block	1.5				
			+102	+102	+105	+105
3	slicing	.72				
			- 2	+100	+ 5	+110
4	slicing	.59				
			- 1	+ 99	+ 7	+117
5	slicing	.45				
			+ 10	+109	+ 27	+144
6	slicing	.31				
			+ 25	+134	+ 38	+182
		.175				
B L O C K 11						
1	cutting of block	1.5				
			+702		+443	
2	splitting of block	1.5				
			+243	+243	+102	+102
3	slicing	.72				
			- 47	+196	-165	- 63
4	slicing	.59				
			- 8	+188	-115	-178
5	slicing	.45				
			- 7	+181	- 66	-244
6	slicing	.31				
			+ 32	+213	- 57	-301
		.175				

11

Table - Relaxations in Cutting the Blocks Free from the Disk and in splitting and slicing of Blocks

B L O C K 12						
			TOP GAGE		BOTTOM GAGE	
Steps	Operations	Remaining thickness in inches	Relaxation, micro inches per inch	Cumulative relaxation in splitting and slicing	Relaxation micro inches per inch	Cumulative relaxation in splitting and slicing
1	cutting of block	1.5				
			+720		+655	
2	splitting of block	1.5				
			+348	+348	+259	+259
3	slicing	.72				
			0	+348	- 65	+194
4	slicing	.59				
			+ 40	+388	- 51	+143
5	slicing	.45				
			+ 35	+423	- 43	+100
6	slicing	.31				
			+ 29	+452	- 76	+ 24
		.175				
B L O C K 13						
1	cutting of block	1.5				
			+786		+804	
2	splitting of block	1.5				
			+274	+274	+243	+243
3	slicing	.72				
			+ 8	+282	- 6	+237
4	slicing	.59				
			+ 2	+284	- 4	+233
5	slicing	.45				
			- 37	+247	- 3	+230
6	slicing	.31				
			- 47	+200	- 35	+195
		.175				

12

Table - Relaxations in Cutting the Blocks Free from the Disk and in splitting and slicing of Blocks

B L O C K 13 <sub>1</sub>						
			TOP GAGE		BOTTOM GAGE	
Steps	Operations	Remaining thickness in inches	Relaxation, micro inches per inch	Cumulative relaxation in splitting and slicing	Relaxation micro inches per inch	Cumulative relaxation in splitting and slicing
1	cutting of block	1.5				
			+832		+724	
2	splitting of block	1.5				
			+282	+282	+241	+241
3	slicing	.72				
			+ 1	+283	0	+241
4	slicing	.59				
			0	+283	0	+241
5	slicing	.45				
			- 10	+273	- 10	+231
6	slicing	.31				
			+ 20	+293	- 41	+190
		.175				
B L O C K 14						
1	cutting of block	1.5				
			+825		+752	
2	splitting of block	1.5				
			+ 32	+ 32	+ 41	+ 41
3	slicing	.72				
			- 10	+ 22	- 10	+ 31
4	slicing	.59				
			- 13	+ 9	- 13	+ 18
5	slicing	.45				
			- 15	- 6	- 18	0
6	slicing	.31				
			+ 5	- 1	- 32	- 32
		.175				



13

Table - Relaxations in Cutting the Blocks Free from the Disk and in splitting and slicing of Blocks

B L O C K 15						
			TOP GAGE		BOTTOM GAGE	
Steps	Operations	Remaining thickness in inches	Relaxation, micro inches per inch	Cumulative relaxation in splitting and slicing	Relaxation micro inches per inch	Cumulative relaxation in splitting and slicing
1	cutting of block	1.5				
			+786		+706	
2	splitting of block	1.5				
			+ 26	+26	+ 25	+25
3	slicing	.72				
			- 2	+24	- 12	+13
4	slicing	.59				
			- 3	+27	- 19	- 6
5	slicing	.45				
			- 4	+17	- 23	-29
6	slicing	.31				
			+ 14	+31	- 42	-71
		.175				
B L O C K 16						
1	cutting of block	1.5				
			+591		+352	
2	splitting of block	1.5				
			+ 86	+86	+ 88	+88
3	slicing	.72				
			- 7	+79	- 2	+86
4	slicing	.59				
			- 8	+71	- 12	+74
5	slicing	.45				
			- 10	+61	- 25	+49
6	slicing	.31				
			0	+61	- 23	+26
		.175				



Table 14  
Strains, Micro Inches per Inch, Relaxed in Cutting  
the Blocks 11 to 16 Free From the Disk

<u>Block No.</u>	<u>Distance from Center</u>	<u>Radial Relaxed Strain</u>	
		<u>Top</u>	<u>Bottom</u>
11	1.5	+702	+443
12	2.0	+720	+655
13	2.25	+786	+804
13,	2.25	+832	+724
14	2.875	+825	+752
14,	2.875	+827	+736
15	3.06	+786	+706
16	3.31	+591	+532
16,	3.31	+594	+487

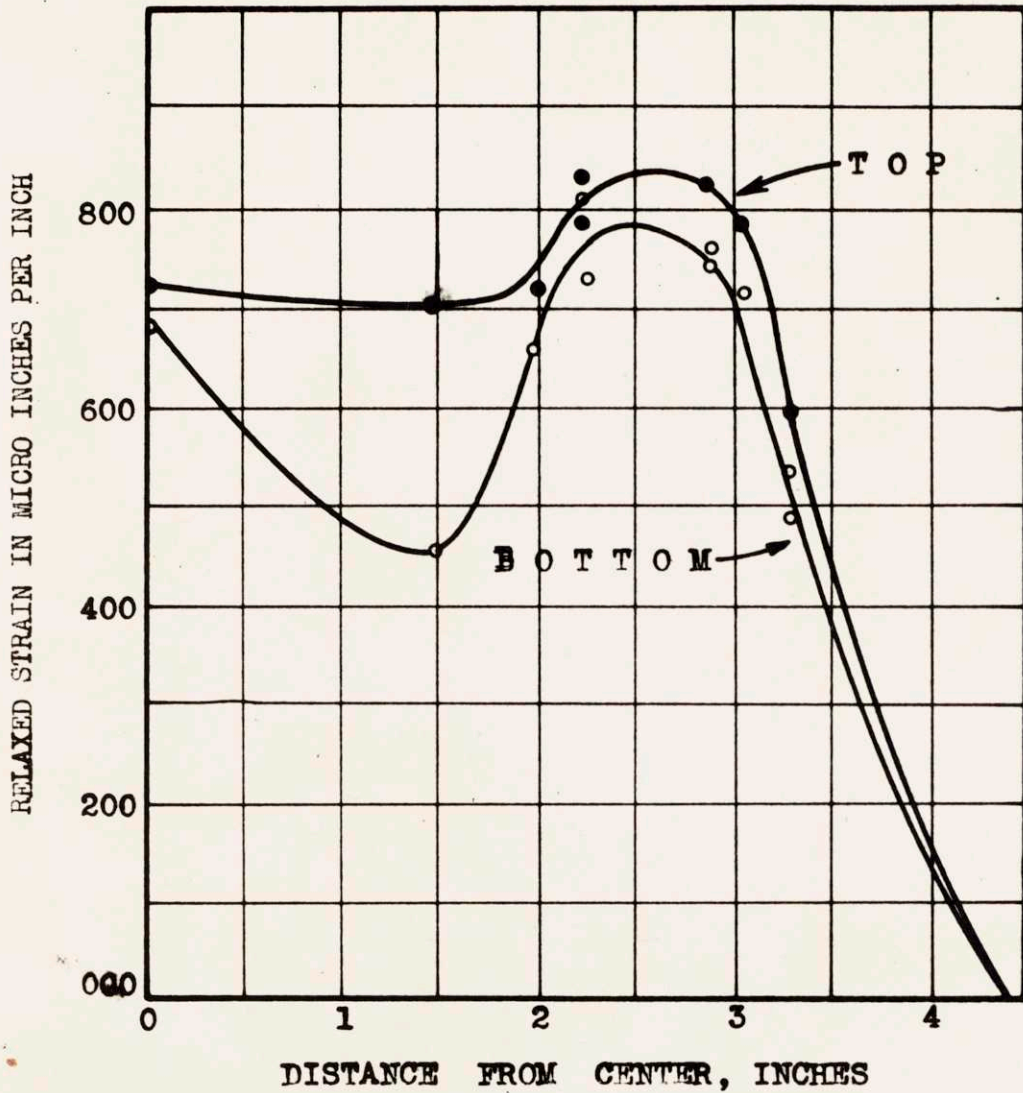


Fig. 18 - Radial Strains Along the Radius of the Disk, Obtained in Cutting the Blocks No. 11 to 16 Free from it

Table 14 shows the strain relaxed in tangential and radial directions for the top and bottom gages.

The strains in Table 15 are used to compute stresses at each point using the equations

$$S_r = \frac{E(e_r + \nu e_t)}{1 - \nu^2}$$

and

$$S_t = \frac{E(e_t + \nu e_r)}{1 - \nu^2}$$

where  $E$  = Young's modulus =  $30 \times 10^6$ ,  $\nu$  = Poisson's ratio = 0.3,  $e_t$  = strain in tangential direction, and  $e_r$  = strain in radial direction. The results are in Table 3.

The average radial and tangential stresses are plotted in Figure 5. It will be seen that there are two curves for the tangential stresses along the radius. Furthermore, Figure 4 indicates that blocks corresponding to the two curves are on two different radiuses of the disk.

From this fact, it is concluded that tangential stresses in the disk are not symmetrical and that these two curves might represent the upper and lower limits. On the other hand, the areas under the curve representing tangential stresses should, plus and minus, add up to zero for the sake of equilibrium, that is, if symmetrical distribution of stress is accepted. In this case the curve T should be taken as the tangential stress pattern in the disk.

Table 15

Strain, Micro Inches per Inch, Relaxed in Cutting the Blocks Free From the Disk

Remaining Relaxation (Splitting and Slicing)

Block No.	Distance from Center	Tangential		Radial		Top		Bottom	
		Top	Bottom	Top	Bottom	Radial	Tangential	Radial	Tangential
		$e_r$	$e_t$	$e_r$	$e_t$	$e_r$	$e_t$	$e_r$	$e_t$
1	0.	+724	+681	+724	+681	-400	-400	-152	-152
2	0.56	+873	+926	+710	+565	-160	-300	-250	-106
3	1.125	+1028	+739	+700	+465	+ 80	-294	-340	-300
4	1.53	+557	+620	+700	+450	+160	+252	-360	-130
5	1.687	+780	?	+706	+510	+240	-214	-370	-355
6	2.09	-164	+122	+750	+700	+500	+198	0	-208
7	2.25	+514	+511	+800	+760	+330	-214	+115	-178
8	2.81	+368	+408	+830	+760	+ 20	- 94	-100	-122
8 <sub>1</sub>	2.81	-752	-752	+830	+760	+ 20	+266	-100	+220
9	3.37	-355	-471	+540	+480	+ 60	- 8	+ 50	+ 56
9 <sub>1</sub>	3.37	-826	-820	+540	+480	+ 60	+190	+ 50	+188
10	3.937	-859	-798	+380	+370	+ 60	+286	+ 70	+192
10 <sub>1</sub>	3.937	-909	-810	+200	+170	+ 60	+190	+ 70	+252



So far, the average stresses in the radial and tangential directions have been shown. To obtain the true stress distribution through the thickness, relaxations in splitting and slicing of the blocks have to be considered. The remaining stress at a layer  $d$  of a block, after it has been cut free from the disk, is given by the equation (2), (Reference 12, eq. 23).

$$S_a'' = E \left[ \frac{1-a}{2} \frac{de''}{da} - 2(e'' - e''_t) + 3(1-a) \int_{.5}^a \frac{e_t'' - e_t''^0}{(1-a)^2} da + (5a - 4) e_t''^0 + (1 - a) e_b''^0 \right] \quad (2)$$

In equation (2)

$E$  = Modulus of elasticity

$a$  = Fraction of total thickness removed

$e_t''^0$  = Total relaxed strain measured on top gage for the position

$e_t''$  = The relaxed strain on top when splitting the block in half.

In order to obtain the values of the terms at the right hand side of this equation for  $d = 0.5, 0.6, 0.7, 0.8, 0.9, 1$ .

The relaxations in splitting and slicing will be represented now in Figures 19 to 26. The end values of these diagrams are determined by extrapolation. The data taken from the Figures 19 to 26 are recorded in Tables 16 to 36.

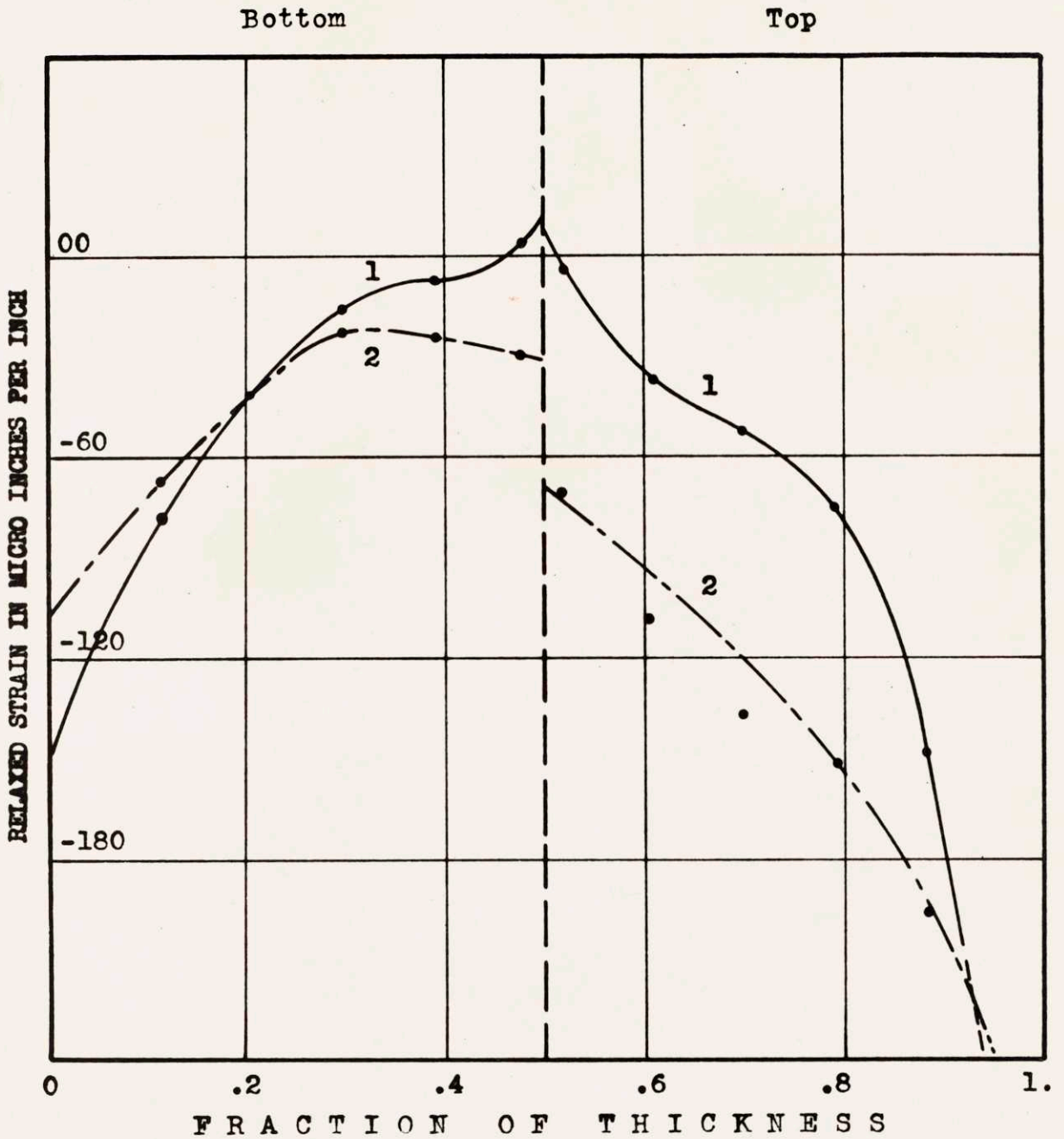


Fig. 19- Strain Relaxed on Top and Bottom in Blocks No. 1 and 2 by Splitting and Successive Slicing from Mid-section Toward Both Faces

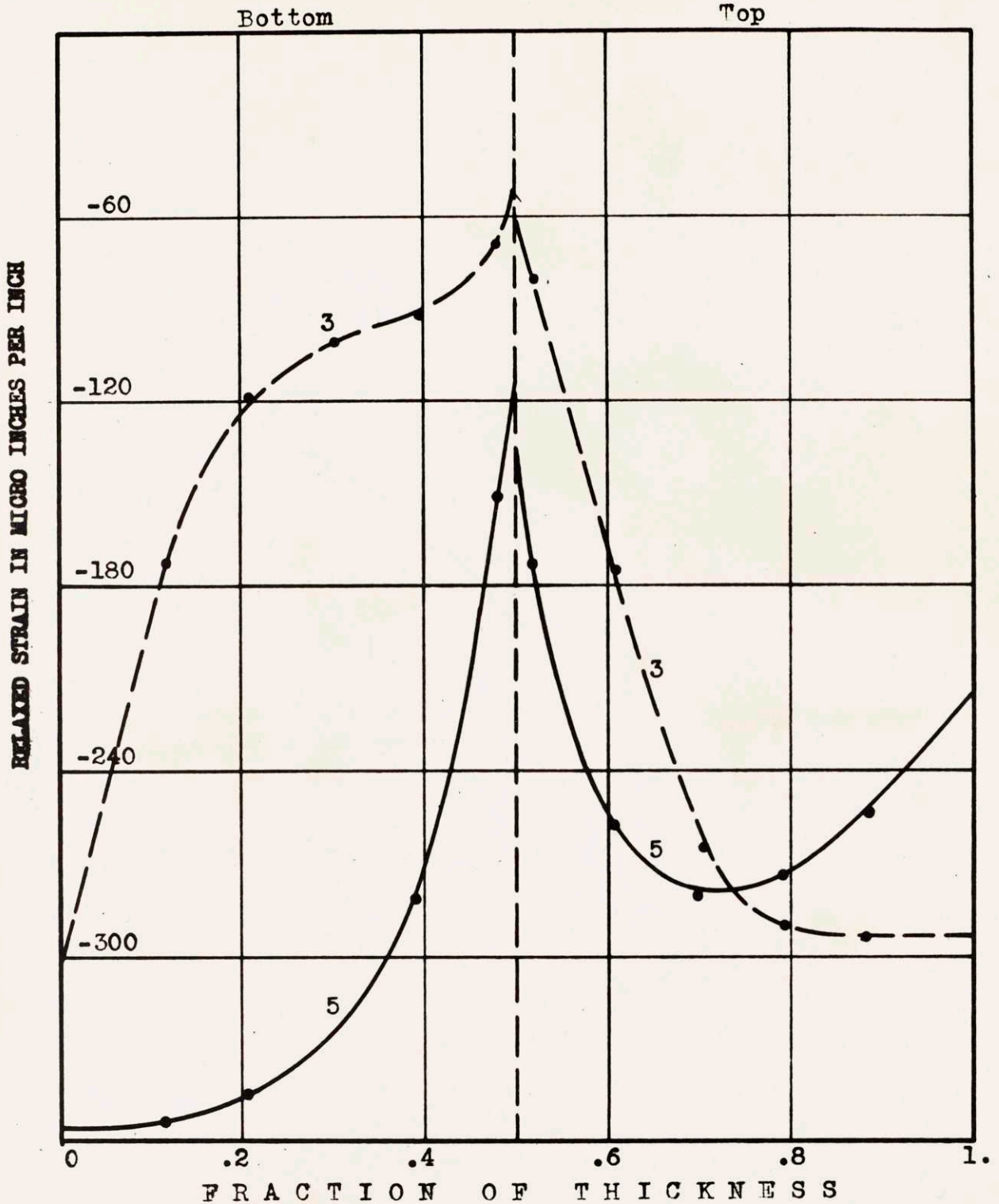


Fig. 20 - Strain Relaxed on Top and Bottom in Blocks No. 3 and 5 by Splitting and Slicing from Mid-section Toward Both Faces.



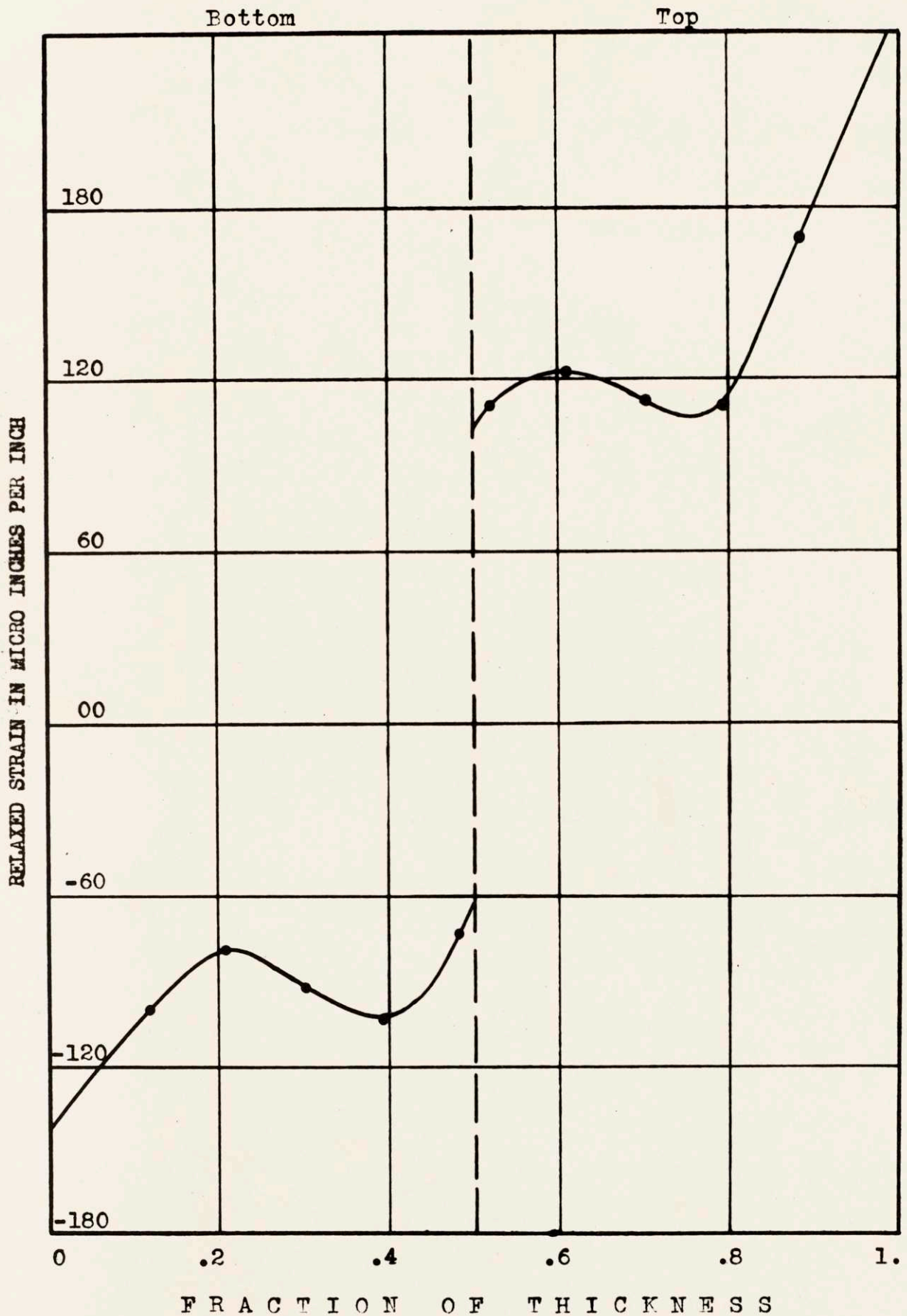


Fig. 21 - Strain Relaxed on Top and Bottom in Block No. 4 by Splitting and Successive Slicing from Mid-section Toward Both Faces

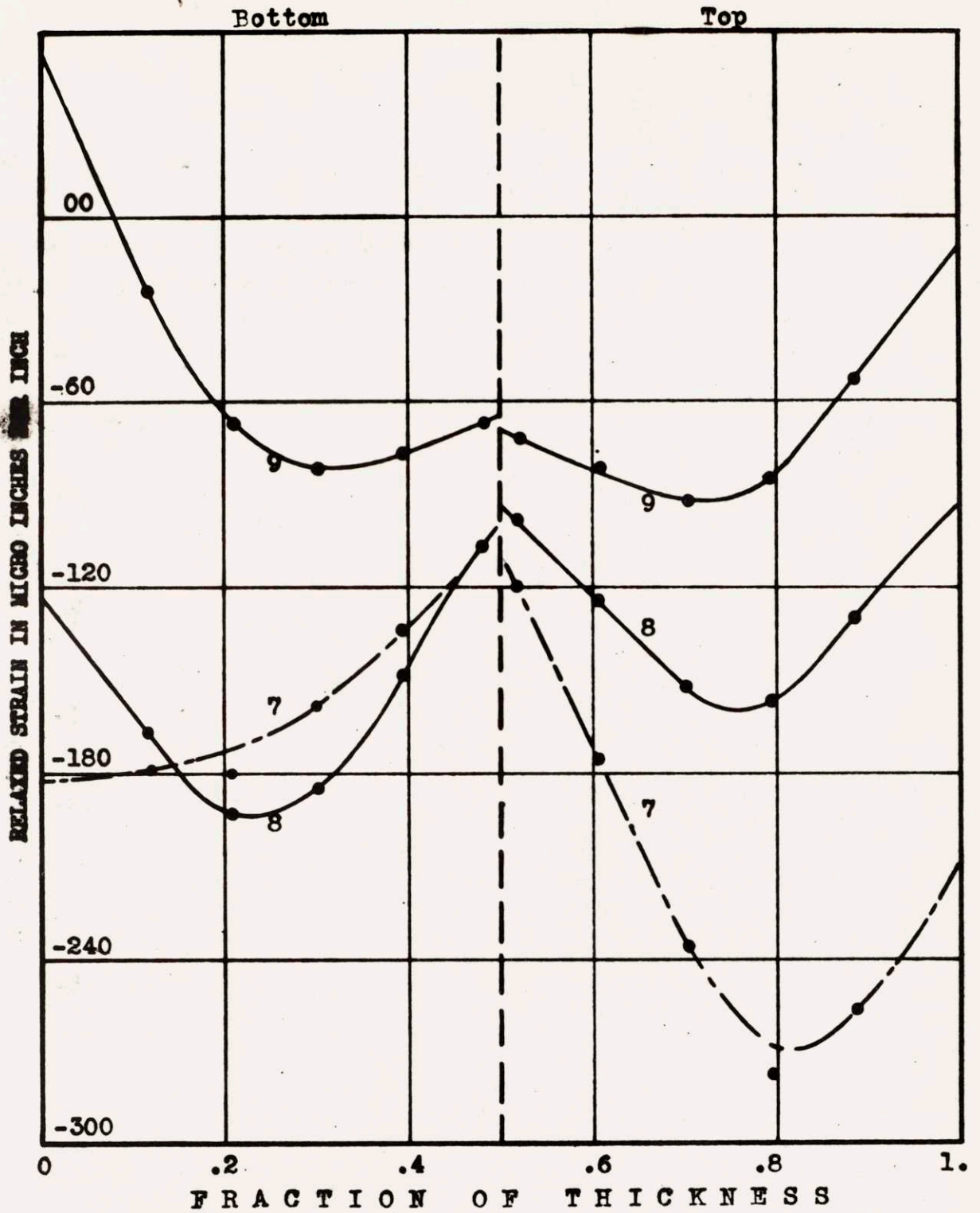


Fig. 22 - Strain Relaxed on Top and Bottom in Blocks No. 7, 8 and 9 by Splitting and Successive Slicing from Mid-section Toward Both Faces

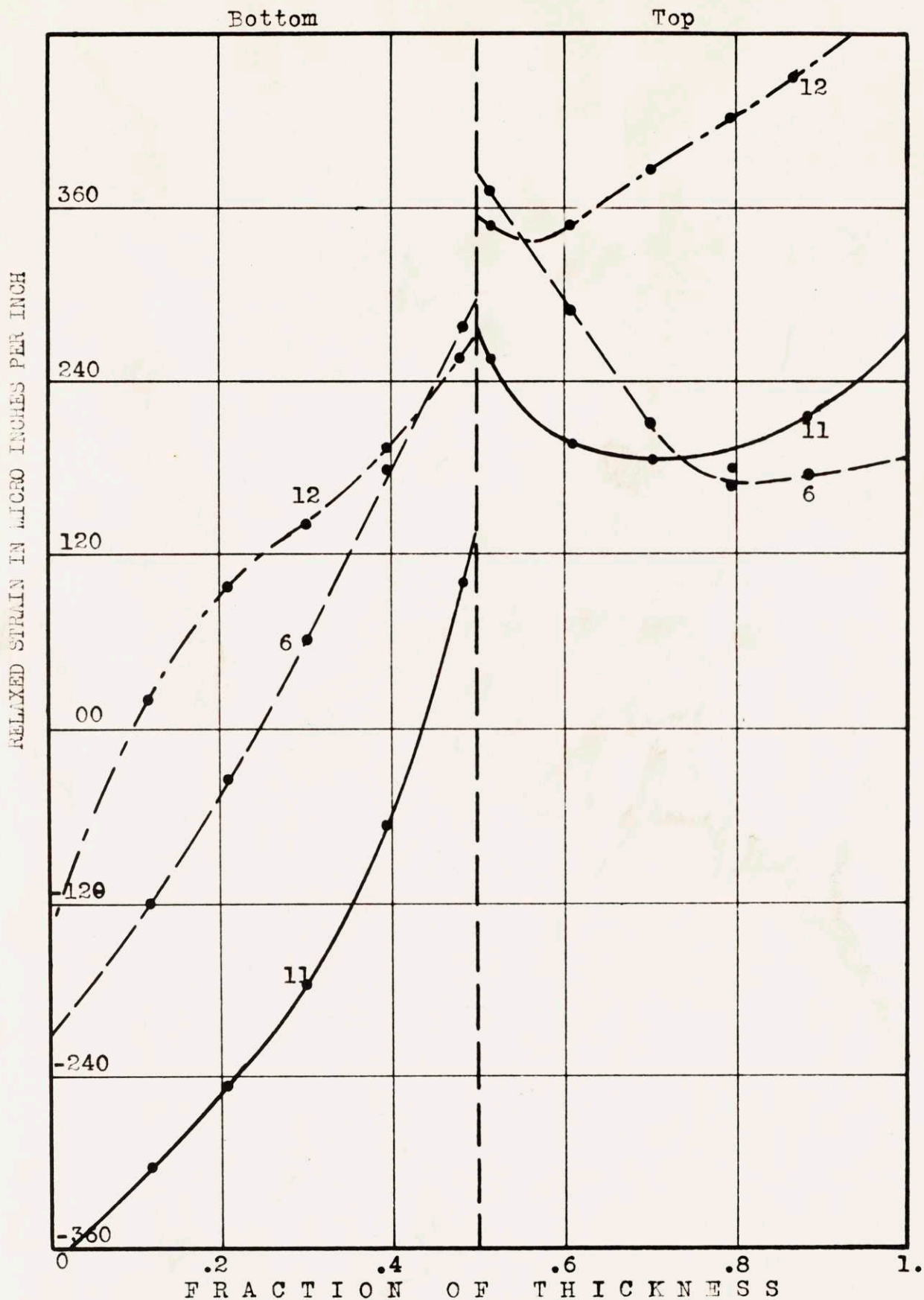


Fig. 23 - Strain Relaxed on Top and Bottom in Blocks No. 6, 11 and 12 by Splitting and Successive Slicing from Mid-section Toward Both Faces.



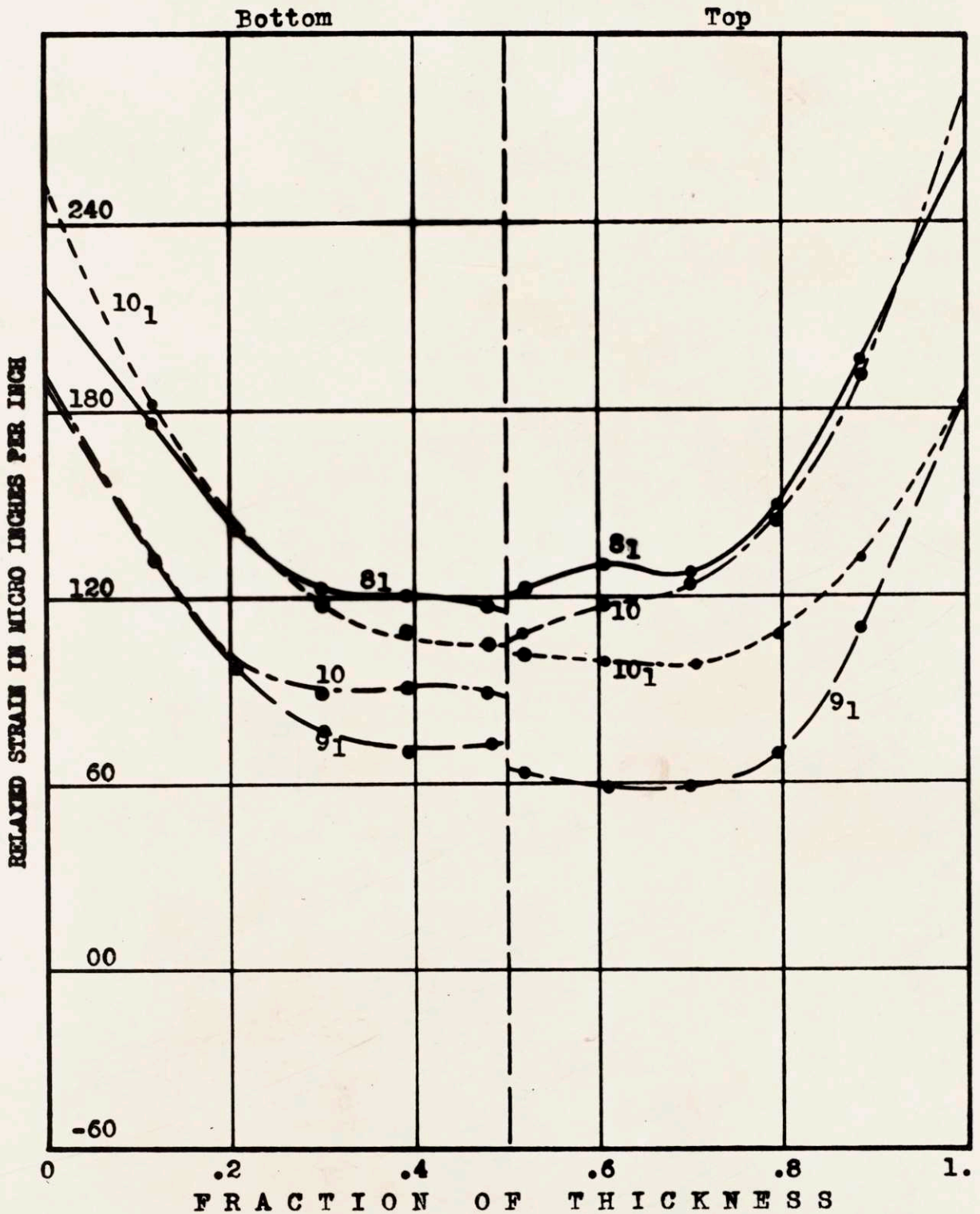


Fig. 24 - Strain Relaxed on Top and Bottom in Blocks No. 8<sub>1</sub>, 9<sub>1</sub>, 10 and 10<sub>1</sub> by Splitting and Successive Slicing from Mid-section Toward Both Faces

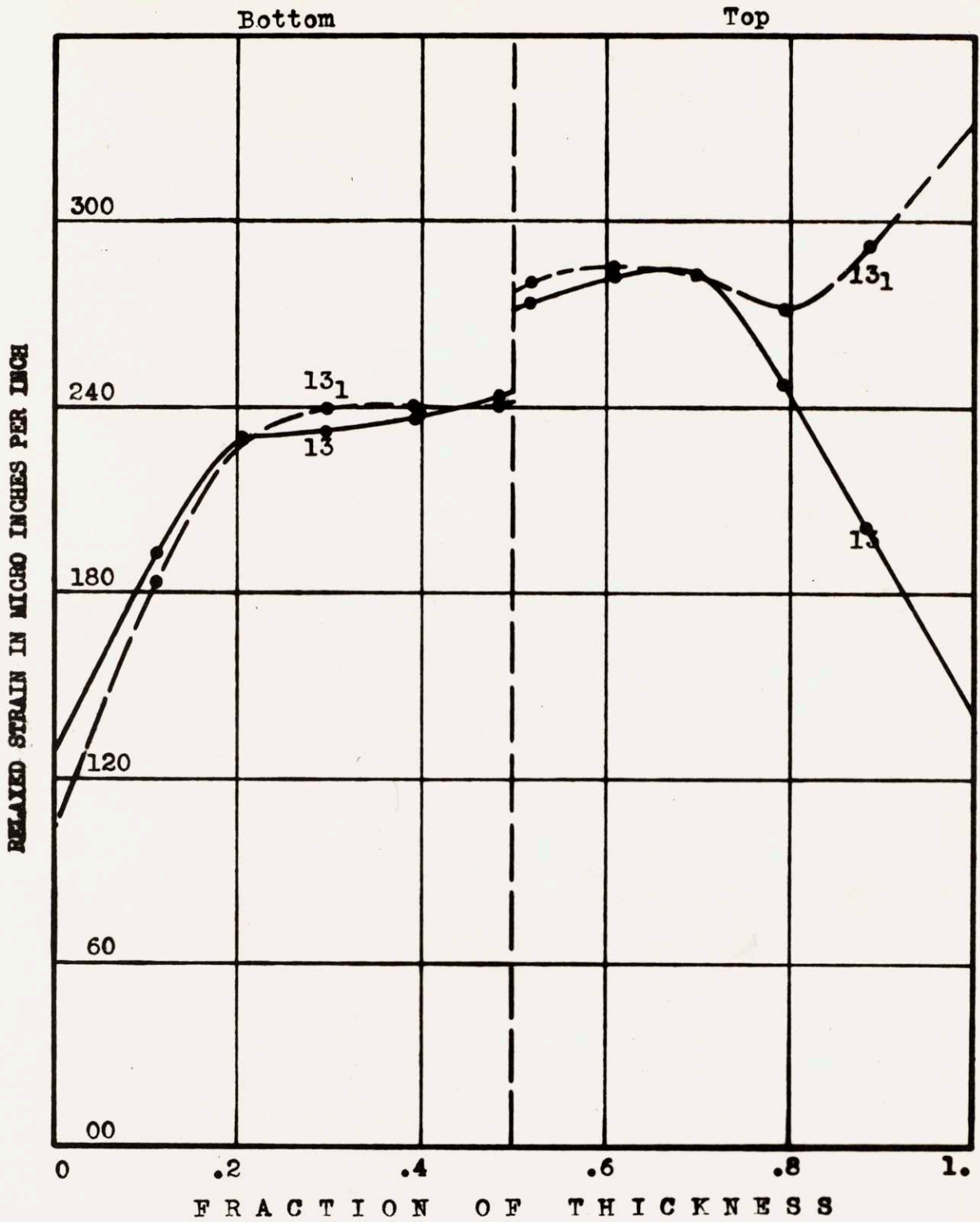


Fig. 25 - Strain Relaxed on Top and Bottom in Block No. 13 and 13<sub>1</sub> by Splitting and Successive Slicing from Mid-section Toward Both Faces

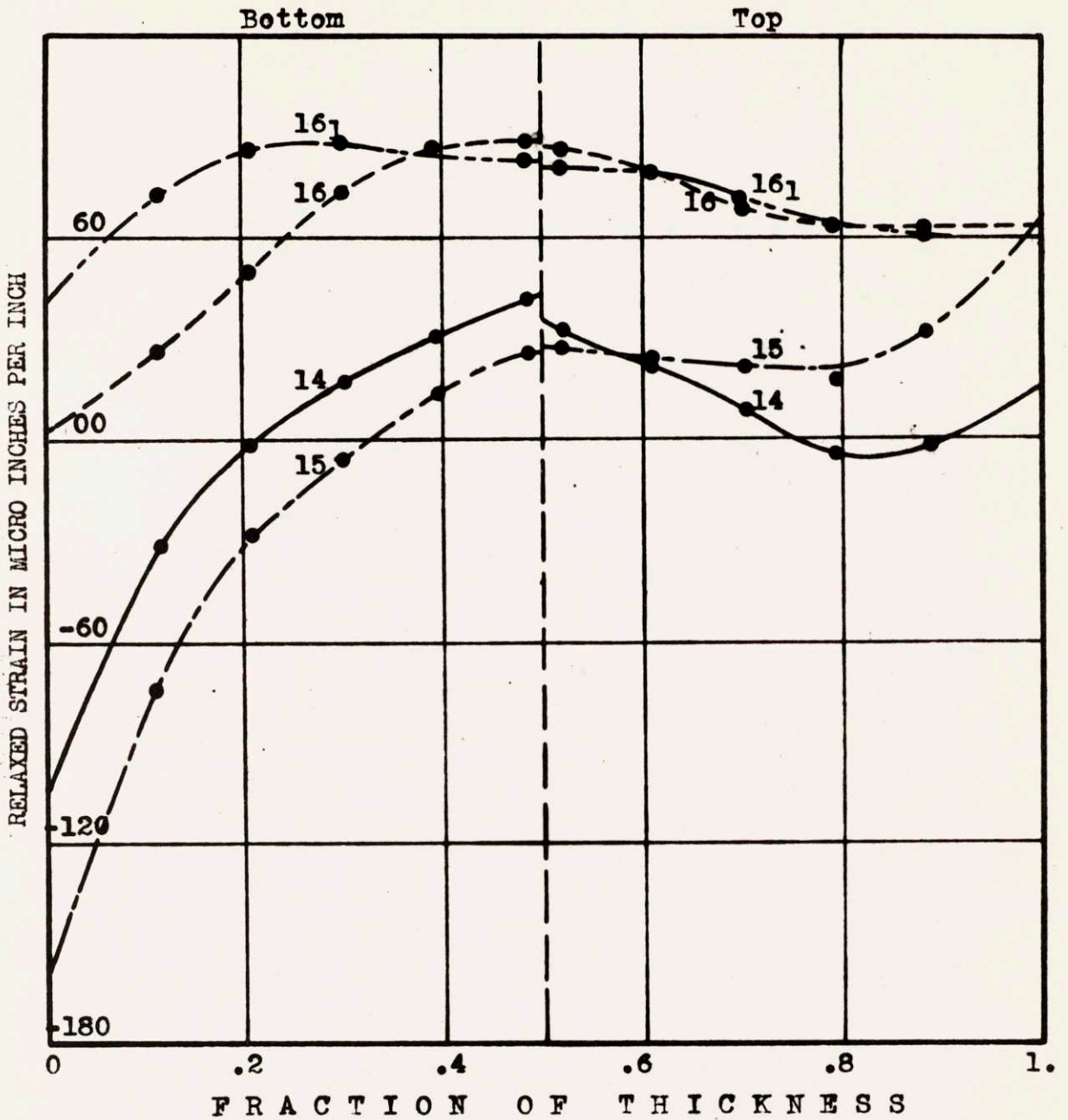


Fig. 26 - Strain Relaxed on Top and Bottom in Blocks No.14, 15, 16 and 16<sub>1</sub> by Splitting and Successive Slicing from Mid-section Toward Both Faces.



16

Table - Tabulation of Data Taken from the Curves, Figs 19 to 26, for the Computation of Stress Relieved in Splitting and slicing of Blocks

BLOCK 1						TOP		
Fraction of thickness, a	Cumulative relaxation in splitting & slicing, e''	$e'' - e''_0$	Slope, $\frac{de''}{da}$	$\frac{e'' - e''_0}{(1-a)^2}$	$\int_a^1 \frac{e'' - e''_0}{(1-a)^2} \cdot da$	Computed stress, S''	Corrected tangential stress, S''*	Corrected radial stress, S''**
.5	+ 4	0	- 580	0	0	+ 4,380	- 5,150	- 5,150
.6	- 36	- 40	- 225	- 250	- 12	+ 600	+ 706	+ 706
.7	- 54	- 58	- 153	- 655	- 96	+ 1,320	+ 1,554	+ 1,554
.8	- 80	- 84	- 400	- 2,100	-180	+ 660	+ 777	+ 777
.9	-176	-180	-1500	-18,000	-934	+ 240	+ 282	+ 282
1.0	-400	-404				-12,100	-14,200	-14,200
BLOCK						BOTTOM		
.5	+ 10	0	- 540	0	0	- 4,440	- 5,220	- 5,220
.6	- 10	- 20	- 20	- 125	- 6	+ 600	+ 706	+ 706
.7	- 16	- 26	- 166	- 289	- 26	0	0	0
.8	- 44	- 54	- 380	- 1,350	- 98	+ 360	+ 424	+ 424
.9	- 89	- 99	- 500	9,900	-573	+ 200	+ 235	+ 235
1.0	-152	-162				- 4,860	- 5,770	- 5,770

\*, \*\*: For explanation see bottom of page 88

17

Table - Tabulation of Data Taken from the Curves, Figs 19 to 26, for the Computation of Stress Relieved in Splitting and slicing of Blocks

BLOCK 2						TOP		
Fraction of thickness, $a$	Cumulative relaxation in splitting & slicing, $e''$	$e'' - e''_0$	Slope, $\frac{de''}{da}$	$\frac{e'' - e''_0}{(1-a)^2}$	$\int_0^a \frac{e'' - e''_0}{(1-a)^2} \cdot da$	Computed stress, $S''$	Corrected tangential stress, $S''_T$ *	Corrected radial stress, $S''_R$ **
.5	- 70	0	-228	0		+ 960	+1,130	-14,500
.6	- 94	- 24	-247	- 150	- 7	+1,422	+1,675	- 2,400
.7	-122	- 52	-283	- 577	- 42	+1,480	+1,740	- 400
.8	-156	- 86	-385	- 2,150	-157	+ 990	+1,165	+ 2,500
.9	-206	-136	-680	-13,600	-807	-1,270	-1,495	+ 800
1.0	-300	-230				-6,900	-8,100	- 4,800
BLOCK						BOTTOM		
.5	- 32	0	+ 76	0		+ 960	+1,130	-14,500
.6	- 25	+ 7	+ 45	+ 44	+ 2	+ 42	+ 50	+ 5,300
.7	- 23	+ 9	- 40	+ 100	+ 9.3	- 618	- 727	+ 8,800
.8	- 42	- 10	-270	- 250	+ 4.2	- 555	- 653	+ 6,600
.9	- 72	- 40	-300	- 400	- 28.4	-2,500	-2,940	- 2,400
1.0	-106	- 74				-2,220	-2,500	-12,200

\*, \*\*: For explanation see bottom of page 88



18

Table - Tabulation of Data Taken from the Curves, Figs 19 to 26, for the Computation of Stress Relieved in Splitting and slicing of Blocks

BLOCK 3						TOP		
Fraction of thickness, a	Cumulative relaxation in splitting & slicing, e''	e'' - e'' <sub>0</sub>	Slope, $\frac{de''}{da}$	$\frac{e'' - e''_0}{(1-a)^2}$	$\int_a^1 \frac{e'' - e''_0}{(1-a)^2} \cdot da$	Computed stress, S''	Corrected tangential stress, S''*	Corrected radial stress, S''**
.5	- 60	0	-1,120	0		- 6,300	- 7,410	-22,200
.6	-170	-110	-1,120	- 687	- 28	+ 80	+ 941	- 4,600
.7	-260	-200	- 800	- 2,220	- 167	+ 4,341	+ 5,100	- 2,300
.8	-292	-232	- 84	- 5,800	- 524	+ 3,940	+ 4,640	+ 2,700
.9	-294	-234	0	-23,400		-14,280	-16,800	+ 2,100
1.0	-294	-234	0		-2,864	- 7,000	- 8,230	- 4,200
BLOCK						BOTTOM		
.5	- 50	0	-1,040	0		- 6,450	-7,600	-22,200
.6	- 90	- 40	- 132	- 250	- 125	+ 1,920	+ 2,260	+ 5,000
.7	-100	- 50	- 146	- 556	- 51.5	+ 1,120	+ 1,380	+ 0,500
.8	-123	- 73	- 344	- 1,825	- 150	+ 300	+ 353	+ 7,800
.9	-188	-138	-1,020	-13,800	-1,380	- 6,600	+ 7,760	- 3,400
1.0	-300	-250				- 7,500	- 8,820	-16,400

\*, \*\*: For explanation see bottom of page 88



19

Table - Tabulation of Data Taken from the Curves, Figs 19 to 26, for the Computation of Stress Relieved in Splitting and slicing of Blocks

B L O C K 4					T O P			
Fraction of thickness, a	Cumulative relaxation in splitting & slicing, e''	e'' - e'' <sub>0</sub>	Slope, $\frac{de''}{da}$	$\frac{e'' - e''_0}{(1-a)^2}$	$\int_0^a \frac{e'' - e''_0}{(1-a)^2} \cdot da$	Computed stress, S''	Corrected tangential stress, S'' <sub>T</sub> *	Corrected radial stress, S'' <sub>R</sub> **
.5	+104	0	+488	+ 0		-1,920	-2,260	-25,000
.6	+124	+ 20	+ 22	+ 125	+ 6	-4,690	-5,520	- 5,600
.7	+134	+ 30	-162	+ 334	+ 28.5	-3,860	-4,540	- 3,350
.8	+136	+ 32	+360	+ 800	+ 80	+ 240	+ 282	+ 2,000
.9	+182	+ 78	+680	+7,800	+465	+1,950	+2,300	+ 3,600
1.0	+252	+448				+4,440	+5,220	+ 400
B L O C K					B O T T O M			
.5	- 60	0	-840	0		-2,040	-2,400	-25,000
.6	-101	- 41	- 66	- 390	- 23	+4,284	+5,050	+ 1,000
.7	- 91	- 31	+182	- 344	- 57	+2,976	+3,500	+ 8,400
.8	- 79	- 19	- 60	- 475	- 92	- 72	- 85	+ 6,600
.9	-104	- 44	-360	-4,400	-310	-1,280	-1,510	- 2,200
1.0	-130	- 70				-2,100	-2,470	-18,000

\*, \*\*: For explanation see bottom of page 88

Table - Tabulation of Data Taken from the Curves, Figs 19 to 26, for the Computation of Stress Relieved in Splitting and slicing of Blocks

B L O C K 5					T O P			
Fraction of thickness, a	Cumulative relaxation in splitting & slicing, e <sup>''</sup>	e <sup>''</sup> - e <sup>''0</sup>	Slope, $\frac{de''}{da}$	$\frac{e'' - e''0}{(1-a)^2}$	$\int_0^a \frac{e'' - e''0}{(1-a)^2} \cdot da$	Computed stress, S <sup>''</sup>	Corrected tangential stress, S <sup>''*</sup>	Corrected radial stress, S <sup>''**</sup>
.5	-130	0	-2,110	0		-11,625	-13,700	-23,400
.6	-254	-124	- 496	- 775	- 39	+ 5,640	+ 6,630	- 5,650
.7	-278	-148	- 54	- 1,645	- 161	+ 5,250	+ 6,170	- 2,570
.8	-272	-142	+ 190	- 3,550	- 392	+ 1,380	+ 1,620	+ 1,450
.9	-246	-116	+ 296	-11,600	-1,147	- 5,200	- 6,120	+ 4,800
1.0	-214	- 84				- 2,520	- 2,960	+ 2,500
B L O C K					B O T T O M			
.5	-110	0	-1,950	0		-11,625	-13,700	-23,400
.6	-270	-160	- 810	- 1,000	- 50	+ 4,680	+ 5,500	- 1,900
.7	-324	-214	- 302	- 2,380	- 184	+ 6,990	+ 8,230	+ 6,500
.8	-346	-236	- 138	- 5,900	- 560	+ 2,886	+ 3,370	+ 6,000
.9	-354	-244	- 32	-24,400	-2,075	- 6,120	- 7,200	- 1,200
1.0	-355	-245				- 7,350	- 8,650	-17,700

\*, \*\*: For explanation see bottom of page 88



21

Table - Tabulation of Data Taken from the Curves, Figs 19 to 26, for the Computation of Stress Relieved in Splitting and slicing of Blocks

BLOCK 6						TOP		
Fraction of thickness, a	Cumulative relaxation in splitting & slicing, e <sup>"</sup>	e <sup>"</sup> - e <sup>"<sub>0</sub></sup>	Slope, $\frac{de''}{da}$	$\frac{e'' - e''_0}{(1-a)^2}$	$\int_0^a \frac{e'' - e''_0}{(1-a)^2} \cdot da$	Computed stress, S <sup>"</sup>	Corrected tangential stress, S <sup>"*</sup>	Corrected radial stress, S <sup>"**</sup>
.5	+384	0	- 864	0		-19,000	-22,360	-14,000
.6	+296	- 88	- 864	- 550	- 21	- 3,252	- 3,830	- 5,800
.7	+208	-176	- 850	-1,955	- 137	0	0	- 2,600
.8	+172	-212	0	-5,300	- 467	+ 6,138	+ 7,210	+ 700
.9	+178	-206	+ 104	-20,600	-1,762	+ 3,330	+ 3,920	+ 7,600
1.0	+198	-186				- 5,670	- 6,660	+ 5,000
BLOCK						BOTTOM		
.5	+304	0	-1,536	0		-19,140	-22,550	-14,000
.6	+184	-120	-1,188	- 750	- 32	- 8,600	-10,110	- 4,700
.7	+ 64	-240	-1,136	- 2,770	- 201	+ 2,760	+ 3,250	+ 850
.8	- 40	-344	- 960	- 8,600	- 768	+ 6,240	+ 7,340	+ 3,300
.9	-130	-434	- 816	-43,400	-3,368	+ 210	+ 318	+ 4,250
1.0	-208	-512				-15,450	-18,200	-12,500

\*, \*\*: For explanation see bottom of page 88



Table - Tabulation of Data Taken from the Curves, Figs 19 to 26, for the Computation of Stress Relieved in Splitting and slicing of Blocks

B L O C K 7						T O P		
Fraction of thickness, a	Cumulative relaxation in splitting & slicing, e''	e'' - e'' <sub>0</sub>	Slope, $\frac{de''}{da}$	$\frac{e'' - e''_0}{(1-a)^2}$	$\int_0^a \frac{e'' - e''_0}{(1-a)^2} \cdot da$	Computed stress, S''	Corrected tangential stress, S''*	Corrected radial stress, S''**
.5	-108	0	-494	0		- 345	- 406	-9,000
.6	-168	- 60	-640	- 375	- 13	+1,333	+1,570	-6,800
.7	-234	-126	-392	- 1,400	- 95	+3,950	+4,650	-3,000
.8	-266	-158	-144	- 3,950	- 335	+2,400	+2,820	+2,200
.9	-254	-146	+300	-14,600	-1,267	-4,110	-4,840	+4,800
1.0	-212	-104				-3,120	-3,670	+ 500
B L O C K						B O T T O M		
.5	-100	0	-428	0		- 330	- 390	-9,000
.6	-132	- 32	-284	- 200	- 9	+1,890	+2,220	-4,470
.7	-158	- 58	-240	- 645	- 49	+1,605	+1,890	-1,100
.8	-174	- 74	- 98	- 1,850	- 161	+ 600	+ 706	+1,600
.9	-178	- 78	0	7,800	- 651	-3,000	-3,530	+5,000
1.0	-178	- 78				-2,340	-2,750	-4,500

\*, \*\*: For explanation see bottom of page 88

23

Table - Tabulation of Data Taken from the Curves, Figs 19 to 26, for the Computation of Stress Relieved in Splitting and slicing of Blocks

B L O C K 8						T O P		
Fraction of thickness, a	Cumulative relaxation in splitting & slicing, e"	e" - e"o	Slope, $\frac{de''}{da}$	$\frac{e'' - e''_0}{(1-a)^2}$	$\int_0^a \frac{e'' - e''_0}{(1-a)^2} \cdot da$	Computed stress, S"	Corrected tangential stress, S <sup>**</sup> <sub>T</sub>	Corrected radial stress, S <sup>**</sup> <sub>R</sub>
.5	- 92	- 0	-296	0		+ 420	+ 495	-3,100
.6	-122	- 30	-296	- 167	- 8	+1,295	+1,525	-1,000
.7	-152	- 60	-280	- 667	- 41	+1,713	+2,020	0
.8	-156	- 64	+116	-1,600	-150	+ 888	+1,045	+1,350
.9	-124	- 32	+342	-3,200	-377	-2,550	-3,000	- 200
1.0	- 94	- 2				- 60	- 70	-2,200
B L O C K						B O T T O M		
.5	-100	- 0	-364	0		+ 390	+ 460	-3,100
.6	-145	- 45	-590	- 281	- 13	+ 600	+ 706	-1,400
.7	-184	- 84	-242	- 930	- 68	+2,790	+3,285	- 400
.8	-194	- 94	+ 76	-2,350	-198	+1,692	+1,891	- 400
.9	-159	- 59	+380	-5,900	-680	-3,780	-4,450	- 100
1.0	-122	- 22				- 660	- 777	-6,300

\*, \*\*: For explanation see bottom of page 88

Table - Tabulation of Data Taken from the Curves, Figs 19 to 26, for the Computation of Stress Relieved in Splitting and slicing of Blocks

BLOCK 8 <sub>1</sub>						TOP		
Fraction of thickness, a	Cumulative relaxation in splitting & slicing, e <sup>''</sup>	e <sup>''</sup> - e <sup>''0</sup>	Slope, $\frac{de''}{da}$	$\frac{e'' - e''0}{(1-a)^2}$	$\int_0^a \frac{e'' - e''0}{(1-a)^2} \cdot da$	Computed stress, S <sup>''</sup>	Corrected tangential stress, S <sup>''*</sup>	Corrected radial stress, S <sup>''**</sup>
.5	+122	0	+136	0		-2,730	-3,215	-3,100
.6	+132	+ 10	+ 32	+ 625	+ 3	-2,580	-3,040	-1,000
.7	+129	+ 7	+ 76	+ 773	+ 9	- 501	- 590	0
.8	+154	+ 32	+408	+ 800	+ 53	+ 954	+1,120	+1,350
.9	+206	+ 84	+771	+8,400	+433	+2,190	+2,580	- 200
1.0	+266	+144				+4,320	+5,080	-2,200
BLOCK						BOTTOM		
.5	+116	0	+ 88			-2,730	-3,215	-3,100
.6	+122	+ 6	+ 20	+ 374	+ 2	-2,190	-2,580	-1,400
.7	+124	+ 8	+100	+ 89	+ 8	- 450	- 580	- 400
.8	+145	+ 29	+324	+ 725	+ 54	+ 930	+1,095	- 400
.9	+176	+ 60	+388	+6,000	+390	+2,300	+3,710	- 100
1.0	+220	+104				+3,120	+3,670	-6,300

\*, \*\*: For explanation see bottom of page 88



Table - Tabulation of Data Taken from the Curves, Figs 19 to 26, for the Computation of Stress Relieved in Splitting and slicing of Blocks

BLOCK 9					TOP			
Fraction of thickness, a	Cumulative relaxation in splitting & slicing, e''	e'' - e'' <sub>0</sub>	Slope, $\frac{de''}{da}$	$\frac{e'' - e''_0}{(1-a)^2}$	$\int_0^a \frac{e'' - e''_0}{(1-a)^2} \cdot da$	Computed stress, S''	Corrected tangential stress, S''*	Corrected radial stress, S''**
.5	-67	0	-152	0		+ 900	+1,060	-3,500
.6	-81	- 14	-144	- 87.5	- 4	+1,070	+1,260	-2,600
.7	-92	- 25	- 46	- 278	-21	+1,155	+1,360	-1,000
.8	-84	- 17	+260	- 850	-82	- 60	- 70	+1,200
.9	-45	+ 22	+382	+2,200	-78	-2,634	-3,100	+1,600
1.0	- 8	+ 59				+1,770	+2,080	-2,400
BLOCK					BOTTOM			
.5	-64	0	-120	0		+ 990	+1,160	-3,500
.6	-75	- 11	-104	- 68.8	- 3.4	+1,020	+1,200	-2,100
.7	-81	- 17	0	- 189	-14.6	+ 990	+1,160	-1,050
.8	-63	+ 1	+320	+ 50	-23.6	+ 60	+ 70	- 400
.9	-12	+ 52	+680	+5,200	+ 3	-2,940	-3,460	+1,700
1.0	+56	+120				+3,600	+4,240	-1,200

\*, \*\*: For explanation see bottom of page 88

26

Table - Tabulation of Data Taken from the Curves, Figs 19 to 26, for the Computation of Stress Relieved in Splitting and slicing of Blocks

BLOCK 91						TOP		
Fraction of thickness, a	Cumulative relaxation in splitting & slicing, e''	e'' - e'' <sub>0</sub>	Slope, $\frac{de''}{da}$	$\frac{e'' - e''_0}{(1-a)^2}$	$\int_0^a \frac{e'' - e''_0}{(1-a)^2} \cdot da$	Computed stress, S''	Corrected tangential stress, S''*	Corrected radial stress, S''**
.5	+ 65	0	-112	0		-2,655	-3,120	-3,500
.6	+ 60	- 5	- 20	- 31.2	- 1.5	- 936	-4,100	-2,600
.7	+ 60	- 5	+ 36	- 55.6	- 5.8	0	0	-1,000
.8	+ 73	+ 8	+260	+ 200	- 5.5	+ 645	+ 760	+1,200
.9	+123	+ 58	+670	+5,800	+314	+1,548	+1,820	+1,600
1.0	+190	+125				+3,750	+4,400	-2,400
BLOCK						BOTTOM		
.5	+ 74	0	- 48	0		-2,715	-3,210	-3,500
.6	+ 72	- 2	+ 12	- 12.5	- .6	-1,270	-1,500	-2,100
.7	+ 77	+ 3	+124	+ 33.4	+ .4	- 138	- 162	-1,050
.8	+100	+ 26	+308	+ 650	+ 24	+ 186	+ 219	- 400
.9	+140	+ 66	+460	+6,600	+389	+1,836	+2,160	+1,700
1.0	+188	+114				+3,420	+4,000	?

\*, \*\*: For explanation see bottom of page 88



27

Table - Tabulation of Data Taken from the Curves, Figs 19 to 26, for the Computation of Stress Relieved in Splitting and slicing of Blocks

BLOCK 10						TOP		
Fraction of thickness, a	Cumulative relaxation in splitting & slicing, e <sup>''</sup>	e <sup>''</sup> - e <sup>''0</sup>	Slope, $\frac{de''}{da}$	$\frac{e'' - e''0}{(1-a)^2}$	$\int_0^a \frac{e'' - e''0}{(1-a)^2} \cdot da$	Computed stress, S <sup>''</sup>	Corrected tangential stress, S <sup>''*</sup>	Corrected radial stress, S <sup>''**</sup>
.5	+108	0	+140	0		-2,460	-2,900	-8,000
.6	+118	+ 10	+ 70	+ 62.5	+ 3	-2,232	-2,625	-7,000
.7	+126	+ 18	+126	+ 200	+ 19	- 810	- 954	-3,000
.8	+149	+ 41	+370	+1,020	+ 69	+ 432	+ 510	+3,000
.9	+203	+ 95	+700	+9,500	+600	+2,640	+3,110	+4,000
1.0	+286	+178				+5,340	+6,290	+0,000
BLOCK						BOTTOM		
.5	+ 90	0	+ 76	0		-1,920	-2,260	-8,000
.6	+ 93	+ 3	- 12	+ 18.7	+ 1	-1,620	-1,910	-4,500
.7	+ 92	+ 2	+ 20	+ 22.2	+ 3	- 330	- 390	-3,500
.8	+103	+ 13	+228	+ 325	+ 16	+ 840	+ 990	-3,000
.9	+142	+ 52	+486	+5,200	+286	+1,860	+2,190	+3,000
1.0	+192	+102				+3,060	+3,600	

\*, \*\*: For explanation see bottom of page 88



Table - Tabulation of Data Taken from the Curves, Figs 19 to 26, for the Computation of Stress Relieved in Splitting and slicing of Blocks

BLOCK 101						TOP		
Fraction of thickness, a	Cumulative relaxation in splitting & slicing, e <sup>n</sup>	e <sup>n</sup> - e <sup>n</sup> <sub>0</sub>	Slope, $\frac{de^n}{da}$	$\frac{e^n - e^n_0}{(1-a)^2}$	$\int_0^a \frac{e^n - e^n_0}{(1-a)^2} \cdot da$	Computed stress, S <sup>n</sup>	Corrected tangential stress, S <sup>n*</sup>	Corrected radial stress, S <sup>n**</sup>
.5	+102	0	- 20	0		-3,180	-3,740	-8,000
.6	+100	- 2	- 20	- 12.5	- .6	-1,830	-2,155	-7,000
.7	+ 99	- 3	+ 32	- 33	- 3	- 351	- 413	-3,000
.8	+111	+ 9	+208	+ 225	+ 2	+ 804	+ 945	+3,000
.9	+140	+ 38	+370	+3,800	+00	+1,920	+2,260	+4,000
1.0	+190	+ 88				+2,640	+3,100	
BLOCK						BOTTOM		
.5	+104	0	- 4	0		-3,108	-3,740	-8,000
.6	+107	+ 3	+ 44	+ 18.7	+ 1	-1,776	-2,090	-4,300
.7	+118	+ 14	+200	+ 155	+ 9	- 340	- 400	-3,500
.8	+146	+ 42	+332	+1,050	+53	+ 42	+ 50	-3,000
.9	+190	+ 86	+550	+8,600	+533	+2,178	+2,560	+3,000
1.0	+252	+148				+4,440	+5,220	

\*, \*\*: For explanation see bottom of page 88

29

Table - Tabulation of Data Taken from the Curves, Figs 19 to 26, for the Computation of Stress Relieved in Splitting and slicing of Blocks

BLOCK 11						TOP		
Fraction of thickness, a	Cumulative relaxation in splitting & slicing, e''	e'' - e'' <sub>0</sub>	Slope, $\frac{de''}{da}$	$\frac{e'' - e''_0}{(1-a)^2}$	$\int_0^a \frac{e'' - e''_0}{(1-a)^2} \cdot da$	Computed stress, S''	Corrected tangential stress, S''*	Corrected radial stress, S''**
.5	+272	0	-1,504	0		-21,390		-25,100
.6	+198	- 74	- 288	- 463	- 23	- 4,692		- 5,520
.7	+188	- 84	0	- 933	- 93	- 2,810		- 3,310
.8	+194	- 78	+ 140	- 1,950	- 233	+ 1,758		+ 2,065
.9	+220	- 52	+ 392	- 5,200	- 590	+ 2,844		+ 3,350
1.0	+274	+ 2				+ 60		+ 70
BLOCK						BOTTOM		
.5	+142	0	-2,480	0		-20,910		-24,680
.6	- 52	-196	-1,200	- 1,225	- 60	+ 1,400		+ 1,650
.7	-178	-320	- 872	- 3,560	- 298	+ 7,548		+ 8,880
.8	-248	-390	- 632	- 9,750	- 960	+ 5,860		+ 6,800
.9	-310	-452	- 588	-45,200	-3,460	- 1,960		- 2,300
1.0	-368	-510				-15,300		-18,000

\*, \*\*: For explanation see bottom of page 88

30

Table - Tabulation of Data Taken from the Curves, Figs 19 to 26, for the Computation of Stress Relieved in Splitting and slicing of Blocks

BLOCK 12						TOP		
Fraction of thickness, a	Cumulative relaxation in splitting & slicing, e''	e'' - e'' <sub>0</sub>	Slope, $\frac{de''}{da}$	$\frac{e'' - e''_0}{(1-a)^2}$	$\int_0^a \frac{e'' - e''_0}{(1-a)^2} \cdot da$	Computed stress, S''	Corrected tangential stress, S''*	Corrected radial stress, S''**
.5	+352	0	- 328	0		-14,160		-16,650
.6	+344	- 8	+ 364	- 50	- 2.5	- 4,650		- 5,470
.7	+388	+ 36	+ 364	+ 400	+ 10	- 3,168		- 3,730
.8	+424	+ 76	+ 364	+ 1,900	+ 125	+ 440		+ 518
.9	+468	+114	+ 428	+11,400	+ 790	+ 7,020		+ 8,260
1.0	+512	+160				+ 4,800		+ 5,650
BLOCK						BOTTOM		
.5	+276	0	- 920	0		-14,040		-16,060
.6	+200	- 76	- 608	- 475	- 23	- 3,970		- 4,670
.7	+144	-132	- 424	- 1,470	-120	+ 1,800		+ 2,120
.8	+ 94	-182	- 640	- 4,550	-420	+ 3,550		+ 4,060
.9	+ 4	-272	-1,160	-27,200	-900	+ 2,670		+ 3,140
1.0	-160	-436				-13,000		-15,300

\*, \*\*: For explanation see bottom of page 88



31

Table - Tabulation of Data Taken from the Curves, Figs 19 to 26, for the Computation of Stress Relieved in Splitting and slicing of Blocks

B L O C K 13					T O P			
Fraction of thickness, a	Cumulative relaxation in splitting & slicing, e''	e''-e'' <sub>0</sub>	Slope, $\frac{de''}{da}$	$\frac{e''-e''_0}{(1-a)^2}$	$\int_a^1 \frac{e''-e''_0}{(1-a)^2} \cdot da$	Computed stress, S''	Corrected tangential stress, S''*	Corrected radial stress, S''**
.5	+272	0	+120	0		-7,680		-9,040
.6	+282	+ 10	+ 64	+ 62.5	+ 3	-5,340		-6,280
.7	+284	+ 12	- 80	+ 133	+ 13	-2,613		-3,075
.8	+243	- 35	-500	- 875	- 9	+1,900		+2,235
.9	+192	- 80	-500	-8,000	-452	+4,800		+5,650
1.0	+142	-130				-3,900		-4,600
B L O C K					B O T T O M			
.5	+244	0	-104	0		-7,680		-9,040
.6	+237	- 7	- 56	- 43.7	- 2	-4,044		-4,750
.7	+232	- 12	- 30	- 133	- 11	- 924		-1,085
.8	+228	- 16	-164	- 400	- 36	+1,540		+1,810
.9	+186	- 58	-532	-5,800	-336	+4,134		+4,860
1.0	+128	-116				-3,480		-4,100

\*, \*\*: For explanation see bottom of page 88

32

Table - Tabulation of Data Taken from the Curves, Figs 19 to 26, for the Computation of Stress Relieved in Splitting and slicing of Blocks

BLOCK 137					TOP			
Fraction of thickness, a	Cumulative relaxation in splitting & slicing, e <sup>''</sup>	e <sup>''</sup> -e <sup>''0</sup>	Slope, $\frac{de''}{da}$	$\frac{e''-e''0}{(1-a)^2}$	$\int_0^a \frac{e''-e''0}{(1-a)^2} \cdot da$	Computed stress, S <sup>''</sup>	Corrected tangential stress, S <sup>''*</sup>	Corrected radial stress, S <sup>''**</sup>
.5	+278	0	+142	0		-7,545		-8,870
.6	+286	+ 8	0	+ 50	+ 1.5	-5,850		-6,880
.7	+282	+ 4	- 76	+ 44.5	+ 2.5	-2,500		-2,940
.8	+273	- 5	+ 20	- 125	- 1	+1,800		+2,120
.9	+300	+ 22	+356	+2,200	- 89	+3,310		+3,900
1.0	+334	+ 56				+1,680		1.975
BLOCK					BOTTOM			
.5	+243	0	- 80	0		-7,365		-8,665
.6	+241	- 2	+ 40	- 12.5	- .5	-3,612		-4,250
.7	+240	- 3	- 52	- 33	- 3	- 978		-1,150
.8	+229	- 14	-292	- 350	- 22	+1,236		+1,455
.9	+180	- 63	-584	-6,300	-322	+4,485		+5,270
1.0	+104	-139				-4,170		4,900

\*, \*\*: For explanation see bottom of page 88

33

Table - Tabulation of Data Taken from the Curves, Figs 19 to 26, for the Computation of Stress Relieved in Splitting and slicing of Blocks

BLOCK 14						TOP		
Fraction of thickness, a	Cumulative relaxation in splitting & slicing, e <sup>"</sup>	e <sup>"</sup> -e <sup>"<sub>0</sub></sup>	Slope, $\frac{de''}{da}$	$\frac{e''-e''_0}{(1-a)^2}$	$\int_a^1 \frac{e''-e''_0}{(1-a)^2} \cdot da$	Computed stress, S <sup>"</sup>	Corrected tangential stress, S <sup>"*</sup>	Corrected radial stress, S <sup>"**</sup>
.5	+ 36	0	-180	0		-2,310		-2,720
.6	+ 22	- 14	- 92	- 87.5	- 4	- 408		- 480
.7	+ 9	- 27	-166	- 300	- 23	+ 108		+ 127
.8	- 6	- 42	0	-1,500	- 98	+1,020		+1,200
.9	0	- 36	+104	-3,600	-348	- 144		- 170
1.0	+ 16	- 20				- 600		- 700
BLOCK						BOTTOM		
.5	+ 44	0	-116	0		-2,310		-2,720
.6	+ 32	- 12	-128	- 75	- 4	-1,080		-1,270
.7	+ 18	- 26	-160	- 290	- 22	- 90		- 106
.8	- 2	- 46	-240	-1,150	- 92	0		0
.9	- 40	- 84	-520	-8,400	-560	0		0
1.0	-104	-148				-5,440		-6,400

\*, \*\*: For explanation see bottom of page 88



Table - Tabulation of Data Taken from the Curves, Figs 19 to 26, for the Computation of Stress Relieved in Splitting and slicing of Blocks

BLOCK 15						TOP		
Fraction of thickness, a	Cumulative relaxation in splitting & slicing, e"	e" - e"°	Slope, $\frac{de''}{da}$	$\frac{e'' - e''^0}{(1-a)^2}$	$\int_0^a \frac{e'' - e''^0}{(1-a)^2} da$	Computed stress, S"	Corrected tangential stress, S <sub>T</sub> **	Corrected radial stress, S <sub>R</sub> **
.5	+ 28	0	- 32	0		-1,110		-1,310
.6	+ 14	- 14	- 32	97.5	- 4	- 24		- 28
.7	+ 11	- 17	- 22	189	- 17	+ 276		+ 325
.8	+ 12	- 16	+ 44	400	- 45	+ 438		+ 515
.9	+ 35	+ 7	+216	700	- 27	+ 160		+ 188
1.0	+ 64	+ 36				+1,080		+1,270
BLOCK						BOTTOM		
.5	+ 26	0	- 48	0		-1,110		-1,310
.6	+ 14	- 12	-188	75	- 3.5	- 978		-1,150
.7	- 6	- 32	-220	356	- 23	+ 170		+ 200
.8	- 32	- 58	-314	1,450	-108	+ 762		+ 896
.9	- 82	-108	-716	10,800	-708	- 492		+ 580
1.0	-160	-180				-5,580		-6,570

\*, \*\*: For explanation see bottom of page 88

Table - Tabulation of Data Taken from the Curves, Figs 19 to 26, for the Computation of Stress Relieved in Splitting and slicing of Blocks

BLOCK 16					TOP			
Fraction of thickness, a	Cumulative relaxation in splitting & slicing, e"	e" - e"°	Slope, $\frac{de''}{da}$	$\frac{e'' - e''^0}{(1-a)^2}$	$\int_a^1 \frac{e'' - e''^0}{(1-a)^2} \cdot da$	Computed stress, S"	Corrected tangential stress, S <sub>T</sub> **	Corrected radial stress, S <sub>R</sub> **
.5	+86	0	- 16	0		-2,670		-3,140
.6	+79	- 7	-100	- 43.7	- 2	-1,776		-2,090
.7	+68	-18	-100	- 200	- 14	- 696		- 820
.8	+62	-24	0	- 600	- 54	+ 996		+1,170
.9	+62	-24	0	-2,400	-204	+1,160		+1,365
1.0	+62	-24				- 720		- 850
BLOCK					BOTTOM			
.5	+88	0	0	0		-2,670		-3,140
.6	+86	- 2	- 54	- 12.5	- .5	-1,830		-2,175
.7	+72	-16	-196	- 178	- 9	- 711		- 836
.8	+47	-41	-272	-1,025	- 69	- 282		- 332
.9	+22	-66	-228	-6,600	-448	+1,164		+1,370
1.0	+ 2	-86				-2,580		-3,030

\*, \*\*: For explanation see bottom of page 88

36

Table - Tabulation of Data Taken from the Curves, Figs 19 to 26, for the Computation of Stress Relieved in Splitting and slicing of Blocks

BLOCK 161						TOP		
Fraction of thickness, a	Cumulative relaxation in splitting & slicing, e''	e'' - e'' <sub>0</sub>	Slope, $\frac{de''}{da}$	$\frac{e'' - e''_0}{(1-a)^2}$	$\int_a^1 \frac{e'' - e''_0}{(1-a)^2} \cdot da$	Computed stress, S''	Corrected tangential stress, S''*	Corrected radial stress, S''**
.5	+80	0	- 16	0		-2,475		-2,910
.6	+80	0	- 28	0	0	-1,572		-1,850
.7	+72	- 8	-112	- 89	- 4	- 585		- 688
.8	+64	-16	- 56	- 400	- 28	+ 786		+ 925
.9	+60	-20	- 10	-2,000	-144	+1,338		+1,575
1.0	+60	-20				- 600		- 705
BLOCK						BOTTOM		
.5	+83	0	0	0		-2,535		-2,980
.6	+84	+ 1	+ 30	+ 6.5	0	-1,410		-1,660
.7	+90	+ 7	+ 48	+ 78	+ 4	- 621		- 730
.8	+87	+ 4	-104	+ 100	+ 12	+ 144		+ 170
.9	+70	-13	-224	-1,300	+ 38	+1,587		+1,870
1.0	+42	-41				-1,230		-1,440

\*, \*\*: For explanation see bottom of page 88



The data for the first six columns in Tables 16-36 are taken from the Figures 19-26, and  $S''$  is computed by applying these data in Tables 16-36 in the equation (2), (Referencel2, equation (23))

$$S_a'' = E \left[ \frac{1-a}{2} \frac{de''}{da} - 2(e'' - e''_0) + 3(1-a) \int_{.5}^a \frac{e_t'' - e_g''}{(1-a)^2} da + (5a - 4) e_t'' + (1-a) e_b'' \right] \quad (2a)$$

a changes from .5 up to 1. for  $a = 1$ .

$$S_{1.}'' = 30(e'' - e''_0)$$

The stresses  $S_a''$  thus found must be corrected for the fact that the length of blocks were only one and one-half times the thickness, instead of twice the thickness. This correction consists of multiplying calculated stresses by  $\frac{100}{100-15}$ .

In tables representing blocks one to ten, data showing radial stresses have been interpolated from Figures 28, 29, and 30 drawn from the data obtained from blocks eleven to sixteen. Figures 27 is used to determine radial relaxations corresponding to the tangential blocks Numbers 1 to 10 from the data of blocks 11 to 16.

\*This correction consists of multiplying the calculated stress  $S_a''$  by  $\frac{100}{100-15}$  for the fact that the length block is one and a half times the thickness instead of two<sup>(12)</sup>.

\*\*These radial stresses for blocks 1 to 10 were intrapolated from the curve of radial stresses computed in blocks 11 to 16, Figures 28, 29 and 30.

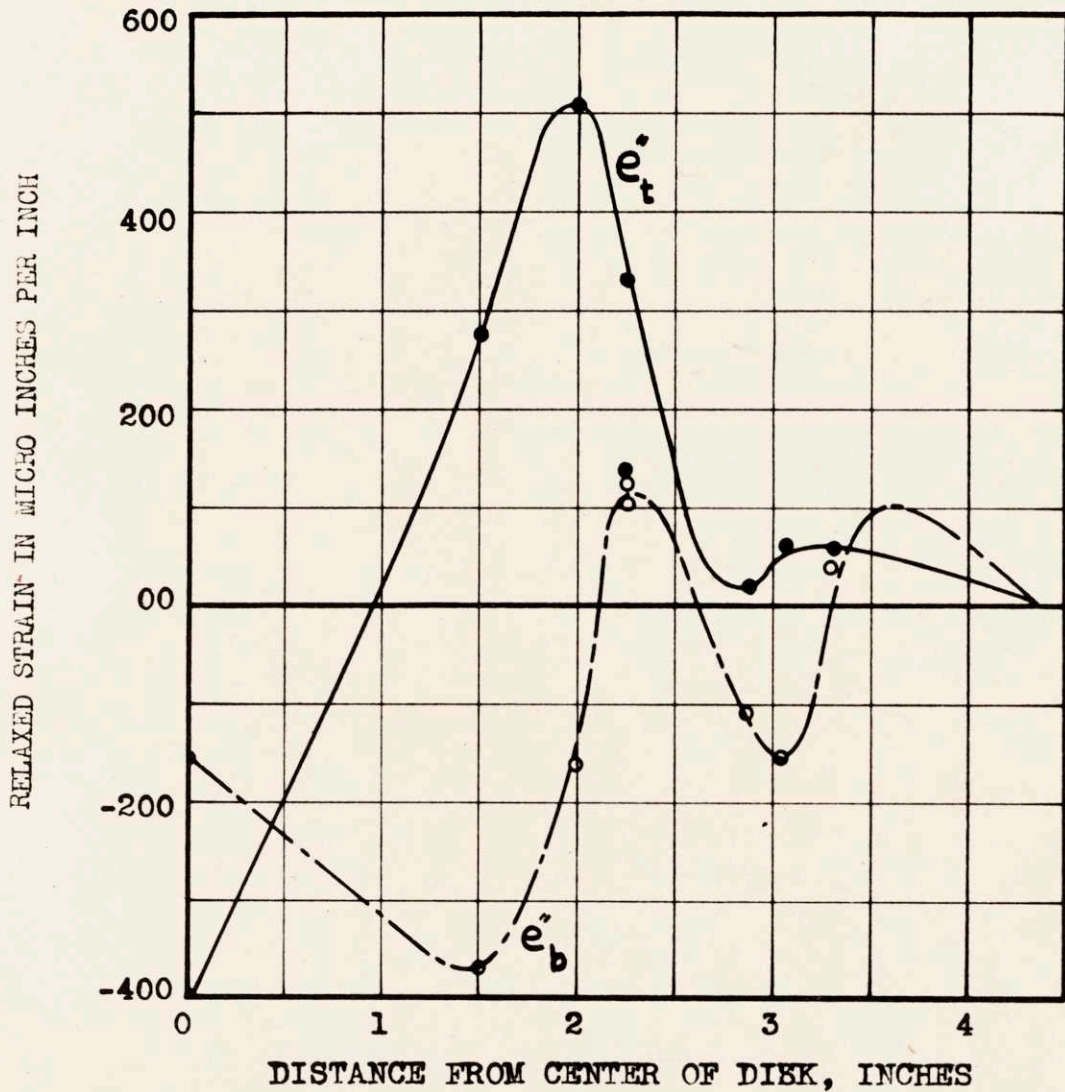


Fig. 27 - The Radial Cumulative Strains Relaxed in Splitting and Slicing of Radial Blocks, No. 11 to 16. These Curves are used to Determine Radial Relaxations Corresponding to the Tangential Blocks No. 1 to 10

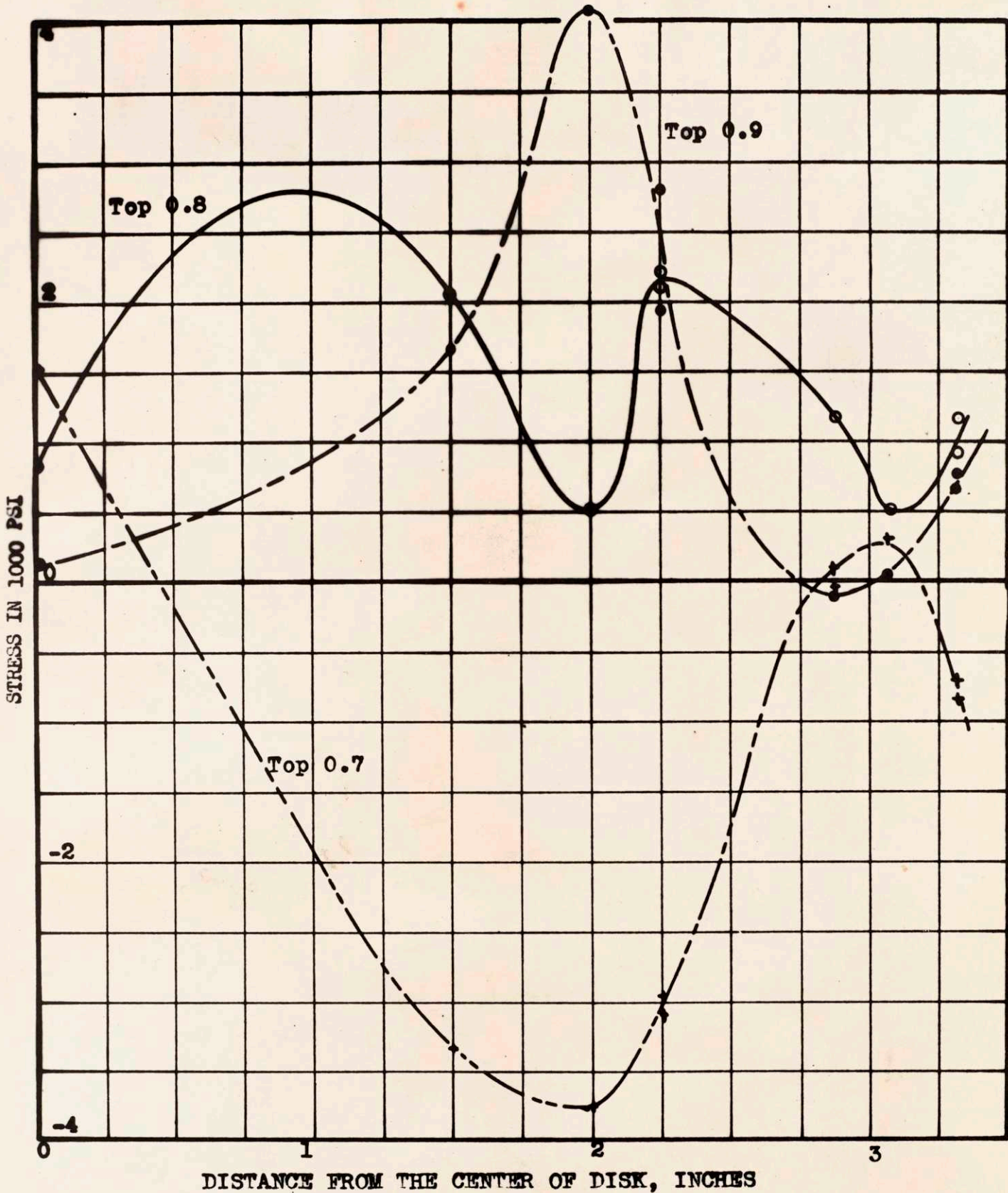
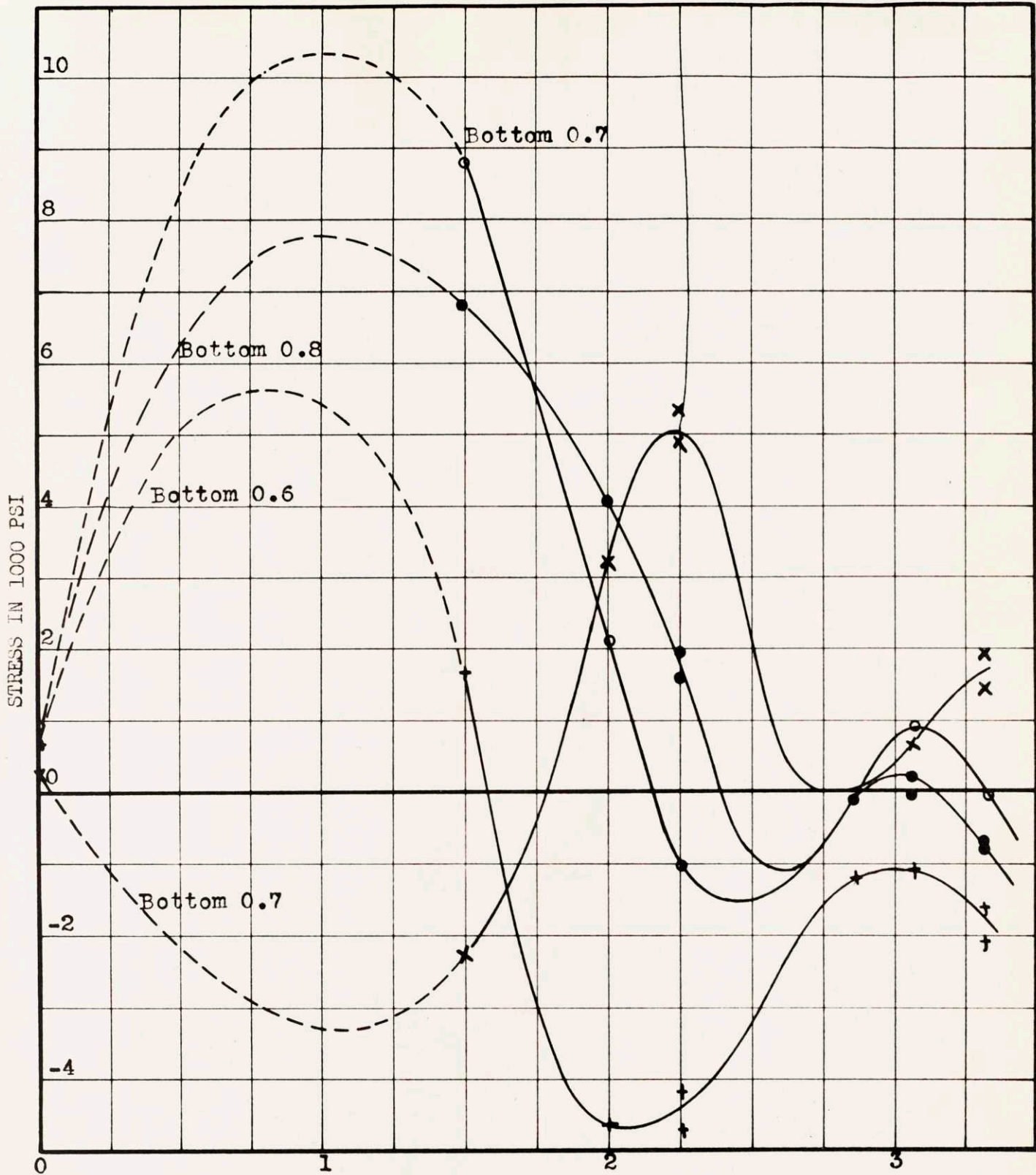


Fig. 28 - Relaxed Radial Stresses due to Slicing of Blocks 11 to 16 at Different Fractions of Thickness





DISTANCE FROM THE CENTER OF DISK, INCHES

Fig. 29 - Relaxed Radial Stresses due to Slicing of Blocks 11 to 16 at Different Fractions of Thickness

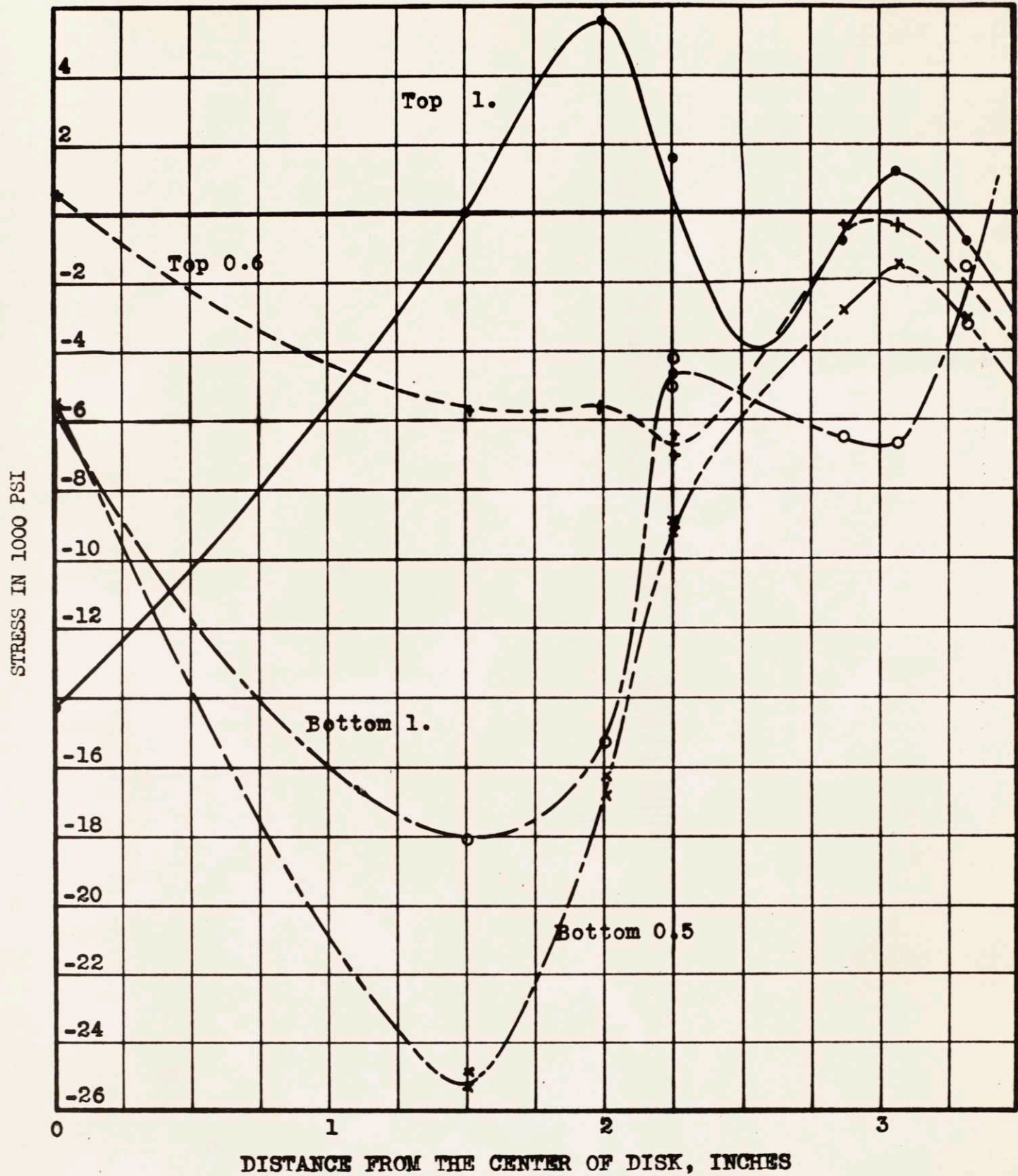


Fig. 30 - Relaxed Radial Stresses due to Slicing of Blocks 11 to 16 at Different Fractions of Thickness



Thus we have average stress for each block and stress remaining at each layer of the individual blocks after they were cut loose from the disk. The stresses measured in these two steps are added up in Figures 6-9 to obtain true stress distribution through the thickness for blocks 1 to 10. True radial and tangential stresses along the radius for fractions of thickness 1. (top), 0.8, 0.6, 0.5, 0.4, 0.2 and 0.0 (bottom) are shown in Figures 31 to 34. From these curves, stress in the thickness direction will be computed.

DETERMINATION OF STRESS IN THE DIRECTION OF THE THICKNESS  
FROM THE VARIATION OF STRESSES IN RADIAL AND TANGENTIAL  
DIRECTIONS IN THE DISK

Solution of the problem of determination of stress in the direction of the thickness from the variation of stresses in radial and tangential directions in the disk is carried out in OSRD Report No. 3580, Serial No. M-244, Page 33-38 by D. Rosenthal, J. R. Clark, S. B. Maloof, and J. T. Norton; and, taking into account the rotational symmetry in the disk, the differential equations below are arrived at

$$\frac{d^2S_z}{dz^2} = \frac{d^2S_r}{dr^2} + \frac{2}{r} \frac{dS_r}{dr} - \frac{1}{r} \frac{dS_t}{dr} \quad (3)$$

is for any point along the radius and

$$\frac{d^2S_z}{dz^2} = 3 \frac{d^2S_r}{dr^2} - \frac{dS_t}{dr^2} \quad (4)$$

for the center of the disk.

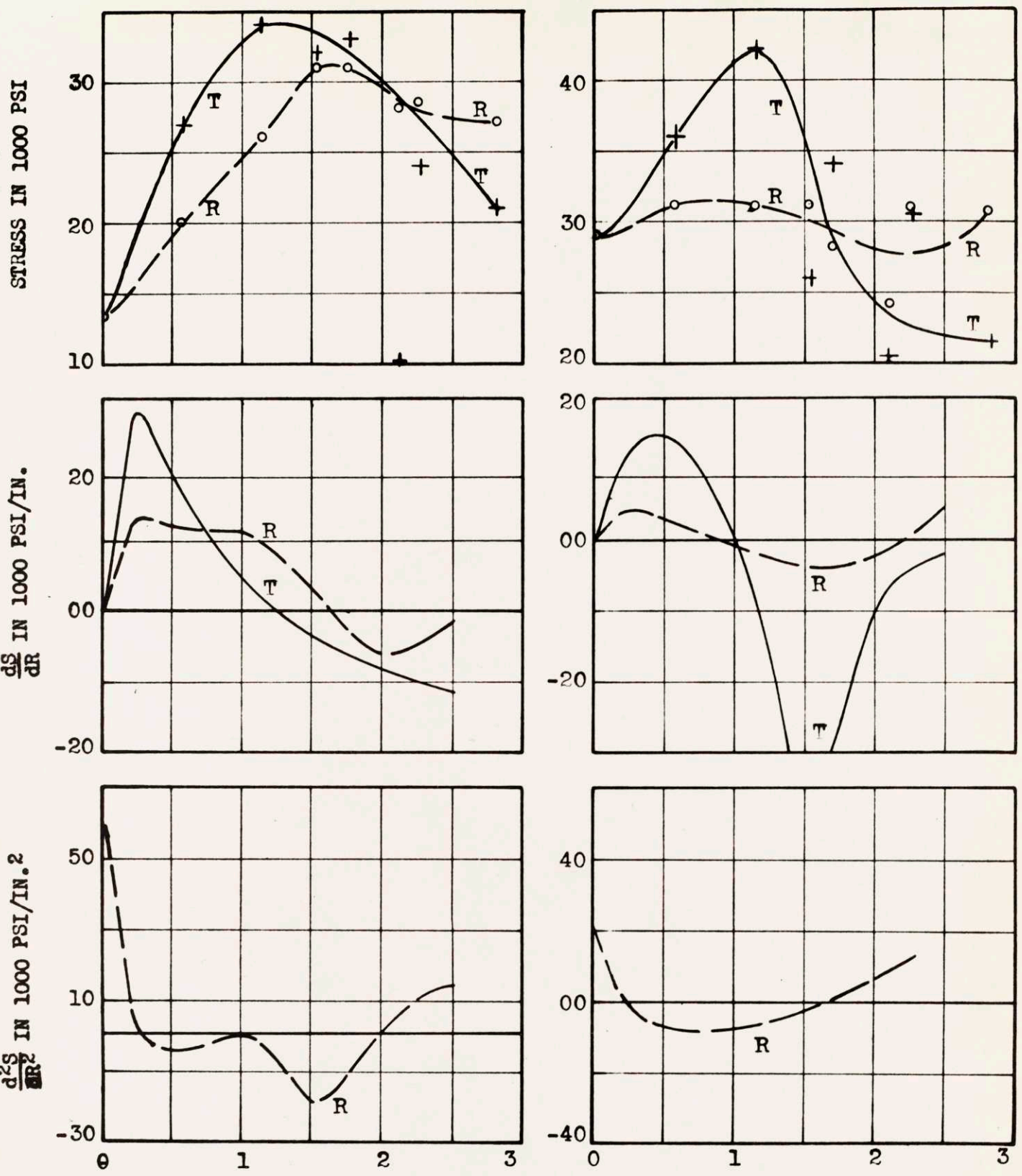


In equations (3) and (4)  $r$  = distance on the radius from the center of the disk to the point considered,  $S_r$  = radial stress in psi at the point considered,  $S_t$  = tangential stress in psi at the point considered;  $S_z$  = stress in the thickness direction, and  $z$  = distance in the thickness direction.

To solve these equations for  $S_z$ , for the fractions of thickness 1.(top), 0.8, 0.6, 0.5, 0.4, 0.2, 0.0 (bottom) true radial and tangential stresses from Figures 6 to 9 are plotted versus radius. Figures 31 to 34.

In Figures 31 to 34, top figure is stress  $S$  in pounds per square inch versus the radius  $R$  of the disk. The center figure is the first derivative (slopes),  $\frac{dS}{dR}$ , of the first curve in pounds per square inch per inch, and the third figure the second derivative,  $\frac{d^2S}{dR^2}$ , of the first curve, that is, slopes of the second curve. From these curves, values of  $\frac{dS}{dR}$ ,  $\frac{d^2S}{dR^2}$ , et cetera, are taken, Table No. 37, and replaced in the equations (3) and (4) to find the values of  $\frac{d^2S_z}{dz^2}$  for the locations 0, 1/2, 1, 1-1/2, and 2 inches from the center of the disk. The values of  $\frac{d^2S_z}{dz^2}$  are plotted versus the fraction of thickness of the disk, Figures 35 to 37, and integrated twice by the graphical method, to arrive at the stress distribution through the thickness of the metal in the thickness direction, Figures 35 to 37 and Figure 10.

On both faces of the disk, stress in the thickness direction must be zero. Therefore, both ends of the curve are connected with a straight line, and the stress in the third direction is measured



RADIUS R IN INCHES  
 Fraction of thickness : 1 (top)

RADIUS R IN INCHES  
 Fraction of thickness : .8

Fig. 31 - Successive Graphical Differentiation of Radial and Tangential Stresses in the Disk versus Radius for Fractions of Thickness 1. (top) and 0.8

R : radial stress  
 T : tangential stress



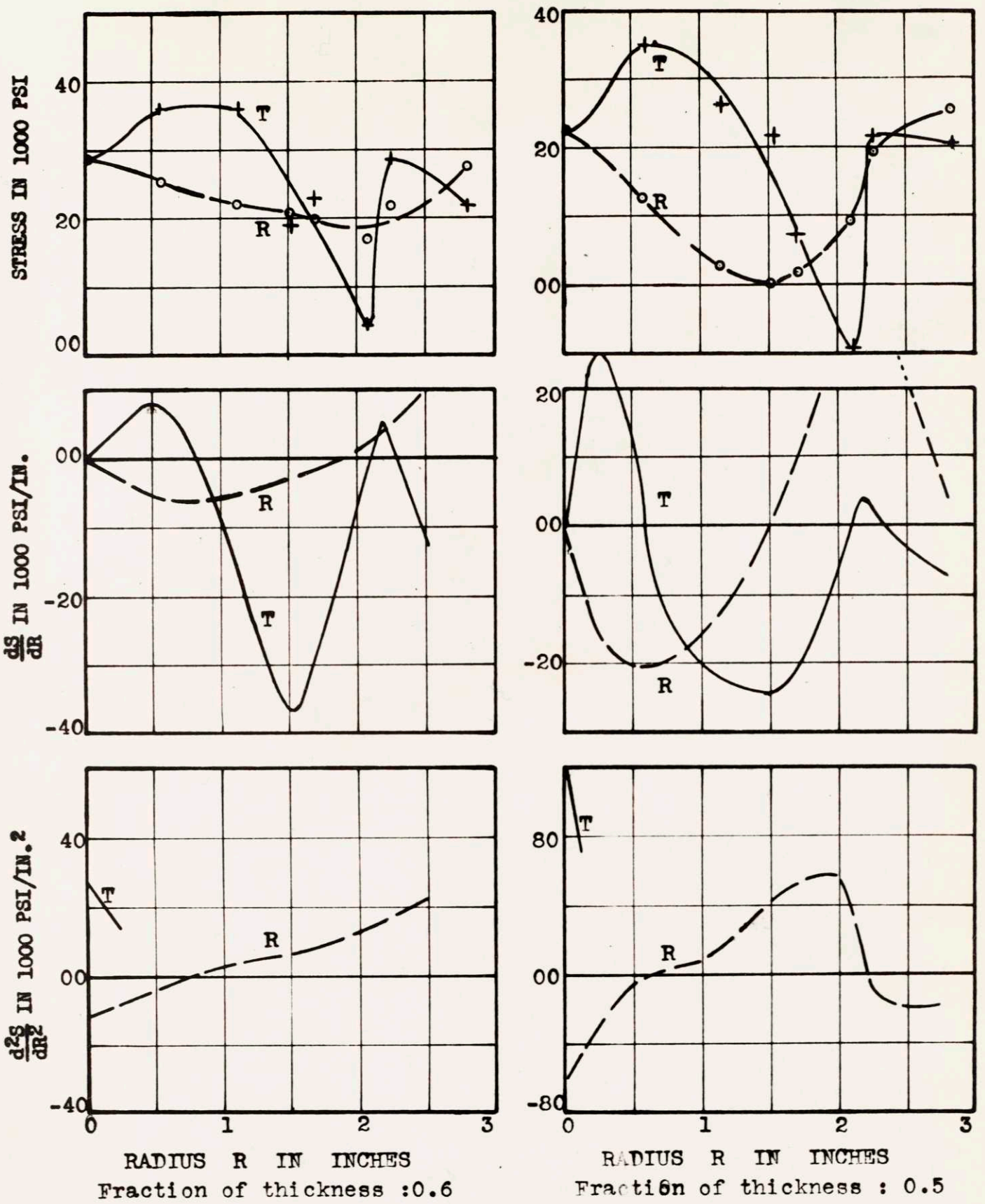


Fig. 32 - Successive Graphical Differentiation of Radial and Tangential Stresses in the Disk versus Radius for Fractions of Thickness 0.6 and 0.5

R : radial stress  
T : tangential stress



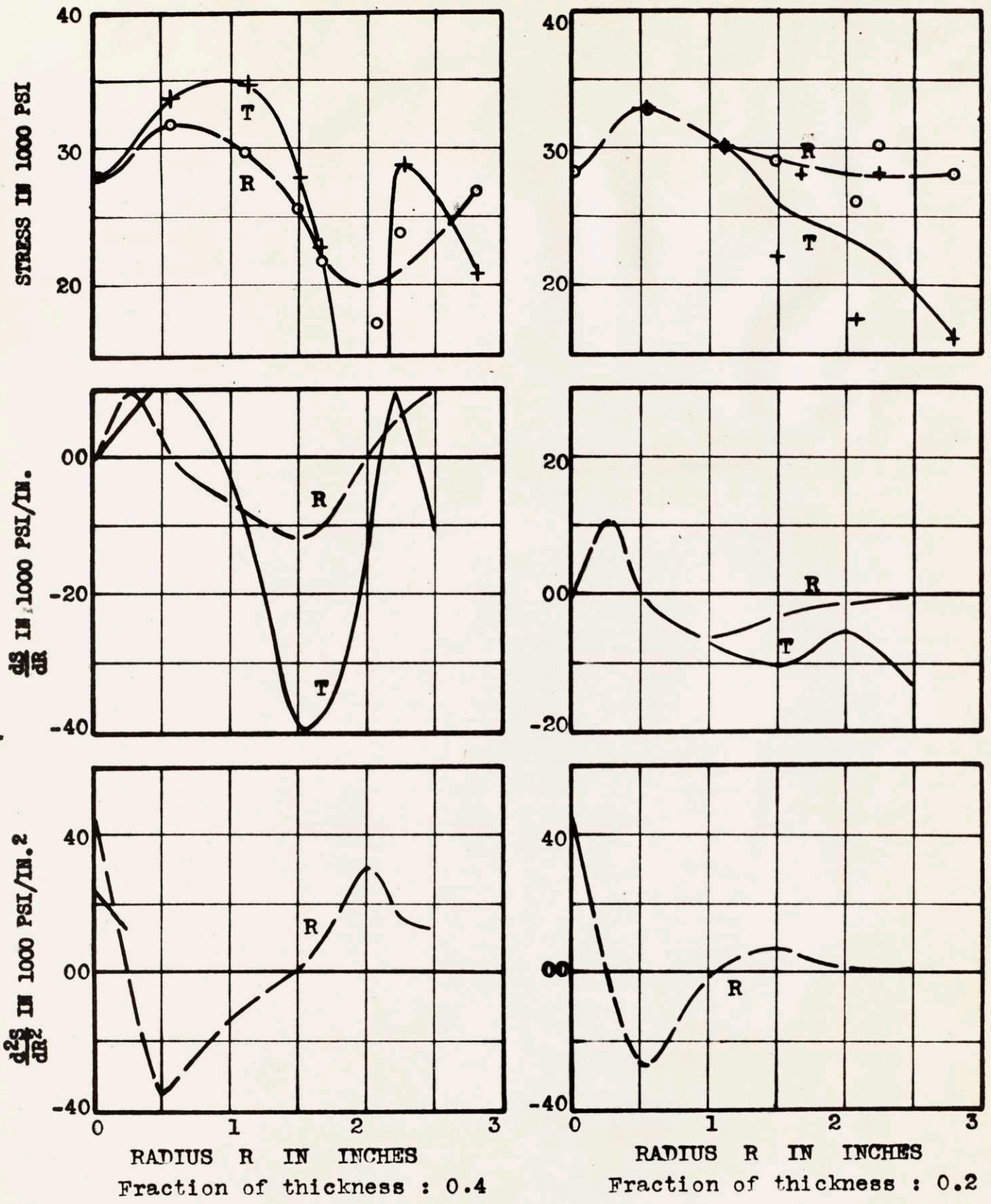


Fig. 33 - Successive Graphical Differentiation of Radial and Tangential Stresses in the Disk versus Radius for Fractions of Thickness 0.4 and 0.2

R : radial stress  
 T : tangential stress

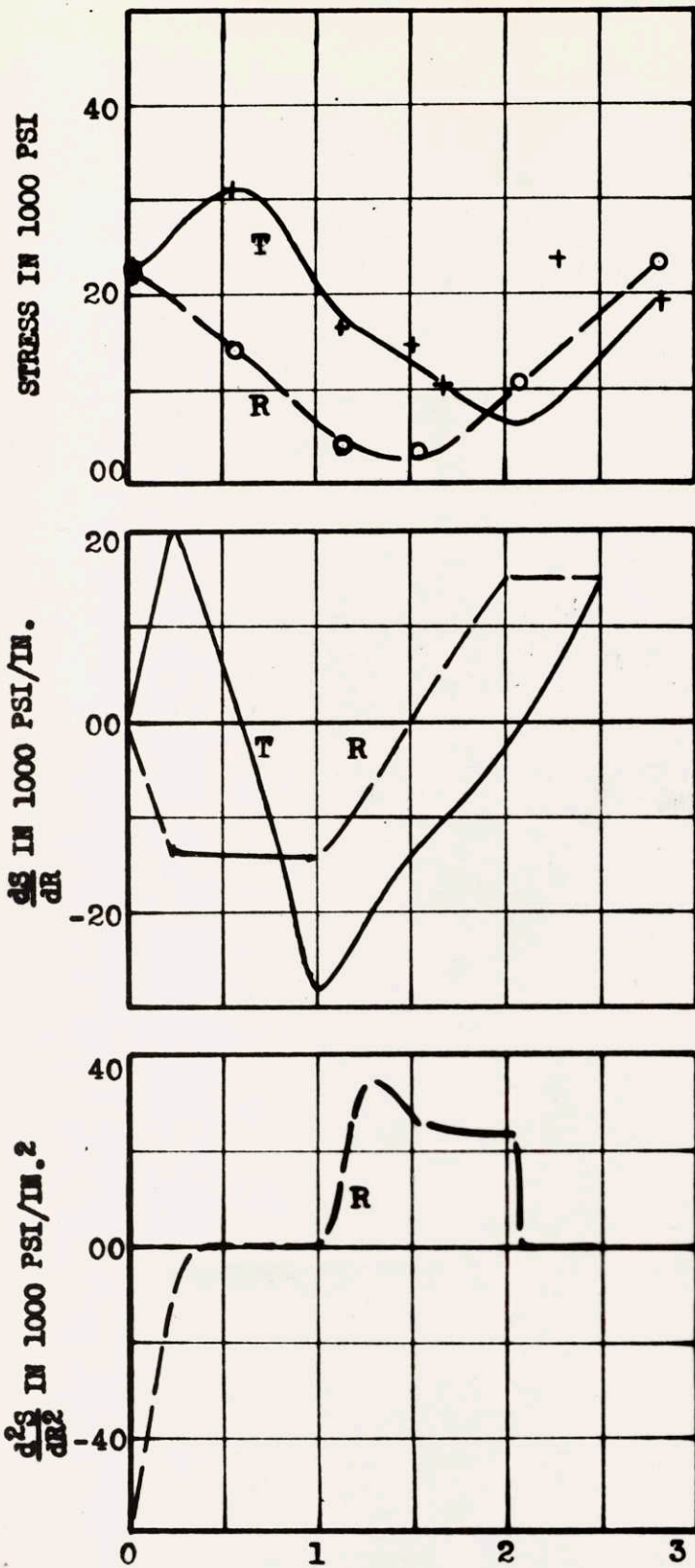


Fig. 34 - Successive Graphical Differentiation of Radial and Tangential Stresses in the Disk versus Radius for Fraction of Thickness 0.0 (bottom)

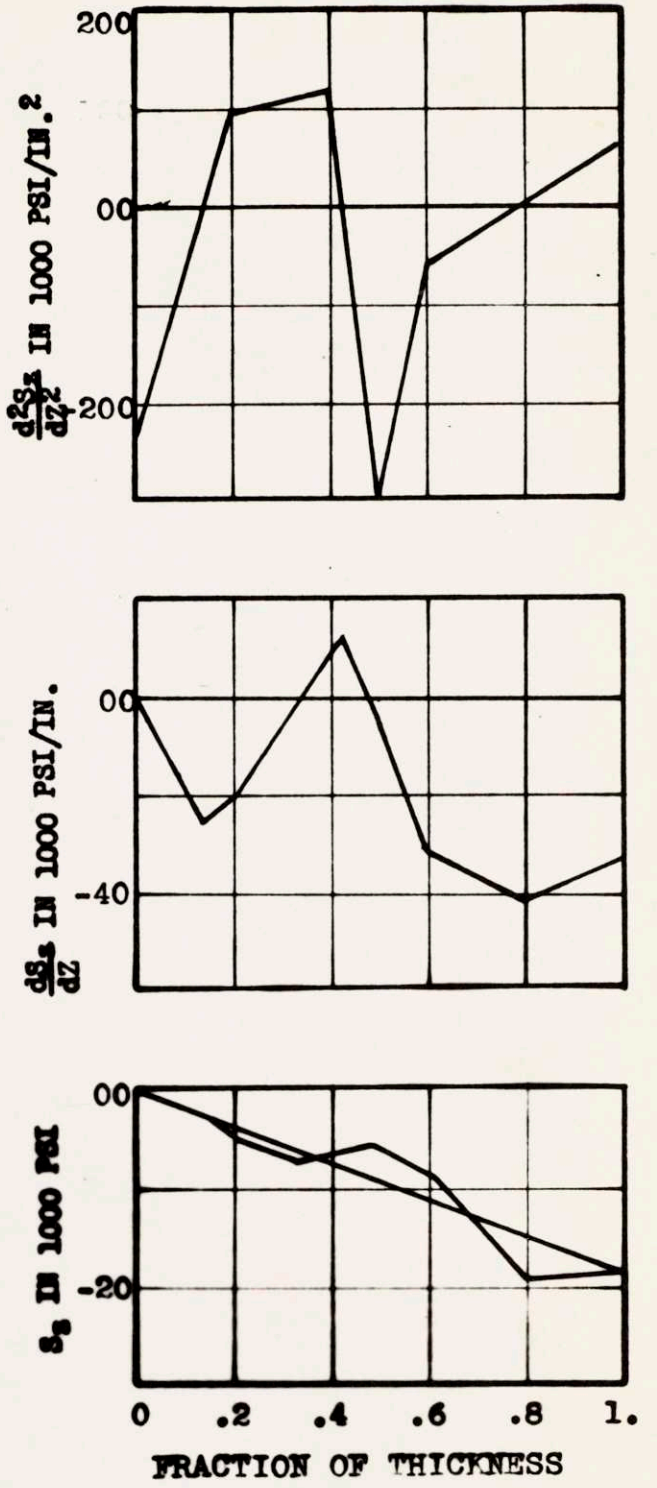


Fig.35 - Successive Graphic Integration for Determination of Stress in Thickness Direction at the Center of the Disk

by the distance from the straight line to the curve

Tables 37a, b, c, d, and e. Numerical values of  $\frac{d^2S_r}{dr^2}$ ,  $\frac{d^2S_t}{dr^2}$ ,  $\frac{dS_r}{dr}$  and  $\frac{dS_t}{dr}$  taken from the curves, Figures 31 to 34, and the calculated value of  $\frac{d^2S_z}{dz^2}$  using equations (3) and (4). All figures are in 1000.

Table 37a

The Center of the Disk

<u>Fraction of Thickness</u>	<u><math>\frac{d^2S_r}{dr^2}</math></u>	<u><math>\frac{d^2S_t}{dr^2}</math></u>	<u><math>\frac{d^2S_z}{dz^2}</math></u>
0.0 (bottom)	56	80	- 24.8
0.2	46	46	+ 92
0.4	46	24	+114
0.5	60	120	-300
0.6	12	28	- 64
0.8	22	66	0
1.0 (top)	60	120	+ 60



Table 37b

One-half From the Center of the Disk

Fraction of Thickness	$\frac{d^2S_r}{dr^2}$	$\frac{dS_r}{dr}$	$\frac{dSt}{dr}$	$\frac{d^2S_z}{dz^2}$
0.0	-58	14	6.5	- 15
0.2	-26	0	0	- 26
0.4	-36	3	11	- 46
0.5	- 1	-20	12	-105
0.6	- 5	- 6	8	- 45
0.8	- 7	2	14	- 27
1.0	- 5	11.5	18	- 15

Table 37c

One Inch From the Center of the Disk

Fraction of Thickness	$\frac{d^2S_r}{dr^2}$	$\frac{dS_r}{dr}$	$\frac{dSt}{dr}$	$\frac{d^2S_z}{dz^2}$
0.0	0	-14	-28	0
0.2	0	- 6	- 6	- 6
0.4	-14	- 6.5	- 3.5	-24
0.5	18	-15	-20	8
0.6	2	- 6	-10	0
0.8	- 7	- 1	0	- 9
1.0	0	11	4	18

Table 37d

One and One-half Inches from the Center of the Disk

Fraction of Thickness	$\frac{dS_r^2}{dr^2}$	$\frac{dS_r}{dr}$	$\frac{dS_t}{dr}$	$\frac{d^2S_z}{dz^2}$
0.0	30	0	-14	39.3
0.2	7.5	- 3	-10	10.1
0.4	0	-12	-40	10.6
0.5	44	0	-24	60
0.6	6	- 3	-37	26.6
0.8	0	- 4	-35	18
1.0	-20	2.5	- 4	14

Table 37e

Two Inches From the Center of the Disk

Fraction of Thickness	$\frac{dS_r^2}{dr^2}$	$\frac{dS_r}{dr}$	$\frac{dS_t}{dr}$	$\frac{d^2S_z}{dz^2}$
0.0	26	15	- 3	42.5
0.2	2	- 1	- 5	3.5
0.4	30	0	-12	36
0.5	56	28	- 6	87
0.6	12	1	- 6	16
0.8	8	- 2	- 8	10
1.0	0	- 7	-10	- 2

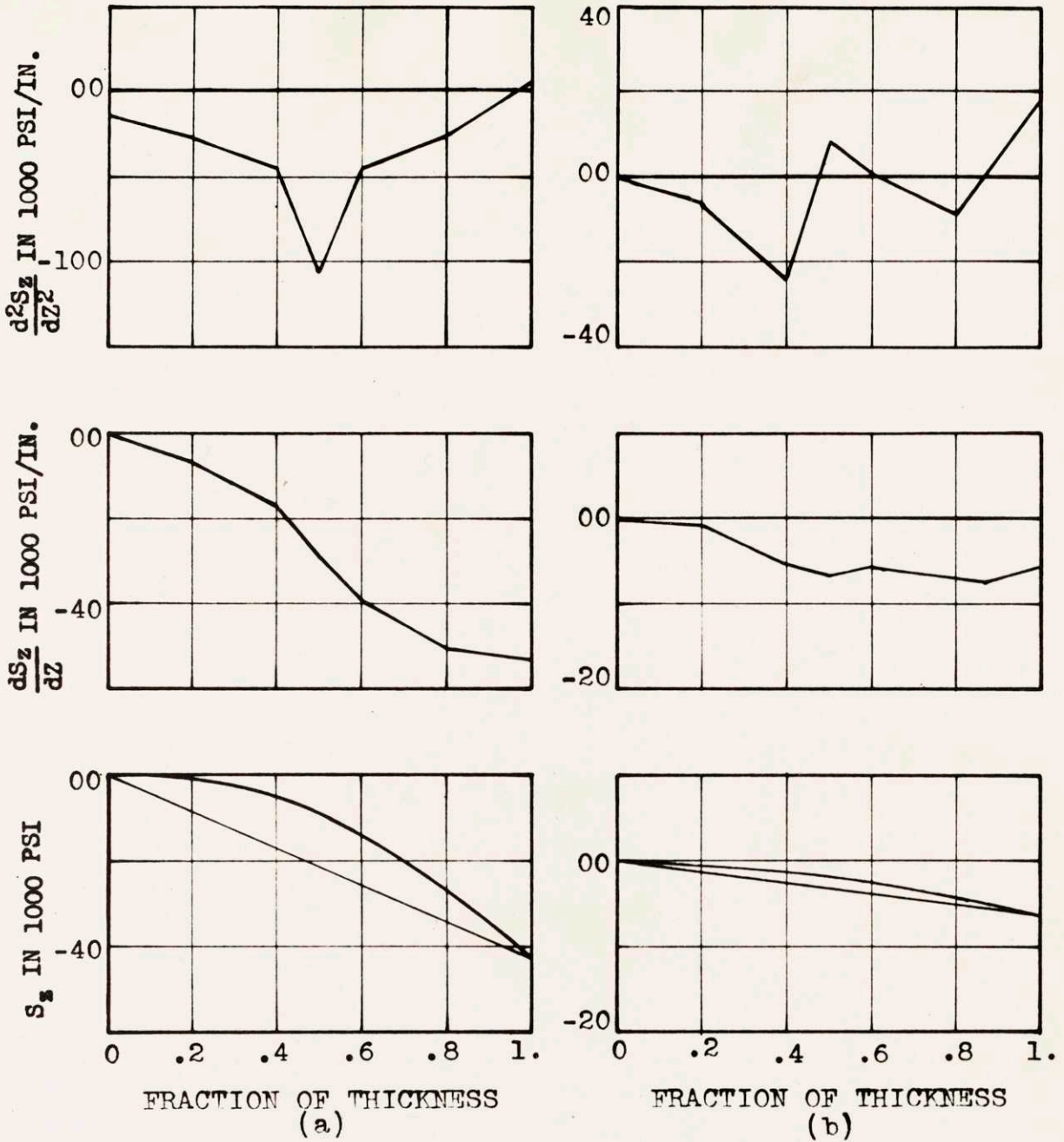


Fig. 36 - Successive Graphical Integration for Determination of the Stress in the Thickness Direction

- a : half an inch from the center of the Disk
- b : one inch from the center of the disk



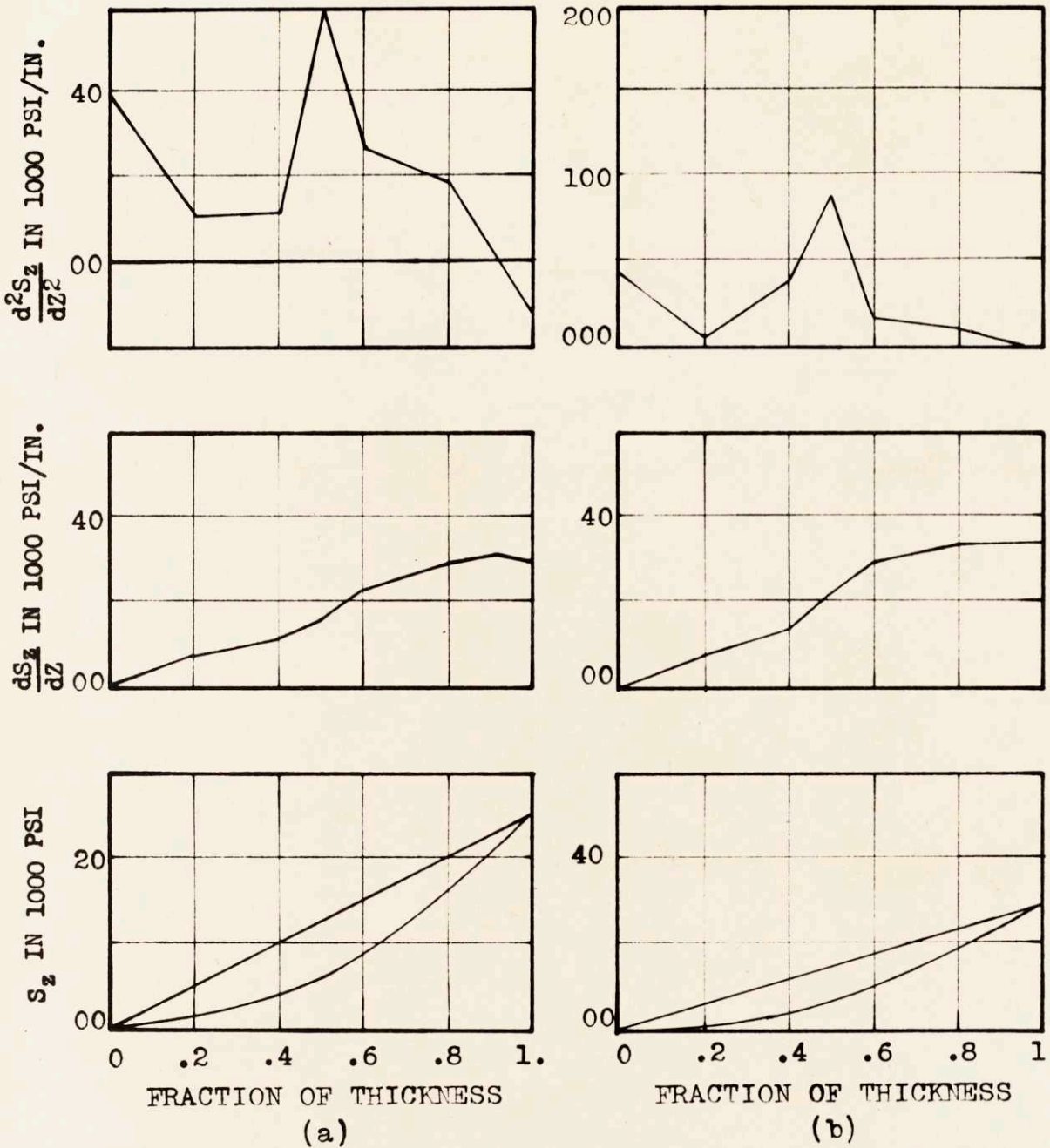


Fig. 37 - Successive Graphical Integration for Determination of the Stress in the Thickness Direction.

a : an inch and a half from the center of the disk

b : two inches from the center of the disk

## PART II

### MEASUREMENT OF STRESSES BELOW THE SURFACE BY RECESSING

#### INTRODUCTION

In measuring stresses below the surface of a specimen, the recessing method has certain advantages over other methods. (For description of other methods see Introduction). This method consists of drilling a hole in the specimen and measuring the stress at the bottom of the hole by means of x-rays and then making corrections for the change in stress caused by the recess. The advantages of this method are as follows:

1. It can be applied to a specimen of any size or shape; therefore, it is very general in application.
2. It is only semi-destructive. The recess can be plugged up easily by welding.
3. It can be applied to a specimen under load.
4. Stress can be measured at any desired depth. There is no need to go through the specimen all the way.
5. Stress is measured directly at any desired depth and corrected for the recessing operation. This is a great advantage over the other methods where stresses are computed.
6. Steep gradients of stress are easily detected by the recessing method. The Sachs method supposes a symmetrical distribution of stresses in a round specimen and takes the average of the measurements around the specimen. In the block method, the length of the block is one and one-half or two times the thickness.

Therefore, the length of the block increases rapidly as the thickness increases, and the measured stress is the average stress over the length of the block. Regardless of the shape or size of the specimen, recessing always measures the stress at a specific point and can detect the steepest gradients across the thickness.

The effect of recessing on the stress at the surface of the metal was studied by J. Mathar<sup>(18)</sup> by drilling a circular recess and measuring the deformation of the hole at the surface of the specimen.

X-ray measurement of stresses at the bottom of the recess is mentioned by L. Frommer and E. H. Lloyd<sup>(13)</sup>. They admit that recessing would influence the stress thus measured but do not make any attempt to measure the change in stress caused by recessing.

As a method of measuring stresses below the surface, recessing has many merits. There are already indications of the type of influence a circular recess has on the surface stresses<sup>(18)</sup>. In Mathar's experiment, in the drilling of the circular hole, surface stresses are relaxed; but the influence of the layers removed from the bottom of the hole decreases very rapidly as the depth of the hole increases; and, from a certain depth on, increasing the depth of the hole is not felt on the surface. This fact suggests that stress at the bottom of the recess; but, as the depth of the recess is increased, this influence, after a certain depth, drops off sharply and becomes negligible. Therefore, the influence that a layer can exercise on the change of stress at the bottom of the recess suggests an exponential function of the distance between the layer considered and the bottom of the recess.



XI THE THEORY OF RECESSING

Professor Daniel Rosenthal developed the following theory to measure the change in stress at the bottom of the recess caused by the recessing operation:

A circular recess in a specimen, (Figure 38), will be considered first, dimensions of which are assumed to be large as compared to the dimensions of the recess. If the change of stress  $ds_z$  at the level  $z$  caused by the removal of the layer  $du$  at a level  $u$  is known, the summation of the influences of the infinitesimal layers from  $u=0$  to  $u=z$  would result in the change of stress at the level  $z$  caused by the recessing operation. The following assumptions are made to calculate the influence of the removal of the layer  $du$  on the change of stress,  $ds$ , at the level  $z$ , Figure 38. Stresses considered are in the same direction.

1. The change of stress  $ds_z$  at the level  $z$  caused by the removal of the layer  $du$  at a level  $u$  is proportional to the stress  $s_u$  at the layer  $du$ .

2. The change of stress  $ds_z$  is also proportional to the thickness  $du$  of the layer  $du$ .

3. The influence of the layer  $du$  is an exponential function of the distance  $(z - u)$ , as suggested by Mathar's experiment and discussed previously.

Hence:

$$ds_z = ks_u e^{-a(z-u)} du \quad (5)$$

where  $k$  and  $a$  are constants, depending on the size and the type of the recess only.

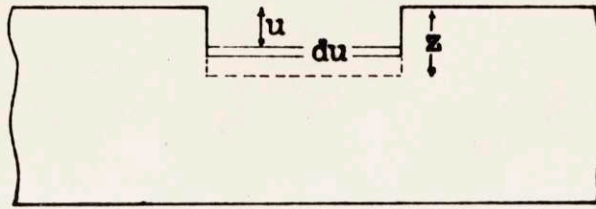


Fig. 38 - Recessing of Specimen

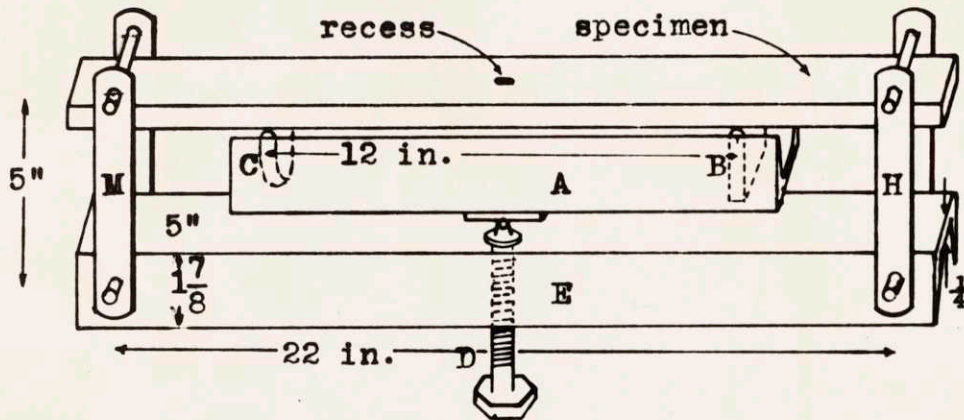


Fig. 39 - The Bending Device. See also Fig. 40

The constant  $k$  is called the stress concentration factor. It will be seen later that the value of  $k$  decreases with the increasing diameter of the recess. The constant  $a$  is called the damping factor because of its damping effect on the influence of the stress with increasing distance from the layer  $du$  considered to the level  $z$ .

If successive layers  $du$  are removed from levels  $u = 0$  to  $u = z$ , the total change of stress  $\Delta s$  at the level  $z$  is shown by equation

(6).

$$\Delta s = s' - s = k \int_0^z s_u e^{-a(x-u)} du \quad (6)$$

or

$$s' - s = k e^{-ax} \int_0^z s_u e^{+au} du \quad (7)$$

$s'$  = apparent stress, i.e., stress measured at the bottom of the recess (level  $z$ ), and  $s$  = true stress at the level  $z$  before recessing.

Equation (7) can be put in the following form, Equation (8):

$$s' e^{+ax} - s e^{+ax} = k \int_0^z s_u e^{+au} du \quad (8)$$

Taking the derivative of the equation (8)

$$\frac{ds'}{du} e^{ax} + a s' e^{ax} - \frac{ds}{du} e^{ax} - a s e^{ax} = k s e^{ax}$$

or

$$\frac{ds'}{du} + a s' = \frac{ds}{du} + (a + k) s \quad (9)$$

In equation (9) the sum  $a + k$  is replaced by  $b$

$$a + k = b \quad \text{or} \quad k = b - a \quad (10)$$



and the equation (8) becomes

$$\frac{ds'}{du} + as' = \frac{ds}{du} + bs \quad (11)$$

The equation (11) shows that  $s$  and  $s'$  are the same kind of function to each other; and, when  $s$  is interchanged with  $s'$  and  $d$  with  $b$ , the equation (11) will remain the same. The same changes can be made in equation (7), by replacing  $k$  by  $(b - d)$  first.

$$s' - s = (b - a) e^{-ax} \int_0^x s_u e^{+au} du \quad (12)$$

then

$$s - s' = (a - b) e^{-bx} \int_0^x s'_u e^{+bu} du \quad (13)$$

$$s = s' - k e^{-(a+k)x} \int_0^x s'_u e^{+(a+k)u} du \quad (14)$$

The equation (14) is the solution of the equation (7), and is the equation of the theory of recessing.

EXPERIMENTAL VERIFICATION OF THE THEORY OF RECESSING

XII A LONG AND NARROW RECESS

To determine the constants in the equation in the theory of recessing, a known pattern of stress is set up so that, from the measurement of stress on the surface of the specimen, stress at any level below the surface may be known. Steel plates are used as specimens, and pure bending and tension are used to produce stresses of known type. The stress produced in tension is uniform at any cross-section of the specimen, and that produced in bending changes linearly from  $+s$  at the tension side to  $-s$  at the compression side, passing from the zero at the mid-section of the specimen. Thus, when stress is set up, it is known what stress value to expect at any level. The stress measured in the recess at that level varies from the stress without recess by the amount caused by the influence of the stress.

Various shapes and sizes of recesses must be examined for possible use in special cases and for the most practical solution of the recessing problem in general.

The first type of recess chosen for investigation is a long and narrow recess. Specimen is a steel flat. Stresses are produced by bending the flat in a specially built bending device and in tension in a tensile strength testing machine.

A. The Bending Device

A four-point bending device was built to produce pure bending, Figures 39, 40. The bending device consists of two steel channels,

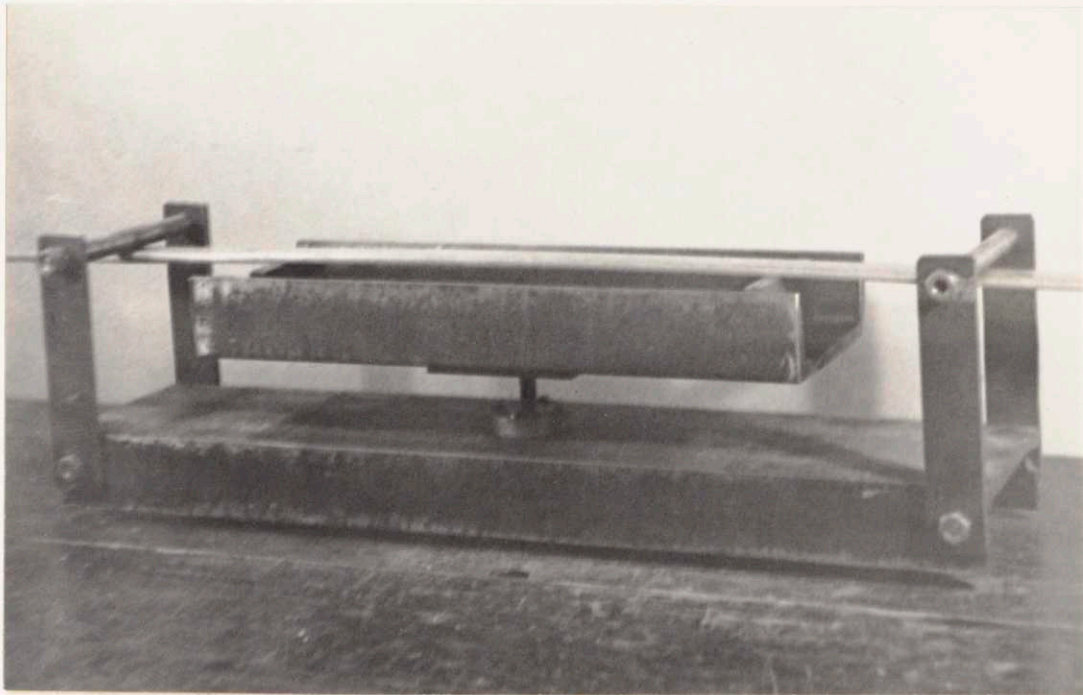


Figure 40. A picture of the Bending Device.  
A wooden stock is placed in the place of the  
specimen to hold the device together.



one of which is longer than the other. The short channel A, has two supports, B and C, close to the ends that support the specimen. One of these supports is fixed to the channel while the other has a round bottom and can rotate to fit the specimen.

The channel A rests on a steel ball at the end of the screw D. The screw D goes through the channel E and is operated with a wrench to raise or lower the channel A. Specimen is pushed by the supports B and C and is pulled by the hinges H and M, hinged to the channel E.

As will be seen later, in the tests conducted, this bending device produces a pure bending in the specimen within the supports B and C.

#### B. Specimen I and Its Preparation

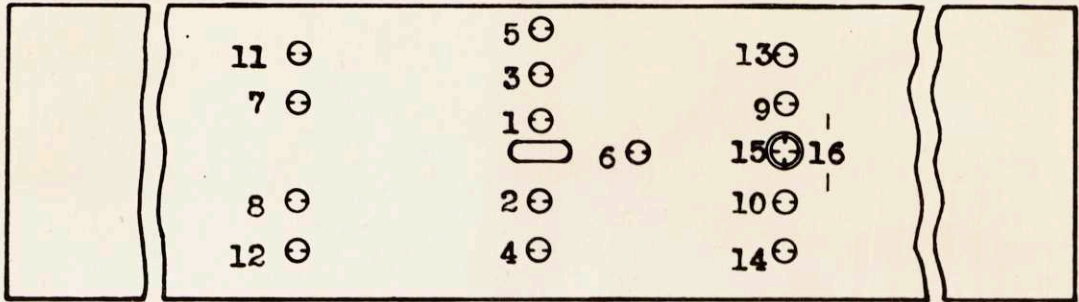
The specimen is a low carbon steel flat twenty-five inches long, three inches wide, and five-eighths inches thick. It was stress relieved by holding it at 1200° F for two hours and cooling it in the furnace at a rate of about 50° F per hour. After the stress relieving treatment, both sides of the specimen are surface ground to remove scale and etched to remove the cold worked layer in grinding. The surface is then polished with emery paper, and stresses are measured with x-rays at different spots of the specimen to test the effect of the stress relieving treatment. Stresses measured varied between -2,000 and +3,500 psi. These stresses are considered unimportant because, in the investigation of recessing, the change in stress rather than the absolute stress is taken into consideration.

## 1. The Layout of Gages

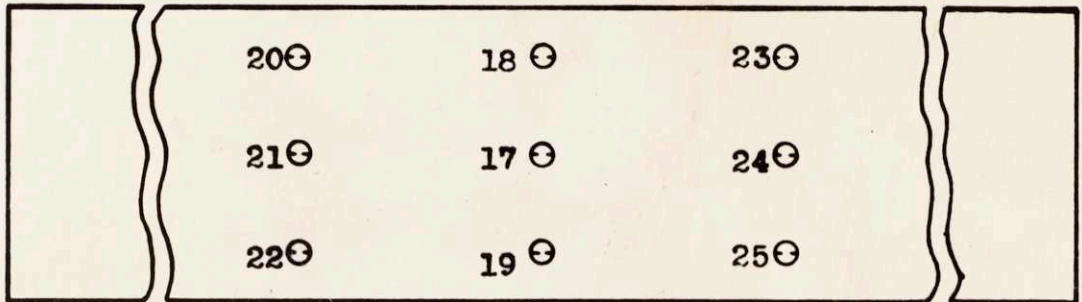
The layout of gages, Figure 41, is so arranged that gages 1, 2, 3, 4, and 5 measure stress variation, if any, from the recess toward the outer edges of the specimen. At the opposite side of the specimen are gages 17, 18, and 19. Gages 18 and 19 are for measuring the stress in compression; and gages 17, opposite the recess, indicates the effect of the recess, if any, at the other side of the specimen. Gages 7 to 25 are placed two and one-half inches away from the recess to check the uniformity of bending.

## 2. Recessing

It was thought that the narrower the recess, the less would be the change in stress in the recess; but, from the practical point of view, two-tenths of an inch is considered the lower limit. Actually, a three-sixteenths inch end mill is used to machine the recess. The length of the recess is 0.6 inches and the depth is 0.078 inches. Electrical resistance strain gages of type SR-4 are cemented on both sides of the specimen, Figure 41, to measure the stress produced in bending. After the machining of the recess, a layer of a minimum of ten thousandths of an inch thick is removed from the bottom of the recess by etching with a 30 percent nitric acid solution. Then the bottom is polished with emery paper, Nos. 1, 0, 00, and 000, and scratches are removed at each step which have been left from the previous step. Finally, at least 1/1000 of an inch layer is removed by etching with 10 percent fresh nital solution. The specimen is now ready for measurement of stresses.



The Top Face of the Specimen I. Slot at the Center is the Recess.



Bottom Face of the Specimen

Fig. 41 - The Layout of the Electrical Resistance Strain Gages  $\otimes$  on the Specimen I. The Sign  $\otimes$  indicates a Cross Gage.

Scale:  $\frac{1}{2}$

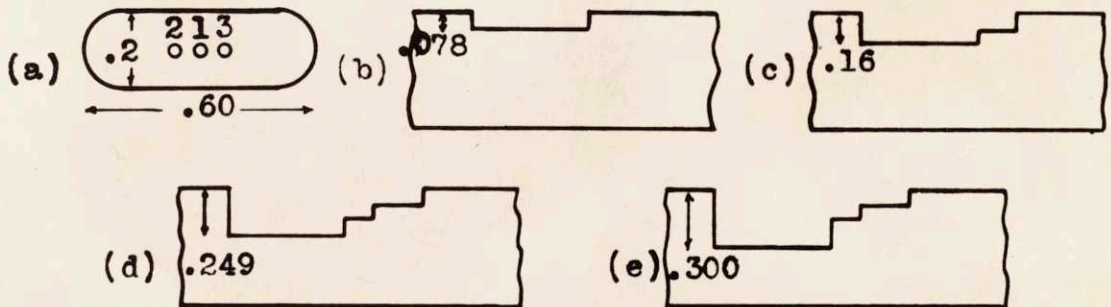


Fig. 42 - (a) Bird's-eye View of the Recess. Scale; 2. (b), (c), (d) and (e) Cross sections of Four Recesses used. Scale: 1.



### 3. The Bending Experiment

For the measurement of stresses in bending, the specimen is placed in the bending device, Figures 39, 40, under the x-ray tube. Strain gage readings are taken and stresses are measured at points 1, 2, and 3 at the bottom of the recess at no load, Figure 42. Then the load is applied to a maximum stress of about 28,000 psi at the outermost layers of the specimen, measured by strain gages. While the specimen is under the load, strain gage readings are again taken and stresses measured with x-rays at points 1, 2, and 3, Figure 42. The difference between various gage readings are usually less than 10 micro inches per inch, which corresponds to 300 psi. After all the measurements on the specimen at load are completed, the load is taken off, and strain gage readings are recorded again at no load to determine whether any plastic deformation has taken place. In the experiments, maximum stress was always below 29,000 psi, and no plastic deformation was observed.

For uniformity of calculations in each experiment, either in bending or in tension, the measured stresses are multiplied with a factor, so as to have a maximum stress of 30,000 psi in the specimen. In bending, 30,000 psi is the stress at the outermost layer of the specimen; and, in tension, it is the uniform stress. In measuring the stress in the specimen, only the gages on the cross-section which cut the recess into two are taken into consideration. The other strain gages are used for checking the uniformity of bending and the effect of the recess on bending in general. As the recess is very small compared with the specimen, the effect of the recess on bending is very small.

#### 4. Successive Recesses

After all the measurements have been taken with the first recess, the depth of the recess is increased in steps to 0.160, 0.249, and 0.300 inches, Figure 42; and at each level, the same measurements are taken as in the first recess, and stresses are measured at the bottom of the recess by x-rays. In order to allow the x-rays to come out of the recess while the oblique pictures are being taken, one end of the recess is lowered in steps, as shown in Figure 42. It will be demonstrated later that the lowering of one end of the recess does not change the stress in the recess to any appreciable extent. In measuring the stress by x-rays at the bottom of the recess, at least two pictures of each spot are taken with a new setting in both perpendicular and oblique directions, and stresses are measured at at least two distinct points at the center of the recess. In the case of the last recess, i.e., the 0.300 inch deep recess, stress in the recess is measured, not by x-rays, but by an electrical strain gage of type A-8. The strain gage type A-8 is very small in size,  $3/32 \times 1/4$  inches, and is ideal for measurement of stress in the recess.

#### 5. Results Obtained from Specimen I in Bending

The first bending of Specimen I is carried out to check the uniformity of the bending obtained in the bending device. The data records are shown in Table 38, Figure 41.

It is seen from Table 38 that only one gage out of eight differed by 1.9 percent from the average, and that the difference of the others from the average is less than one percent. Therefore, it is concluded that a pure bending is obtained in the above experiment.

Table 38

Relaxations in Micro Inches per Inch, Recorded in Strain  
Gages in Bending of Specimen 1, in the Bending Device

<u>Strain Gage No.</u>	<u>Strain Shown in Bending</u>	<u>Differences From the Average</u>
11	-470	+1
12	-465	-4
13	-465	-4
14	-468	-1
20	+473	+4
22	+466	-3
23	+477	+8
25	+468	-1
Compression side, average	-467	
Tension side, average	+471	
Average, both sides	469	



Table 39 shows strains recorded in the gages attached to Specimen 1 in bending for four recesses of different depths, Figure 42. Strains are in micro inches per inch and are multiplied by a factor making the average of gages 1, 2, 3, 4, and 5 1000 micro inches per inch. This correction is made to compare results. The average strain of gages 1 to 5 is taken to calculate the true stress in the recess; and, again, for the sake of comparison, this average is increased to 1000 micro inches per inch. The actual gage readings vary between 800 and 950 micro inches per inch. In test bendings, it is seen that, no matter what the load is, strains recorded by gages are always proportional to each other. The transverse stress on the tension side of the flat resulting from the bending, as computed from the strains of the cross-gage 15 and 16, is:

$$S_t = 33(-236 + 0.3 \times 926) = 1385 \text{ psi tension.}$$

Stresses measured at the bottom of the recesses are shown in Figure 50.

### C. Use of Strain Gage in the Recess

The use of the electrical strain gage to measure the change of stress at the bottom of a recess has certain advantages over the use of x-rays:

1. The use of the strain gage takes less time than that of the x-ray.
2. While the gage can detect 300 psi easily, the accuracy of x-rays is no better than plus or minus 2,000 psi.

Table 39

Strains Recorded in Micro Inches per Inch, by Gages, of Specimen1 in Bending for Four Recesses of Different Depths

<u>Gage No.</u>	<u>0.078 Inch Recess</u>	<u>0.160 Inch Recess</u>	<u>0.249 Inch Recess</u>	<u>0.300 Inch Recess</u>	<u>Average Strain</u>
1	1005	1025	1025	-	1018
2	1020	1008	1006	1003	1009
3	983	990	992	1034	1000
4	1011	990	990	983	993
5	985	987	989	982	986
6	952	950	917	-	940
7	-	-	-	-	-
8	-	-	-	-	-
9	955	966	920	937	945
10	978	971	914	939	951
11	965	987	952	930	959
12	972	966	950	932	955
13	973	954	936	932	949
14	993	976	929	929	957
15	-	953	912	914	926
16	255	-	222	-	236
17	1015	945	951	957	967
18	998	-	984	975	986
19	1000	-	980	983	988
20	1006	-	922	-	964
21	-	-	919	943	931
22	970	-	923	942	945
23	-	-	933	942	938
24	972	955	944	935	951
25	973	935	940	937	947

3. With the strain gage attached to the recess, stress measurements can be taken at different loads below the yield point of the specimen. The strain gage is especially practical when the effect of the length of the recess is to be examined. For this purpose, the length of the recess can be increased without touching the gage.

4. With the gage in the recess, the specimen can be tested both in bending and in tension. To use an x-ray in the tensile test would require a special set-up of the x-ray tube.

5. The area over which the strain gage measures the stress ( $3/32 \times 1/4$  inches) is much larger than that of the x-ray, but the measurement of the stress with an x-ray at different points close to the center of the bottom of the recess shows that the area covered by the strain gage has about the same stress in loading.

Therefore, in the investigation of stress in the recess, the strain gage will be used rather than x-rays. In the application of the recessing method, however, x-rays are the only means of measuring stresses.

#### D. Preparation and Testing of Specimen II

With the second specimen, the effect of the length of the narrow and long recess is to be examined.

The specimen is a mild steel flat,  $25 \times 3 \times 0.6$  inches in size. It is stress relieved at the same time as Specimen I. Two recesses are machined in Specimen II, one 0.08 inches deep, and the other 0.175 inches deep. The width of the recesses is  $3/16$  inches, and their length is at first 0.60 inches. The length of both recesses



is then increased in steps up to 2.34 inches, in order to study their effect on the stress measured in the recess. The layout of gages and recesses is shown in Figure 43. The bending tests are made in the bending device in the same manner as in Specimen I, Figure 44, except that the stress in the recess is measured with the strain gage and not with the x-rays. Tests are made in bending only. For each test, measurements are taken at the maximum loads of about 15,000, 22,000, and 29,000 psi at the outer layer of the specimen. Data taken at each step is then corrected for maximum load of 30,000 psi, and the average of the three readings is taken. The maximum variation of stresses from each other (not from the average) in these three tests is rarely more than 300 psi.

Stress at the opposite side of the recess is 29,700 psi for the recess 0.08 inches deep, and 29,000 psi for the recess 0.175 inches deep.

The results of testing on Specimen II are tabulated in Table 40, and shown in Figures 50, 51, and 52, and they are discussed later.

#### E. Preparation and Testing of Specimen III

In the previous two specimens, stresses in a long and narrow rectangular recess are examined while the specimen is bent. Specimen III is prepared with rectangular recesses of the previous size ( $3/16 \times 0.6$  inches) and varying depth, in order to measure stresses, both in tension and in bending. The specimen is a cold rolled mild steel flat, 50 inches long, 3 inches wide, and one inch thick.

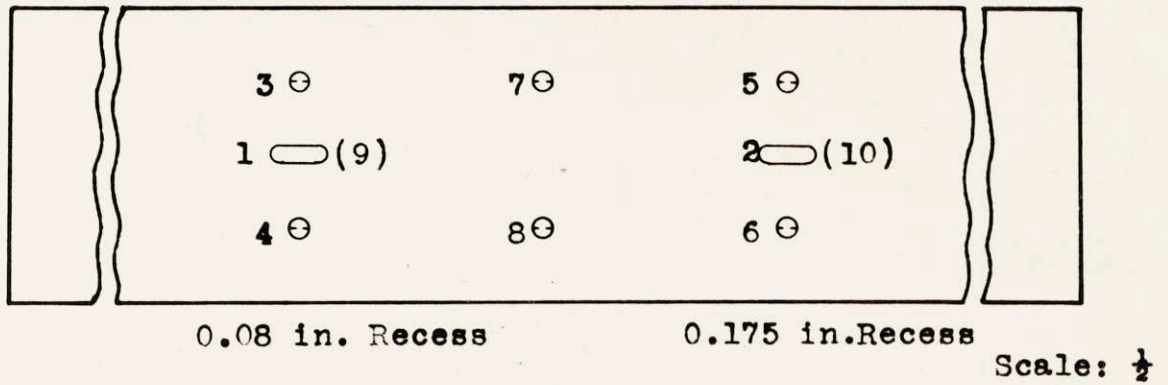


Fig. 43 - The Layout of Strain Gages and Recesses of Specimen II. Numbers Indicate Strain Gages. Number in in Paranthesis are gages Directly opposite to the Recesses.

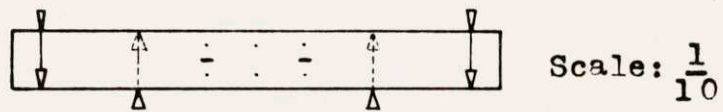
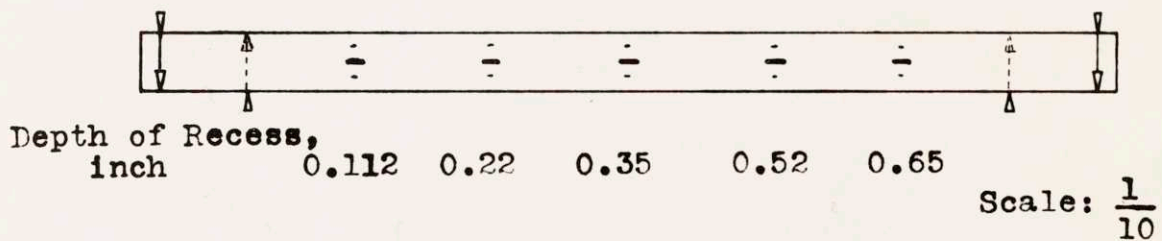


Fig. 44 - Application of Load in Bending Specimen II.



Depth of Recess,  
inch      0.112    0.22    0.35    0.52    0.65

Fig. 45 - Location of Strain Gages and Recesses on the Specimen III .

Table 40

Stress Measured at the Bottom of the Recesses as a Function  
of the Length of Recess

<u>0.08 inch deep recess. True stress at this level in the solid specimen is 22,000 psi</u>		<u>0.175 inch deep recess. True stress at this level in the solid specimen is 12,500 psi</u>	
<u>Length of Recess in Inches</u>	<u>Stress in the Recess in psi</u>	<u>Length of Recess in Inches</u>	<u>Stress in the Recess in psi</u>
0.60	24,000	0.60	15,500
0.94	22,900	0.94	14,000
1.24	22,520	1.26	13,850
1.54	22,280	1.48	13,280
1.76	22,050	1.96	12,925
2.10	22,030	2.34	12,700



Electrical resistance strain gages are used to measure strains, both on the specimen and in the recess; therefore, no stress relieving treatment is necessary. Five recesses,  $3/16$  inches wide and 0.60 inches long, are machined in the specimen, with depths of 0.112, 0.22, 0.35, 0.52, 0.65 inches, as shown in Figure 45. In addition to a small strain gage ( $1/4 \times 3/32$  inches) in each recess, four gages are placed on the specimen for each recess, two on one face and two on the opposite face; so that, if there is a slight bending in the tensile testing machine, the average of the four gage readings is taken. The SR-4 gages on the specimen are of the type A-1.

After the strain gages are cemented on the specimen and left to dry for twenty-four hours over the hot radiator in the laboratory, the gages are covered with petrosene, and long wire leads are soldered on the strain gage wires. The specimen is then placed in a Riechle Universal testing machine of 400,000 pounds capacity, Figure 46, for tensile tests. Before any reading is taken, an 80,000 pound load is put on the specimen and taken off. Then, at the loads of zero, 60,000 pounds, and 70,000 pounds, and then again at zero pounds, strain gage readings are recorded.

At each cross-section of the specimen containing the recess, the average of the four gage readings is taken at the loads of 60,000 and 70,000 pounds. For comparison of results, the average in each case is taken as 1,000 micro inches per inch, and the strain recorded in the recess is multiplied by the factor,  $\frac{1,000}{\text{average}}$  for correction. Then the average of these corrected loads for 60,000 and 70,000 pound loads is taken. The results are shown in Table 41.

Table 41

Results of the Tensile Test of Specimen III

Depth of the Recess in Inches	Strain in Micro Inches per Inch in the Recess for 1000 Micro Inches per Inch in the Cross-section of the Recess			Difference Between Strain in Recess and That on the Specimen
	For 60,000 Pounds	For 70,000 Pounds	Average	
0.112	996	1013	1005	5
0.220	1052	1053	1052	52
0.350	1085	1075	1080	80
0.520	1030	1000	1015	15
0.650	1055	1022	1036	36

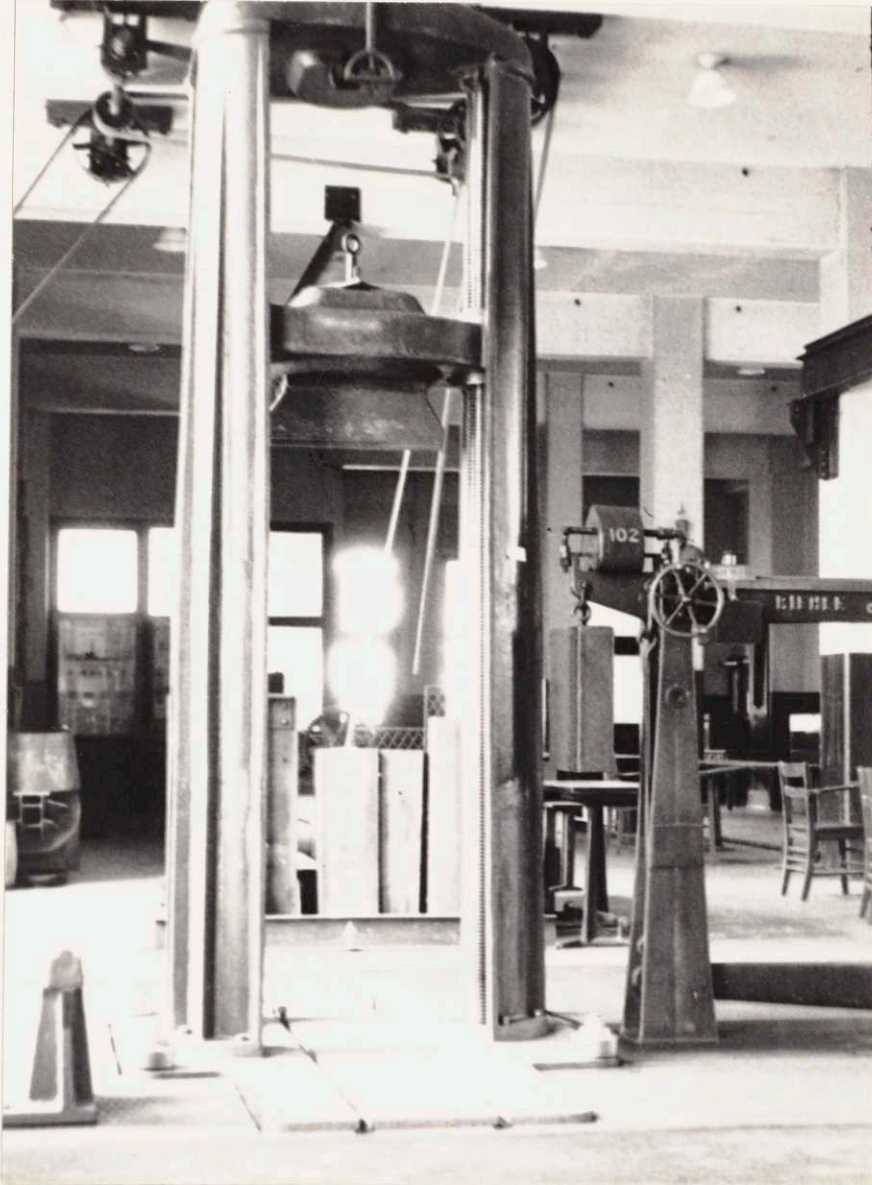


Figure 46. A picture of the Riehle Universal Testing Machine of 400,000 pound capacity used for the tensile testing.



In testing Specimen III in bending, the specimen is placed on a Riehle Universal testing machine of 100,000 pounds capacity, Figure 47. The side containing the recesses is placed downward, so that the recesses will be on the tension side, Figure 45. The data on the results of the bending test are in Table 42 and in Figure 53.

Table 42

Stresses in psi at the Bottom of the Recesses and at  
the Corresponding Layers in the Specimen

<u>Depth of Recess</u>	<u>Stress at the Depth</u>	<u>Stress in Recess</u>	<u>Increase Caused by Recess</u>
0.112	23,400	25,100	1,700
0.220	16,800	17,900	1,100
0.350	9,000	10,260	1,260
0.520	- 1,200	1,140	2,340
0.650	- 8,950	- 8,100	850

F. Preparation and Testing of Specimen IV

In Specimens I, II, and III, long and narrow rectangular recesses have been examined in bending and in tension. So far, the effect of the depth and length of the recess has been studied. It may be said that the effect of the recess on the change of stress was found to be very low. But, before the question of the influence of a transverse stress on a long rectangular recess is answered, no decision can be made as to the practicability of a rectangular recess. Specimen IV has been chosen for the purpose of examining the effect of

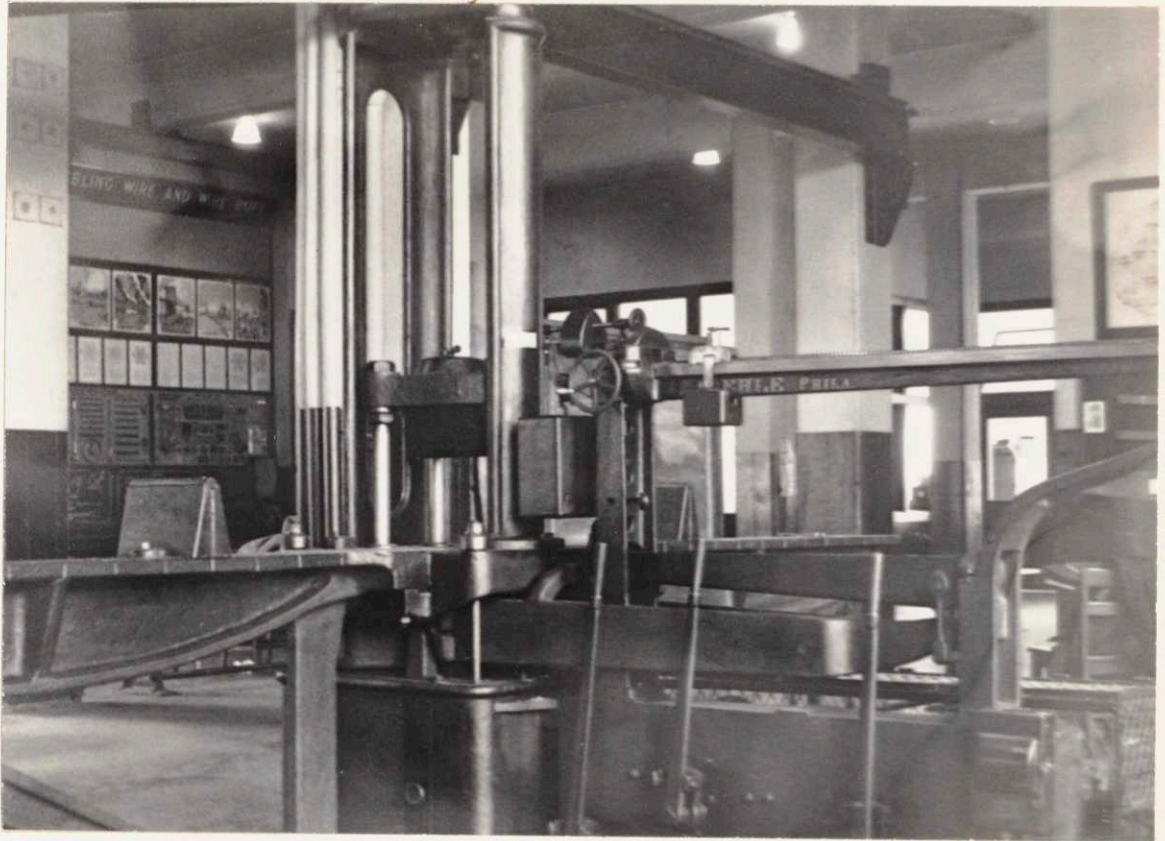


Figure 47. A picture of the Riehle Universal Testing Machine of 100,000 pound capacity used for bending tests.

the transverse stress on a rectangular recess. The specimen is a mild steel flat, 54 x 3 x 1 inches.

As shown in Figure 48, four recesses are machined on this flat, two transverse and two longitudinal. Recesses are of equal size, 3/16 inches wide, 0.6 inches long, and about 0.3 inches deep. The layout of the gages is shown in Figure 48. In one of the longitudinal recesses, a special strain gage, 1/8 inches long and 3/8 inches wide, is placed across the recess; and, in the other, a regular A-7 gage is placed in the longitudinal direction of the recess. Likewise, in one of the transverse recesses, a special gage is placed across the recess; and, in the other, an A-7 gage is placed along the recess. The specimen is tested in tension only. Table 43 shows the result of the test.

Table 43

Results of Testing Specimen IV in Tension. Strain

Figures Are in Micro Inches per Inch.

(For location of gages see Figure 48)

Load in Pounds	Recess Gage 1	Recess Gage 2	Recess Gage 3	Recess Gage 4	Gages 6 and 7	Gages 8, 9, 10 and 11	Gages 13 and 14
40,000	-140	1062	-180	500	460	449	468
60,000	-200	1574	-267	743	683	666	718

In Table 43, strains for the 60,000 pound load are taken for calculation of the stress. If strains measured at the 40,000 pound load are multiplied by  $\frac{60}{40}$ , they come very close to the strains at the 60,000 pound load.



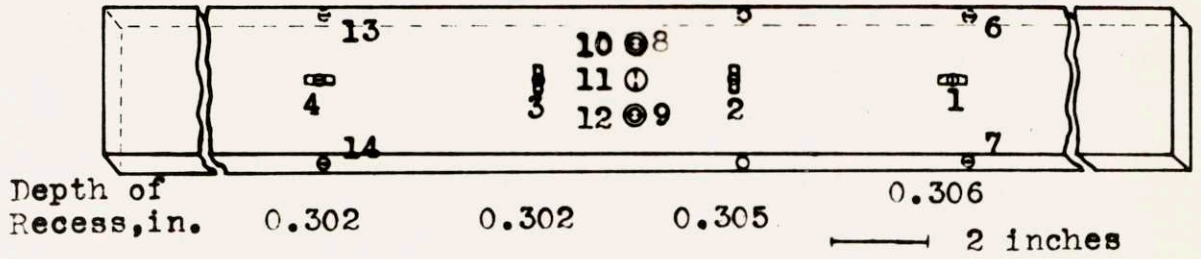


Fig. 48 - Layout of Strain Gages and Recesses on the Specimen IV. Small Circles are gages on top and the Large Circles Gages on the opposite Side of the Specimen. The Line in the Circle shows the direction of the Gage.

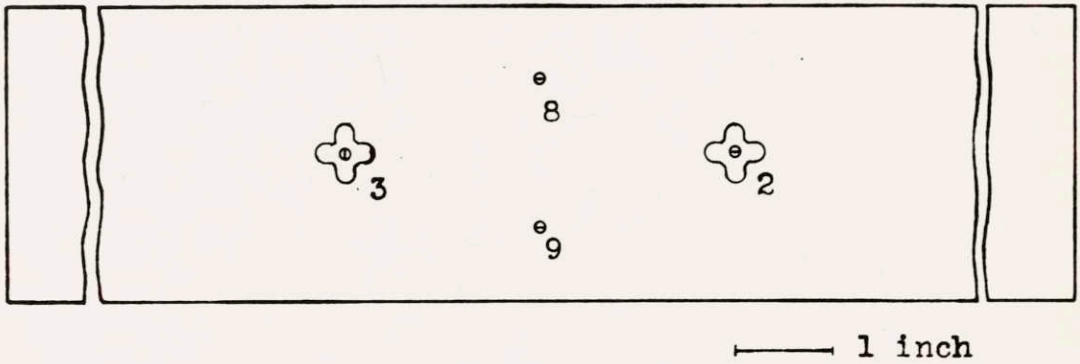


Fig. 49 - Recess Number 2 and 3 on the Specimen IV Machined into Rosettes

Considering the strains in recesses Nos. 1 and 4,  $e_1$  and  $e_4$ , respectively, the transverse stress in the recess No. 1 is

$$S_1 = \frac{E}{1-\nu^2} (e_1 + \nu e_4) \quad (15)$$

where

$E = 30 \times 10^6$ , modulus of elasticity for steel

$\nu = 0.3$ , Poisson's ratio

$e_1, e_4$  = strain in micro inches per inch in the direction of the respective gages.

After simplification, the equation becomes:

$$S_1 = 33(e_1 + 0.3 e_4)$$

Stress in the transverse direction  $S_1$  in recess No. 1 is

$$S_1 = 33(-200 + 0.3 \times 743) = 755 \text{ psi}$$

while stress in the direction of the recess in recess No. 4 is

$$S_1 = 33(743 - 0.3 \times 200) = 22,500 \text{ psi.}$$

Stress in the specimen itself at the cross-section, containing recess No. 1, is

$$S = 30 \times 683 = 20,500 \text{ psi.}$$

The above results show that, when the rectangular recess is in the direction of a uniaxial stress, the transverse stress, 755 psi, appearing in the recess, can be ignored as compared with the longitudinal stress of 22,500 psi.

Considering the transverse recesses Nos. 2 and 3, stress in the longitudinal direction is:

$$S_2 = 33(1574 - 0.3 \times 267) = 49,300 \text{ psi,}$$

and the stress in the transverse direction is:

$$S_3 = 33(-267 + 0.3 \times 1574) = 6,760 \text{ psi.}$$

It is seen from the above figures that, when there is a stress of 20,500 psi perpendicular to the direction of the recess, such as in recess No. 3, stress in the direction of and at the bottom of the recess is increased by 6,760 psi, or by 33 percent of the stress across the recess. Obviously, when the specimen is in pure tension, the transverse stress of 6,760 psi, measured at the bottom of recess No. 3 is caused by the notch effect of the recessing. Therefore, a long and narrow recess cannot be used to measure stresses when there is a biaxial stress condition in the specimen.

The stress of 49,300 psi measured in recess No. 2 shows also that plastic deformation occurred in the transverse recesses. However, when the load on the specimen is removed, no residual stress is indicated by gage 3, while gage 2 shows only -1,560 psi in compression. This low figure might be due to the very small area of plastic deformation, as compared with the remaining section of the specimen.

#### 1. The Effect of the Cross Recess

It is seen from the preceding pages that the notch effect makes it impossible to use a rectangular recess when biaxial stresses exist in the specimen. To see the notch effect of the two rectangular recesses which cross at the center, recesses Nos. 2 and 3 are machined as shown in Figure 49, without removing the gages in the recesses. The specimen is then tested in the tensile machine. The results are shown in Table 44.

In calculating the stresses from the data in Table 44, it is found that, while, in the rectangular recess No. 4, the stress is



Table 44

The Results of Testing Specimen IV in Tension After the

Cross Recesses are Machined, Figure 49. Strain

Figures are in Micro Inches per Inch

<u>Load in</u> <u>Pounds</u>	<u>Recess</u> <u>Gage 1</u>	<u>Recess</u> <u>Gage 2</u>	<u>Recess</u> <u>Gage 3</u>	<u>Recess</u> <u>Gage 4</u>	<u>Gages</u> <u>6 and 7</u>	<u>Gages 8, 9,</u> <u>10 and 12</u>	<u>Gages</u> <u>13 and 14</u>
50,000	-178	816	-244	630	570	567	588
60,000	-208	866	-321	746	680	680	698

22,550 psi, in the cross recess No. 2, the stress is 25,400. Considering that the stress in the specimen is 20,500 psi, the notch effect of the cross gage is about 20 percent, while that of the simple long recess No. 4 is about 10 percent. Stress in the crossed recess No. 3 in the transverse direction is -2,015 psi. It should be noticed that, while, in the rectangular stress, the stress was tension, it is compression when the recess is crossed. The crossed recess decreased the stress of the rectangular recess by one-half in the longitudinal direction.

G. Discussion of Results on the Long and Narrow Recess

In Specimens I, II, III, and IV, a known pattern of stress was produced by bending or by pulling, and stress at the bottom of a long and narrow recess was measured by x-rays or electrical resistance strain gages. For a recess 3/16 inches wide and 0.6 inches long, stresses measured at different depths down to one-half the thickness of the specimen are shown in Figure 50. In this figure the straight line shows the stress introduced to the specimen and

the curve stresses measured in the recesses. Stresses measured by strain gages are lower than those measured by x-rays, but the difference is always less than 2,000 psi, which is the best accuracy obtainable by x-rays.

Figure 53 shows the results obtained in measuring stresses in the recesses  $3/16$  inches wide and 0.6 inches long on a one-inch thick specimen. Strain gages were used exclusively for this experiment. It is to be noticed that the scale of Figure 53 is half that of Figure 50, and the results shown in both are in agreement.

In Figures 51 and 52, the effect of the length of the recess is shown for recesses of two different depths, 0.08 inches and 0.175 inches. It is observed that, at first, the notch effect of the recess decreases sharply with increasing length of the recess of 0.175 inches depth, and even sooner for the recess 0.08 inches deep.

The conclusion drawn from the data in Figures 50 to 53 is that a long and narrow recess, when used in the direction of a uniaxial stress, causes a small change in the value of the stress, depending on the length of the recess. Further, it can be said that, if the recess is  $3/16$  inches wide and long enough to permit the reflected x-rays to come out of the recess, when shooting at the center of the recess at an angle of forty-five degrees for the oblique picture, and not shorter than 0.6 inches, the stress introduced by the notch effect of the recess is less than 2,000 psi for a maximum uniaxial stress of 30,000 psi, or less than six percent.

When x-rays from a cobalt target strike on a flat surface of a steel specimen at an angle of forty-five degrees, the reflected



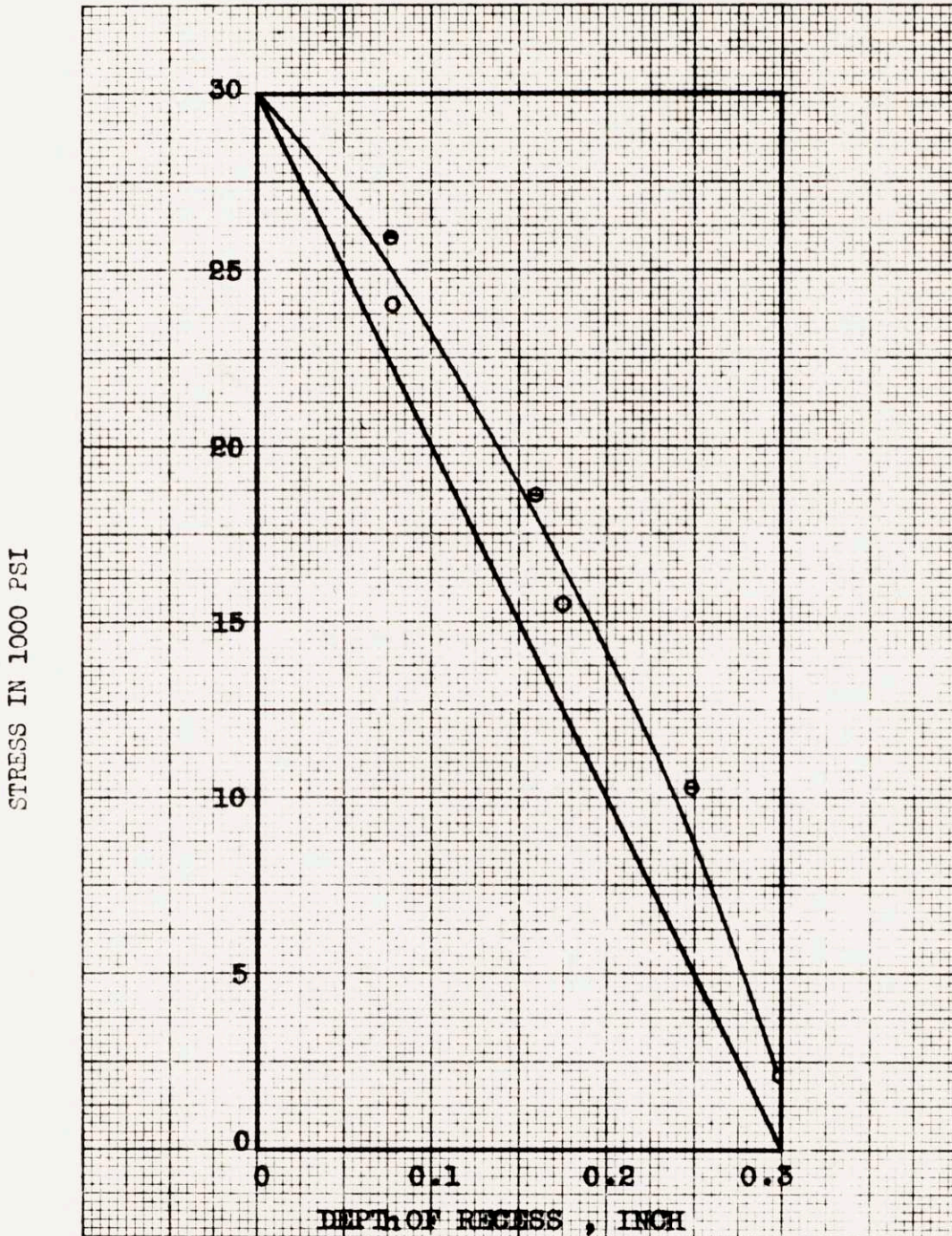


Fig. 50 - Stress Measured at the Bottom of Recesses (curve) Compared with the Stress Introduced to the Specimens I and II in Bending (straight line)

- e stress measured by x-rays
- o stress measured by strain gage



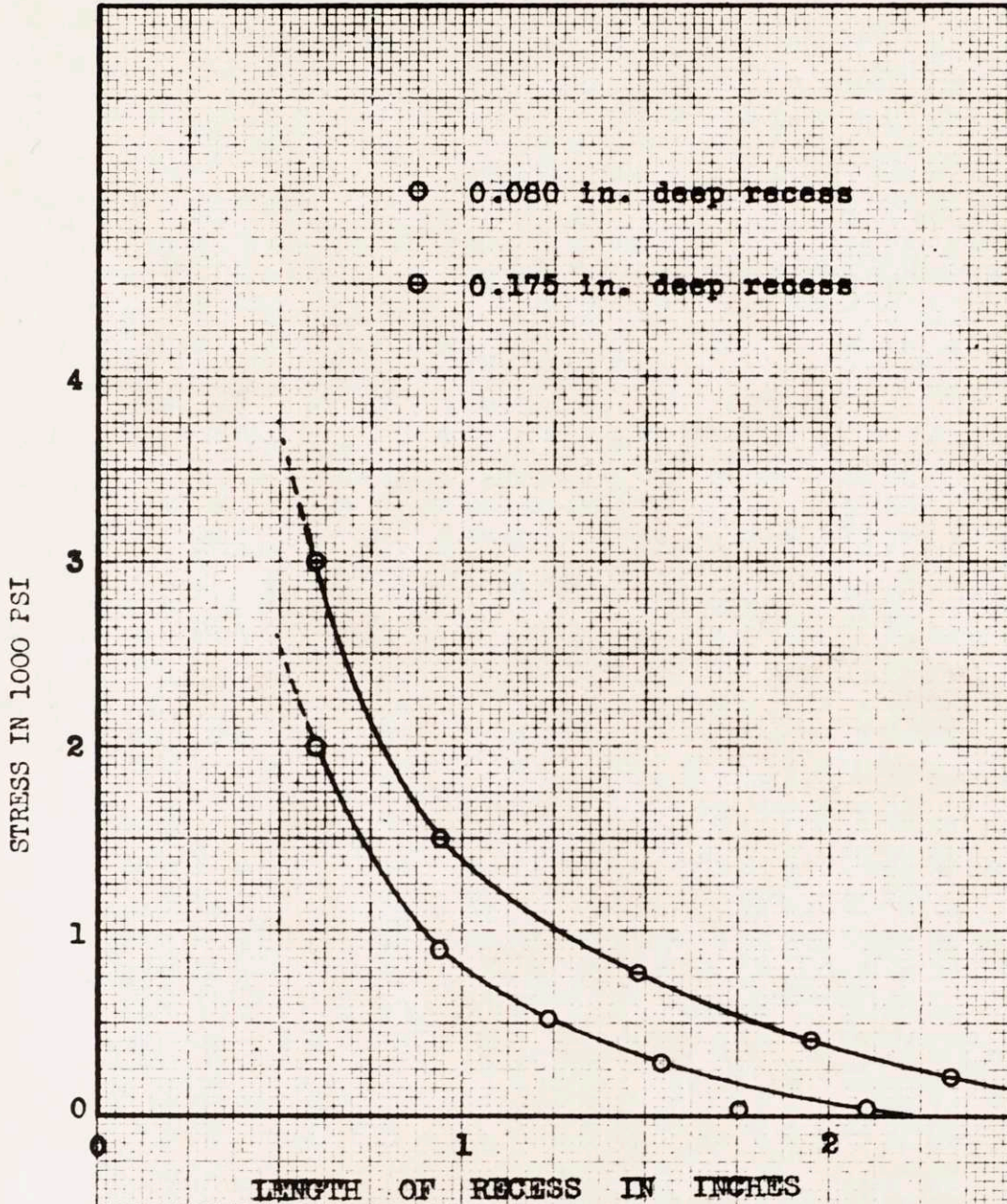


Fig. 51 - Increase in Stress by the Notch Effect of a Long and Narrow Recess versus the Length of the Recess for two different depth of Recesses.



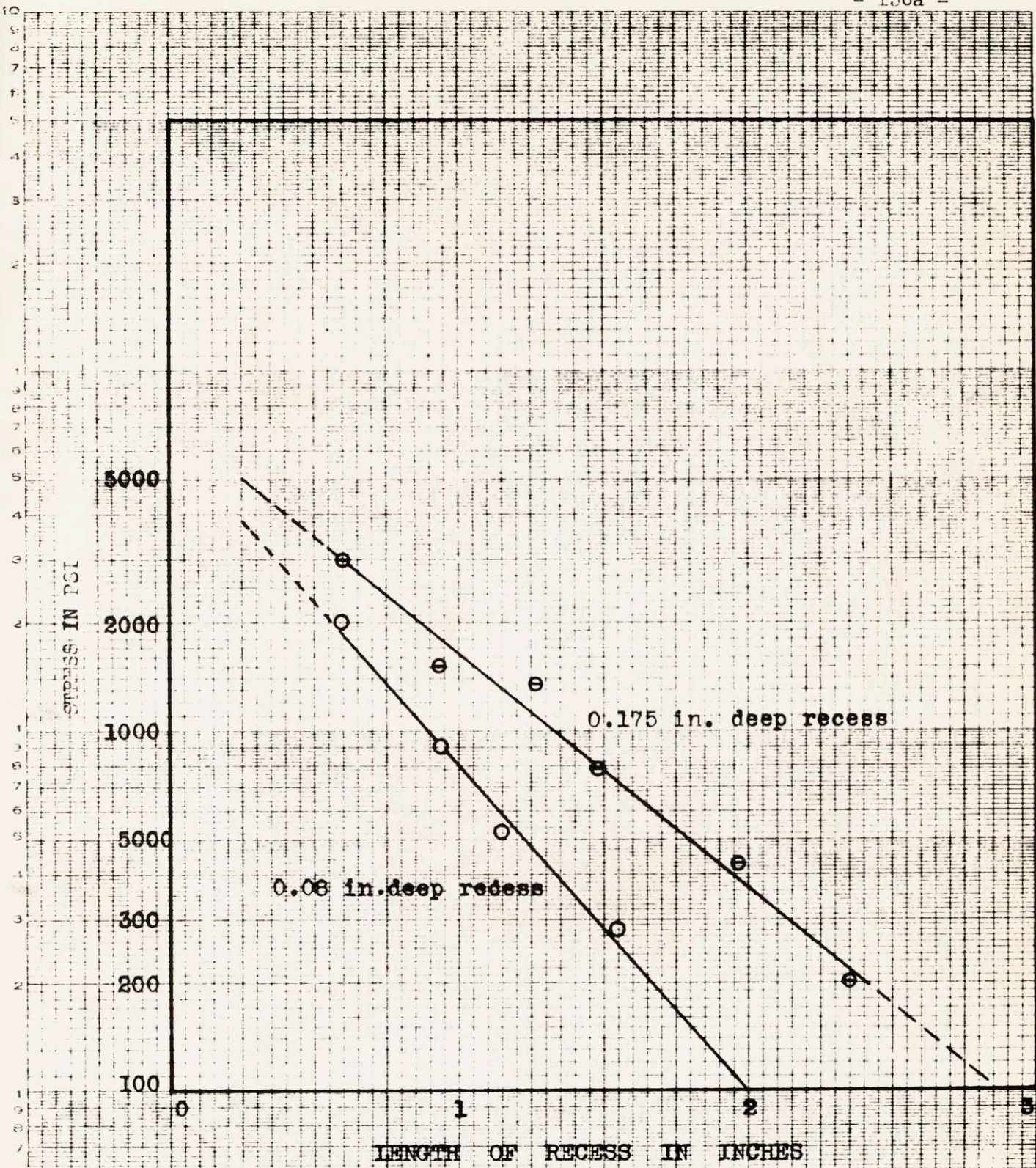


Fig. 52 - Increase in Stress in the Long and Narrow Recess versus the Length of the Recess for two depths of Recesses.



rays nearest to the surface make an angle of about twenty degrees. Therefore, the relation between the length and the depth of a recess is as follows:

$$1/2 \times \text{length of recess} \times \tan 20 = \text{depth}$$

or

$$L \times 0.182 = D \quad (16)$$

where L and D are the length and depth of the recess, respectively.

As the x-ray method of measuring stresses is the only method that can be used in application of the recessing method, the required length of the recess for the reflected x-rays to come out of the recess will limit its notch effect to a small value, so that correction of the measured stress is not necessary.

In the experiments on Specimen IV, the notch effect across the narrow and long recess was considered; and it was found that when the recess is along the uniaxial stress, the transverse notch effect was found to be 755 psi, which can be ignored as compared to the 20,500 psi stress in the longitudinal direction of the recess. However, when the uniaxial stress of 20,500 psi is perpendicular to the direction of the recess, it causes a 6,760 psi stress inside and in the direction of the recess; i.e., stress in the direction of the recess is changed to 33 percent of the stress acting in the direction perpendicular to the recess. Therefore, whenever biaxial stress is known to exist, a narrow and long recess cannot be used without making too great an error in measurements.

#### H. Conclusions on the Long and Narrow Recess

It is concluded from the discussion of the results obtained from the experiments on the narrow and long recess that:



(a) If uniaxial stresses are known to exist in a specimen, and the value of stress below the surface is to be measured, it is sufficient to machine a narrow and long recess and to measure the stress at the bottom center of the recess by means of x-rays. In order to have the error caused by the notch effect of the recess below that detected by the x-ray method, the width of the recess will be about  $3/16$  inches and its length not less than that determined by equation (16a)

$$L = 5 \frac{1}{2} D \quad (16a)$$

where L is the length and D the depth of the recess.

(b) If biaxial stresses exist, the stress in the direction of and inside the recess will be changed by 33 percent of the stress acting in the direction perpendicular to the recess.

The theory of recessing discussed above was not applied to the long and narrow recesses because, when stress is uniaxial, no correction of the measured stress is necessary; and, when stress is biaxial, the 33 percent notch effect of the stress in the transverse direction is too high for the recess to be of any use. In order to eliminate the effect of the transverse stress, a circular recess will next be considered.

### XIII THE CIRCULAR RECESS

It was concluded, from the investigation of the long and narrow recess that, whenever biaxial stresses existed, it could not be used to measure stresses below the surface. Because of the narrow width ( $3/16$  inches) of the recess, the notch factor in the transverse direction is very high (2.4), and the effect of transverse stress on the stress in the direction of the recess is 33 percent of the transverse stress. To decrease the notch effect in the transverse direction, a circular recess will be investigated.

#### A. The Choice of Specimen V and Its Preparation

In the investigation of the circular recess, the effect of the diameter and depth on the longitudinal and transverse stresses is to be examined. As the circular recess removes more material than a long and narrow recess, the specimen chosen was much larger than those used so far. Specimen V is a mild steel flat, 1 x 6 x 82 inches in size. The layout of the recesses with their depths is shown in Figure 54. In the machining of the recesses, the specimen is clamped on a milling machine and bored with a one-fourth inch drill close to the desired depth, Figure 56a. Then, with a centerless end mill, one-half inch in diameter, the recess is machined to the exact depth, producing a flat bottom. The bottom of the recess is then polished with abrasive powder, as described in the application of the recess below, to remove the chips from the machining. After all the machining operations are done and the recesses of one-half inch diameter are polished and degreased with acetone, electrical strain gages of special type are attached to the gages as shown in



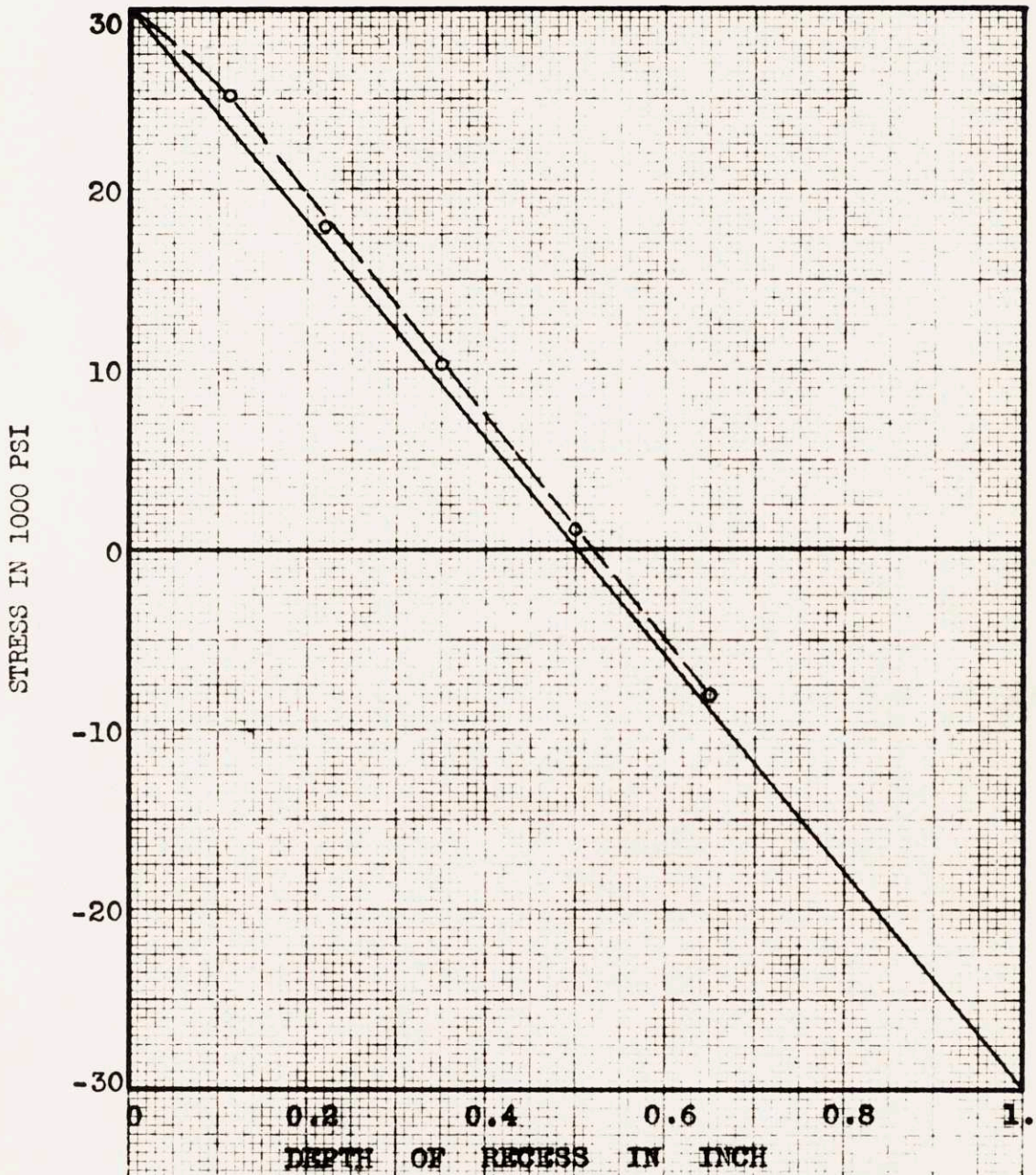


Fig.53 - The Stress in Recess (curve) Compared with the Stress Introduced to Specimen III in Bending (straight line)





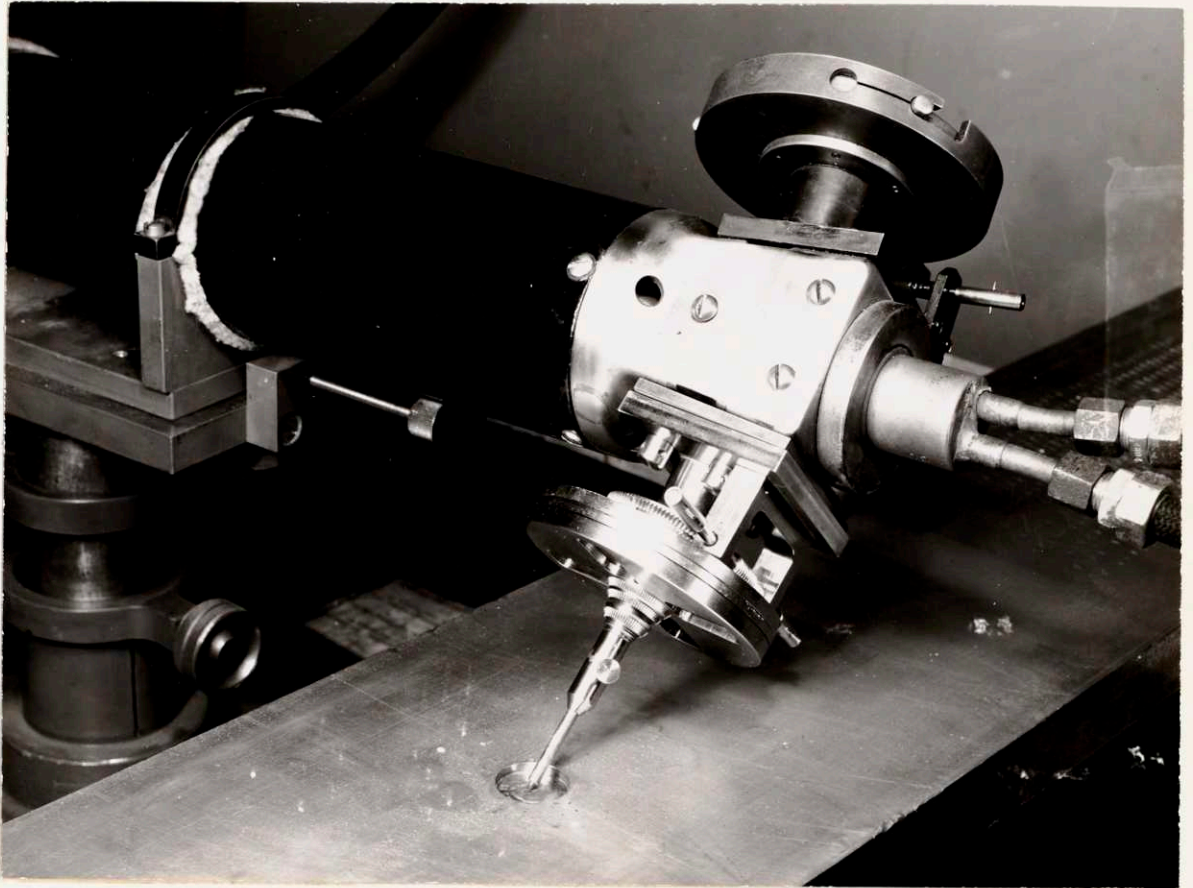


Figure 56a. Picture of a Recess under X-ray  
Tube.

Figure 55, with the remaining gages to measure the strain in the specimen itself. Recesses Nos. 1 and 4 are 0.1 inches deep, recesses Nos. 2 and 5 are 0.2 inches deep, and recesses Nos. 3 and 6 are 0.3 inches deep. Recesses Nos. 1, 2, and 3 have their gages in the longitudinal direction of the specimen, while recesses Nos. 4, 5, and 6 have their gages in the transverse direction. Recess No. 7 is 0.498 inches deep, and the strain gage is in the longitudinal direction. The effective size of the gages are as follows:

Gages - 1 to 4	1/8 inch long	1/8 inch wide
Gages - 5 to 7	1/8 inch long	3/32 inch wide
Gages - 8 to 26	1/2 inch long	(Type A-5)

After the strain gages have been attached, the specimen is left over the hot radiator in the laboratory for twenty-four hours; and then, while the specimen is still hot, the gages are covered with petrosene wax to protect them. Long insulated and numbered wire leads are soldered to the leads of the strain gages for measuring the strains in tension and in bending.

#### B. Testing of Specimen V in Tension and in Bending

For the tensile test, a Riehle Universal testing machine of 400,000 pounds capacity is used, Figures 46 and 57. Tests for bending are conducted in a Riehle Universal testing machine of 100,000 pounds capacity used mainly for transverse testing, Figure 47. Figure 56 shows the application of the load in bending the specimen.

In making the tensile test, first a load of 110,000 pounds is applied to the specimen and relieved. Then, strain gage readings



143

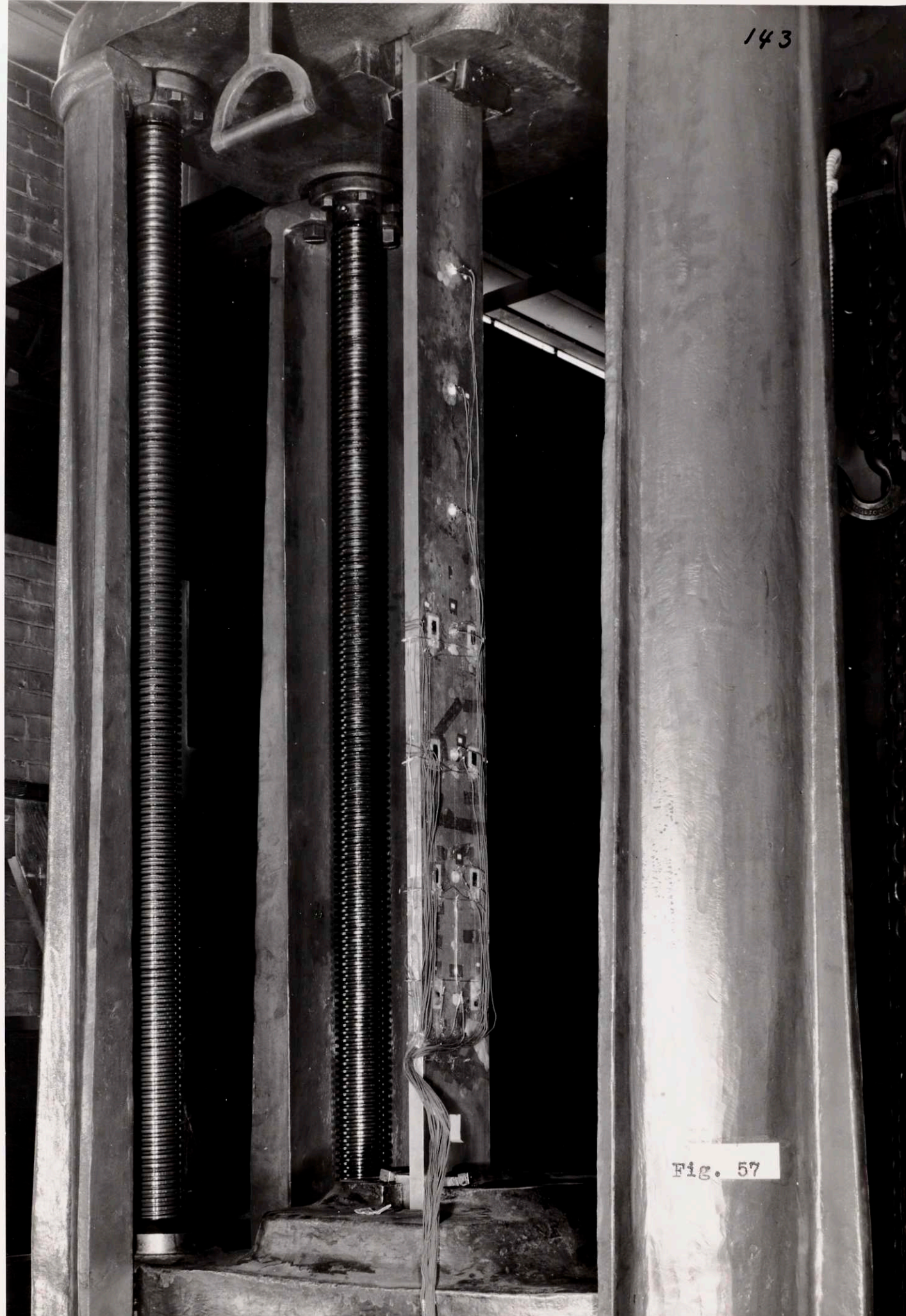


Fig. 57



are taken at no load, 70,000 pound load, 90,000 pound load, and then at zero load again. The averages of the front gages and those of the back gages are taken for each load reading; and, from the slight bending, if any, the strain at the layer of the recess is computed. The strains thus computed and the strain in the recess are then multiplied by  $\frac{1000}{\text{Computed Strain}}$  to obtain a uniform strain in the base metal for each recess. Then the average of the computed values of the strain for the loads of 70,000 and 90,000 pounds is taken to represent the strain in the recess. For recesses containing gages in the transverse direction, Figure 55, the strain measured on the specimen at the other gage of the same depth is taken for comparison, as these recesses are symmetrical in the specimen.

After the investigation of the recesses one-half inch in diameter, both in tension and in bending, is completed, the gages in the recesses are removed and the diameter of the recesses increased to three-quarters of an inch. Strain gages are then placed in the recesses and the same tensile testing and bending operations repeated that were done in the case of the recess one-half inch in diameter. In the third step, the diameter of recesses Nos. 2, 3, 5, and 6 are enlarged to one inch. The depth of recess No. 1 is increased to 0.855 inches and that of recess No. 7 to 0.641 inches. Strain gages are cemented in the recesses, and the same tensile and bending tests are repeated once more.

### C. Results of Experiments in Tension and in Bending

As has been explained before, for easy comparison and uniformity of results in all the tensile tests, strains measured were in-

creased proportionally to obtain a strain of 1000 micro inches per inch in the specimen. Thus, no matter what the diameter or the depth of the recess is, or the actual load applied on the specimen, the strains measured in the recesses can be shown together, and the effects of the depth and the diameter of the recess are easily observed.

In the bending tests, measured strains are increased proportionally to get the strains on the surface of the metal to 1000 micro inches per inch. The data recorded in the bending tests of Specimen V are summarized in Table 45, in which the figures represent the strain in micro inches per inch in recesses for 1000 micro inches per inch strain at the surface of the specimen. Data for the recesses one-half inch in diameter represents the average of two tests at different loads. Of the four sets of data given for recesses three-fourths inches in diameter, the first two had 3,100 and 4,150 pound loads, respectively; and the effective length of strain gages in the recesses was one-fourth inch. In the last two sets of data, the loads on the specimen in testing were 3,860 and 4,000 pounds, respectively, and the length of the strain gage was one-eighth inches, as in all other cases.

In the calculation of stresses for the recesses three-fourths of an inch in diameter, the average of the four sets of readings is considered.

Stresses calculated from the strain data in Table 45 are in Table 46. Equation 15 is used to determine stresses from the strains. In Table 46, for each diameter of a recess, the first figure in each



Table 45

Strain in recesses, in micro inches per inch, obtained in bending tests of specimen V. Figures with minus sign are strains in the transverse direction, except for the last two columns

Diameter of Recess in Inches	Depth of Recesses in Inches					
	0.100	0.200	0.301	0.498	0.641	0.855
1/2	950	805	572	135		
	-219	-196	-170			
3/4	926	797	600	173		
	-222	-191	-159			
3/4	940	792	598	175	-168	-820
	-205	-189	-154			
3/4	915	758	616	175		
	-210	-187	-148			
3/4	895	745	591	162		
	-214	-197	-148			
Average 3/4	920	773	601	171	-168	-820
	-213	-191	-152			
1		766	597			
		-197	-140			

Table 46

Stress in recesses in pounds per square inch obtained in bending specimen V. First figure is the stress in the longitudinal direction, and the second figure is the stress in the transverse direction. The third figure is the stress in the longitudinal direction, ignoring the transverse strain in the calculation.

<u>Diameter of Recess in Inch</u>	<u>Depth of Recesses in Inch</u>					
	<u>0.100</u>	<u>0.200</u>	<u>0.301</u>	<u>0.498</u>	<u>0.641</u>	<u>0.855</u>
	29,200	24,600	17,200			
1/2	2,180	1,520	66			
	28,500	24,200	17,200	4,050		
	28,300	23,600	18,400			
3/4	2,080	1,350	925			
	27,600	23,200	18,000	5,130	-5,040	-24,600
		23,350	18,300			
1		1,090	1,250			
		23,000	17,400			

column of the recess is the stress measured in the longitudinal direction; the second figure is the stress in the transverse direction; and the third figure is the stress in the longitudinal direction, calculated without considering the effect of the strain in the transverse direction. The discrepancy between the stress computed by equation (15) and the stress obtained by ignoring the transverse strain and multiplying the strain by thirty is only 2.5 percent, thus justifying the use of stresses obtained in the last three columns of Table 46.

Measured stresses in Table 46 are also shown in Figure 58, where the straight line is the stress pattern introduced to the specimen in bending, and the curves are stresses measured in the recesses.

The strains in micro inches per inch recorded in the recesses in the tensile test of specimen V are summarized in Table 47. Figures with minus signs are strains in the recesses in the transverse direction. In all these data, strains measured in the experiment are increased proportionally, in order to obtain a uniform strain of 1000 micro inches per inch in the specimen itself.

Table 49 contains stress in recesses computed from strains in Table 48 by equation (15).

Before the results in Table 49 are plotted, it is of interest to discuss what happens as the recess gets deeper and the bottom of the recess approaches to the opposite side of the flat specimen.

When the depth of the gage was less than one-half inch, the strain gage at the opposite side of the recess was not affected by



Table 47a

Strain in recesses in micro inches per inch obtained in the tensile test of Specimen V. Figures with minus signs are strains in the transverse direction

<u>Diameter of Recess in Inches</u>	<u>Load in Tensile Test, 1000 Pounds</u>	<u>Depth of Recesses in Inch</u>					
		<u>0.100</u>	<u>0.200</u>	<u>0.301</u>	<u>0.498</u>	<u>0.641</u>	<u>0.855</u>
1/2	100	1160	1240	1275	1325		
		- 268	- 322	- 416			
1/2	60	1160	1250	1285	1310		
		- 270	- 293	- 418			
Average		1160	1245	1280	1317		
		- 269	- 308	- 417			
1	85		1177	1300			
			- 346	- 370			
1	99.3		1215	1275			
			- 322	- 342			
1	83		1210	1296			
			- 327	- 312			
1	98		1209	1272			
			- 324	- 309			
Average			1203	1286			
			- 330	- 333			

Table 47b

Strain in recesses in micro inches per inch obtained in the tensile test of Specimen V. Figures with minus signs are strains in the transverse direction

Diameter of Recess in Inches	Load in Tensile Test, 1000 Pounds	Depth of Recesses in Inches					
		0.100	0.200	0.301	0.498	0.641mm	0.855
3/4	100	1165	1216	1300	1400		
		- 302	- 334	- 350			
3/4	59.5	1138	1194	1300	1400		
		- 296	- 330	- 351			
3/4	103	1105	1160	1264	1380		
		- 312	-	- 324			
3/4	83	1125	1178	1304	1335		
		- 317	- 346	- 370			
3/4	105	1100	1172	1292	1366		
		- 316	- 333	- 354			
3/4	99	-	-	1285	1370		
		-	-	- 360			
3/4	85				1462	1680	
3/4	99.3				1410	1685	
3/4	83				1450	1700	
3/4	98				1440	1688	
Average		1127	1184	<b>1291</b>	1392	1440	1688
		- 309	- 336	- 352	-	-	-

Table 48

Average strain in recesses taken from Tables 47a and b  
in micro inches per inch obtained in the tensile tests  
of Specimen V. Figures with minus sign are strains in  
the transverse direction.

Diameter of Recess in Inches	Depth of Recess in Inches						
	<u>0.100</u>	<u>0.200</u>	<u>0.301</u>	<u>0.498</u>	<u>0.641</u>	<u>0.855</u>	<u>1.00*</u>
1/2	1160	1245	1280	1317			
	- 269	- 308	- 417				
3/4	1127	1184	1291	1392	1440	1688	3,000
	- 309	- 336	- 352				-2,000
		1203	1286				
		- 330	- 333				

\*Strain for the recess all the way through the thickness of the plate has been calculated theoretically.



Table 49

Stress in pounds per square inch, in recesses obtained in the tensile test of Specimen V. For each diameter of a recess, the first figure is the stress in the longitudinal direction, the second in the transverse direction and the third stress in the longitudinal direction, where the effect of the transverse strain is ignored.

Diameter of recess in inches	Depth of Recesses in Inches						
	0.100	0.200	0.301	0.498	0.641	0.855	1.00
	35,600	33,000	38,100				
1/2	2,540	2,120	1,090				
	34,800	37,350	38,400	39,500			
	34,200	35,800	39,100				79,200
3/4	950	626	1,150				-36,300
	33,800	35,600	38,800	41,800	43,200	50,600	90,000
		36,040	39,100				
1		1,020	1,750				
		36,100	38,600				

the recess at all. In Table 50, the effects of the recesses of 0.498 and 0.641 inches depth are shown, respectively.

It is observed from Table 50 that, when the depth of the recess is 0.498 inches, the effect is just beginning to be felt at the other side of the specimen; but, when this depth is increased to 0.641 inches in the specimen one inch thick, the strain gage opposite the recess records 103 micro inches per inch more than the other gages, for an actual strain of 1000 micro inches per inch.

For the limiting case, i.e., when the depth of the recess reaches the thickness of the plate, the strain has been computed theoretically.

D. The Shape of a Circular Hole in an Infinite Plate Under the Uniform Biaxial Stresses

If  $a$  is the radius of the circular hole and the translations of the points  $U$  and  $V$  caused by the stresses  $S_1$  and  $S_2$  are given by equations (17) and (18)<sup>(18)</sup> for uniform tension, where  $S_2 = 0$ ,

Figure 61.

$$U = \frac{a^2 s_1}{2Er} \left[ \frac{2r^2}{a^2} + (5 + \nu) - \frac{a^2}{r^2} (1 + \nu) \right] \quad (17)$$

$$V = \frac{a^2 s_1}{2Er} \left[ -\frac{2\nu r}{a^2} - (3 - \nu) + \frac{a}{r^2} (1 + \nu) \right] \quad (18)$$

where  $E$  is the modulus of elasticity and  $\nu$  Poisson's ratio.

As applied to the problem of recessing, the strain produced in an infinitely thin sheet at the end of the hole is:

$$\frac{U}{a} = 3000$$

micro inches per inch in the direction of stress  $S_1$ , and

$$\frac{V}{a} = -2000$$

micro inches per inch in the transverse direction.



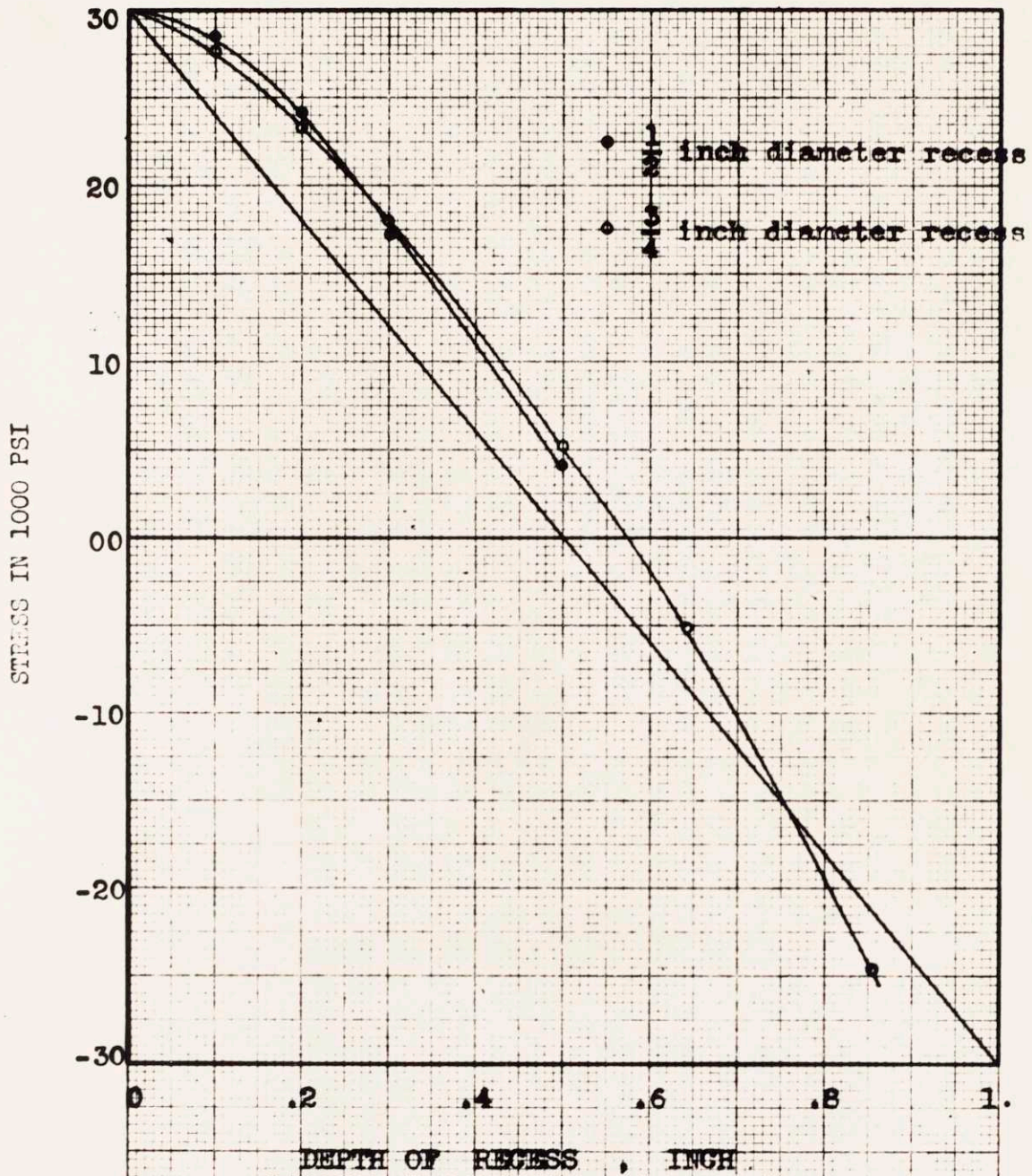


Fig. 58 - Stress Measured at the Bottom of Recesses (curves) and the true Stress Pattern (straight line) in Specimen V.



Table 50

Strain in micro inches per inch recorded by gages No. 25 and the deviation of these readings  
compared with the average of gages Nos. 24 and 26

<u>Diameter of Recess in Inches</u>	<u>Depth of Recess in Inches</u>	<u>Strain Recorded</u>		<u>Deviation of Gage 25 from the Average of 24 and 26</u>	<u>Deviation per 1000</u>	<u>Average Deviation</u>
		<u>Gage 25</u>	<u>Gages 24 and 26</u>			
1/2	0.498	500	498	2	4	2
		299	299	0	0	
3/4	0.498	499	498	1	2	8
		282	283	- 1	- 3	
		512	506	6	12	
		414	410	4	9	
		528	518	10	20	
		494	485	9	18	
3/4	0.641	458	415	43	104	103
		543	495	48	97	
		445	403	42	104	
		543	490	53	107	

The results of tensile tests, Table 49, are shown in Figure 59.

E. Discussion of Results in Bending and in Tension

As noted in Figure 59, in a plate one inch thick, when the depth of the recess is less than one-half inch, the opposite side of the recess is not affected by the recess, and the plate can be considered as infinitely thick. At a depth of one-half inch, the strain gage directly opposite the recess of one-half inch diameter showed only 0.2 percent increase, while that opposite the recess of three-fourths inch diameter showed 0.8 percent increase caused by the recess, Table 50. However, when the remaining thickness from the bottom of the recess to the opposite face of the specimen is less than one-half inch for a recess three-fourths inches in diameter, the plate can no longer be considered infinitely thick, Figure 59. Actually in practice it is not necessary to go close to the other side of the specimen. Instead a recess should be started from the other side.

When the depth of the recess of one-half inch diameter reaches one-half inch, the notch effect of the recess does not increase any more and stays constant. The shape of the curve for the recess three-fourths inches in diameter suggests that, Figure 59, the notch effect would be at the maximum at about a depth of three-fourths inches, but the limited thickness of the specimen does not permit the observation of this phenomenon.

It can generally be said that the notch effect of a recess of one-half inch diameter increases faster than that of a recess of three-fourths inch diameter, but the curve for the recess of one-

half inch diameter flattens down, reaching the maximum stress at a depth of one-half inches, while the stress of the recess of three-fourths inch diameter reaches a higher maximum at about a depth of three-fourths inches.

The maximum notch effect of the recess of one-half inch diameter is about thirty-three percent and that of the recess of three-fourths inch diameter is about forty-three percent. The notch effect in the transverse direction for a circular recess is usually less than seven percent; and, only in one case was it found to be eight percent, Tables 46 and 49. As, in most cases, the probable error in measuring the stresses by the x-ray method is not less than 10 percent, the transverse effect of the stress in circular recesses can be ignored. Therefore, the circular recessing method can be used to measure stresses below the surface, where a multiaxial stress pattern exists, if a law is found for correcting the measured stress in the direction of the stress. Equation (14), derived in the discussion of the theory of recessing, will be applied to the data obtained in the circular recess for correction of stresses measured.

A recess of one inch diameter is not very different in results from a recess of three-fourths inch diameter, Figure 59, and sufficient data is lacking for a full discussion of it.

#### F. Application of the Recessing Data to the Theory of Recessing

The solution of the theory of recessing was equation (14):

$$S = S' - ke^{-(a+k)z} \int_0^z S'_u e^{+(a+k)u} du$$



where  $S$  = true stress at the bottom of the recess,  $S'$  = stress measured at the bottom of the recess,  $a$ ,  $k$  = constants,  $z$  = total depth of the recess,  $S'_u$  = stress measured at depth  $u$ , and  $u$  = variable. The constants  $a$  and  $k$  vary with the changing diameter of the recess. To determine their values for a recess of one-half inch diameter, the values of  $S$ ,  $S'$ ,  $z$  and the variation of  $S'_u$  with the depth  $u$  must be known. By application of these experimentally determined figures in tension, Figure 59, to equation (14) at two definite points at least, the values of constants  $a$  and  $k$  are determined by trial and error.

The values of constants  $a$  and  $k$  thus determined are in Table 51.

Table 51

The Figures for Constants  $a$  and  $k$  for the Recesses of One-half Inch and Three-fourths Inch Diameters, Determined Experimentally.

<u>Diameter of Recess in Inches</u>	<u>Damping Factor <math>a</math></u>	<u>Stress Concentration Factor <math>k</math></u>
1/2	6.8	2.25
3/4	2.61	1.40

The values of stress concentration factor  $k$  and that of the damping factor are increasing with the decreasing diameter.

From the data in bending and in tension for the recess of one-half inch diameter, Figures 58 and 59, true stresses will be calculated and the computed results will be compared with the known values in order to determine the degree of precision of the recessing method.

Table 52 contains values of the different terms in equation (14), and Table 53 the true stresses introduced and calculated at different depths of Specimen V in bending. In Table 54 true stresses are calculated from the measurements in tension for the one-half inch diameter recess and the results compared with the stress introduced to the specimen. Data in the first four columns in Table 52 are not shown in Table 54.

The computed stresses in Table 54 are very close to 30,000 psi, introduced to the specimen in tension, Figure 60. This agreement was to be expected because, in the determination of the stress concentration factor  $k$  and the damping factor  $a$ , data obtained in tension was used. However, when the theory of recessing is applied to the tests in bending, with values of  $a$  and  $k$  determined from the data in the tensile test, the agreement between the computed true stresses and the known stresses introduced to the specimen is almost as good as that in tension, Table 53, Figure 60.

From the above results, it is concluded that the experimental result and the theory of recessing are in perfect agreement, and that stresses below the surface can be measured by the recessing method and corrected for the error introduced by the recessing operation.

#### G. Conclusion

In the investigation of the circular recessing method to measure stresses below the surface, the conclusions reached are as follows:

Table 52

The Values of the Terms Appearing in Equation (14) to Calculate True Stresses in Recessing

Depth of Recess z	$(a + k)z$	$e^{-9.05z}$	$e^{+9.05z}$	Apparent Stress* $S'_u$	$S'_u e^{+9.05u}$	$\int_0^z S'_u e^{+9.05u} du^{**}$
0.0	0.000	1.	1.	30,000	30,000	0
0.1	0.905	0.4041	2.472	28,500	70,452	5,023
0.2	1.810	0.1641	6.1101	24,200	147,862	15,939
0.3	2.715	0.066	15.104	17,300	261,300	36,397
0.4	3.620	0.0268	37.337	11,000	410,607	70,000
0.5	4.525	0.0108	92.296	4,050	373,800	111,000

\* from Table 46 and Figure 58.

\*\* Area under the curve, where  $S'_u e^{+9.05u}$  is plotted versus the depth of recess, z



Table 53

Stresses introduced to Specimen V in bending and stresses  
computed from the measurement in recesses

<u>Depth of</u> <u>Recess z</u> <u>in Inches</u>	<u>Stress</u> <u>Introduced</u> <u>in Psi</u>	<u>Stress</u> <u>Computed</u> <u>in Psi</u>	<u>Difference Between</u> <u>the True Stress</u> <u>and Stress Measured</u>
0.0	30,000	30,000	0
0.1	24,000	23,935	- 65
0.2	18,000	18,335	+ 335
0.3	12,000	11,896	- 104
0.4	6,000	6,780	+ 780
0.5	0,000	1,350	+1,350

Table 54

The values of the terms appearing in equation (14) and true stresses computed from the data obtained in the one-half inch diameter recess in tension. Stress figures are in psi

Depth of Recess z in Inches	Apparent Stress* $S'_u$	$S'_u e^{9.05u}$	$\int_0^z S'_u e^{9.05u} du$ **	Computed Stress $S$	Deviation from Stress Introduced, 30,000
0	30,000	30,000	000	30,000	00
0.1	34,800	86,025	5,790	29,540	-460
0.2	37,350	228,208	20,800	29,660	-340
0.3	38,400	580,000	58,000	29,800	-200
0.4	39,050	1,458,000	152,000	30,037	+ 37
0.5	39,500	3,644,635	390,000	30,000	00

\* Data from Table 49 and Figure 59.

\*\* Area under the curve where  $S'_u e^{9.05u}$  is plotted versus the depth of recess z.

(1) In a specimen with uniform stress, the effect of a circular recess on the stress measured at the bottom of the recess increases with increasing depth and reaches its maximum at about a depth equal to the diameter of the recess. This maximum is about 30 percent higher than the stress introduced to the specimen, for a recess of one-half inch diameter, and higher for a larger diameter recess.

(2) The effect of the stress in the transverse direction is less than eight percent of the transverse stress, which can be ignored, considering that x-rays are to be used exclusively to measure stress in recesses and the accuracy of the x-ray method of measuring stresses is not better than 90 percent.

(3) Stresses introduced by recesses can be corrected easily and accurately by the theory of recessing explained above.

The above conclusions are for specimens large enough as compared with the recess, so that the stress pattern in the specimen is not altered by the recess.

In Part III of this paper the recessing method of measuring stresses below the surface will be applied to a bent plate, and the results obtained will be compared with those obtained by the block method.



PART III

APPLICATION OF THE RECESSING METHOD TO MEASURE STRESSES  
THROUGH THE THICKNESS IN A PLATE BENT BEYOND THE  
ELASTIC LIMIT

XIV RESIDUAL STRESSES IN A ONE-INCH THICK BENT PLATE

A. Investigation

In practice, when metal plates are bent beyond their elastic limit, thick plates fail with a brittle fracture while thinner plates of the same material do not fail for the same percentage of plastic deformation as the thick plates. In the x-ray laboratory of the Department of Metallurgy of Massachusetts Institute of Technology, Mr. Kenneth Bohr has undertaken the problem of measuring residual stresses in plates bent to one percent plastic deformation on the surface. Specimens of three different thicknesses were to be examined in order to determine the trend of the stress pattern with increasing thickness, and the size factor, if any, causing the brittle fracture in the thick plates. The thickness of the plates was one-half inch, one inch, and one and one-half inches, respectively.

The block method of measuring stresses through the thickness, described earlier, was to be used to measure stresses. It was decided that stresses in the one inch thick plate should also be measured by the recessing method, using a recess of one-half inch diameter.

### B. Preparation of the Specimen

The specimen is a mild steel plate, one inch thick, six inches wide, and twenty inches long. It is surface ground to remove the oxidized layers on both faces and stress relieved by heat treatment. The stress, measured by x-rays on the surface of the specimen after heat treatment, was found to be 1350 psi.

Two SR-4 strain gages of Type A-3 are cemented to the specimen to measure the percent deformation in bending, Figure 62; and the specimen is bent in a Riehle Universal testing machine of 100,000 pounds capacity, Figure 47, as shown in Figure 63. The data recorded in bending are shown in Table 55. The specimen is bent to obtain one percent plastic deformation at the surface.

In the bending of the specimen beyond 19,000 pounds, a small increase in load caused a large increase in the strain on the specimen. For this reason, no attempt was made to reach 10,000 micro inches per inch deformation on the specimen; and 9943 micro inches per inch was considered sufficiently close.

### C. Measurement of Residual Stresses in the Bent Plate by X-rays

As observed in Table 55, the specimen is bent to obtain one percent plastic deformation on the tension side of the plate. The residual stress pattern caused by the bending will be determined by the x-ray method of measuring stresses, using the recessing method of measuring stresses below the surface.

To measure the stress on the surface of the specimen, the surface is etched ten-thousandths of an inch deep by thirty percent nitric acid; and the rough surface left by the etching is polished



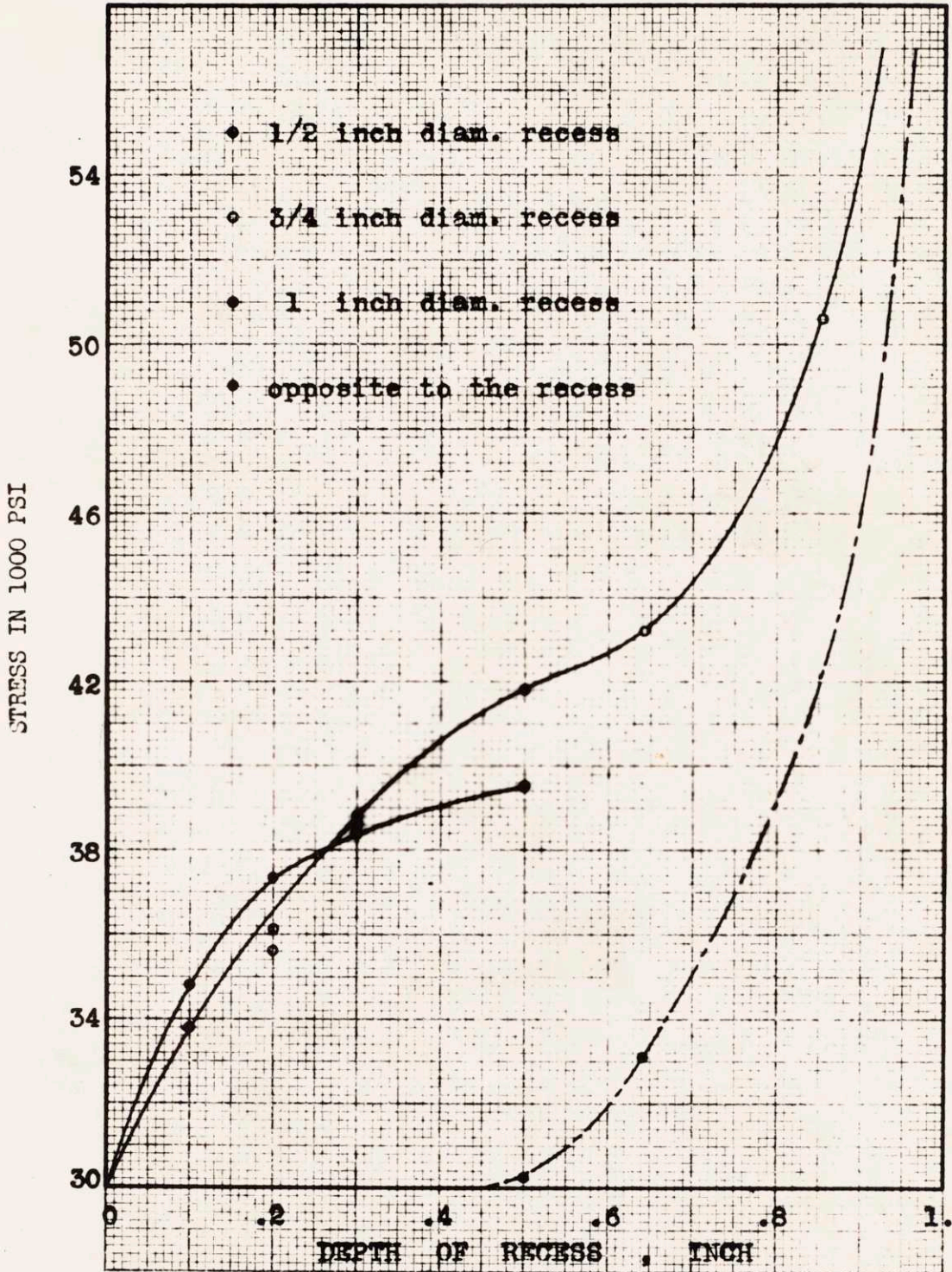


Fig. 59 - Stresses Measured at the Bottom of Recesses of Specimen V in Tension



Table 55

The data recorded in bending of the specimen. Strains are in  
micro inches per inch

<u>Load in</u> <u>Pounds</u>	<u>Strains</u> <u>in Gage 1</u>	<u>Strains</u> <u>in Gage 2</u>	<u>Average</u> <u>Strain</u>	<u>Deflection in Thou-</u> <u>sandths of an inch</u>
00	0	0	0	0
1,400	222	262	242	-
5,660	849	909	879	50
10,000	1,404	1,457	1,430	84
12,250	1,808	1,805	1,836	706
14,650	2,337	2,403	2,370	130
17,400	4,101	4,233	4,167	180
18,500	6,468	6,588	6,528	234
18,920	7,578	7,738	7,658	260
19,180	8,858	9,060	8,959	290
19,290	9,842	10,043	9,943	314
00	3,252	3,285	3,270	137

by emery paper Nos. 1, 0, 00. In each step, the scratches left from the previous step are removed. Finally, a one-thousandth of an inch layer is removed by ten to twenty percent nital solution. By this process of polishing and etching, any possible cold worked layer on the surface of the specimen is removed, and the surface is then ready for measuring of the stresses by x-rays.

The thickness of the layer removed by polishing or etching is measured by a mechanical dial fastened to a three-point support, Figure 66. Two of these three points are sharp and are slightly hammered into the specimen for reference points. In etching, these reference points are covered by vaseline.

On the surface of the specimen, stresses are measured at three points, Figure 62, on the line across the specimen, close to each other; and the stresses measured at point 1 are taken as the representative of the stress at the surface of the specimen. These measured stresses are in Table 56.

Table 56

Stresses measured at the surface of the bent plate

<u>Location,</u> <u>Figure 62</u>	<u>Stress Psi in</u> <u>Longitudinal Direction</u>	<u>Stress psi in</u> <u>Transverse Direction</u>
1	-29,200	+13,200
2	-28,700	+10,000
3	-29,600	+16,000

The next step in the experiment is to machine the recess and prepare it for the stress measurement by x-rays as follows:

(1) The specimen is clamped in a milling machine, and a recess of one-half inch diameter is machined, using a centerless end mill of one-half inch diameter.

(2) A layer of at least 0.010 inches is removed from the bottom of the recess by etching with thirty percent nitric acid to remove the cold worked layer.

(3) To smooth the bottom of the recess roughened in the previous step, a liberal amount of carborundum abrasive powder No. 150 is placed in the recess with some water. A hardwood cylinder of about one-fourth inch diameter is attached to the grips of a hand drill, which in turn is plugged to a Variac transformer to adjust the speed, Figure 64, then while the drill is rotating at a slow speed, a piece of cotton is held at the flat end of the hardwood cylinder, the cylinder is then rotated in the recess containing the abrasive powder and water. The cotton holds on the abrasive powder and polishes the bottom of the recess. It is replaced with a new piece of cotton before it wears out.

After carborundum abrasive powder No. 150 has been used, powders No. 200, 320, and 500 are used in succession to obtain a smooth surface at the bottom of the recess.

(4) The polished surface is etched with a nital solution to remove at least a 0.001 inch layer. The recess is now ready for measuring the stress by x-rays.

At least two x-ray pictures are taken in every direction with new settings; and, if the stresses measured are not close enough, the process is repeated.



STRESS IN 1000 PSI

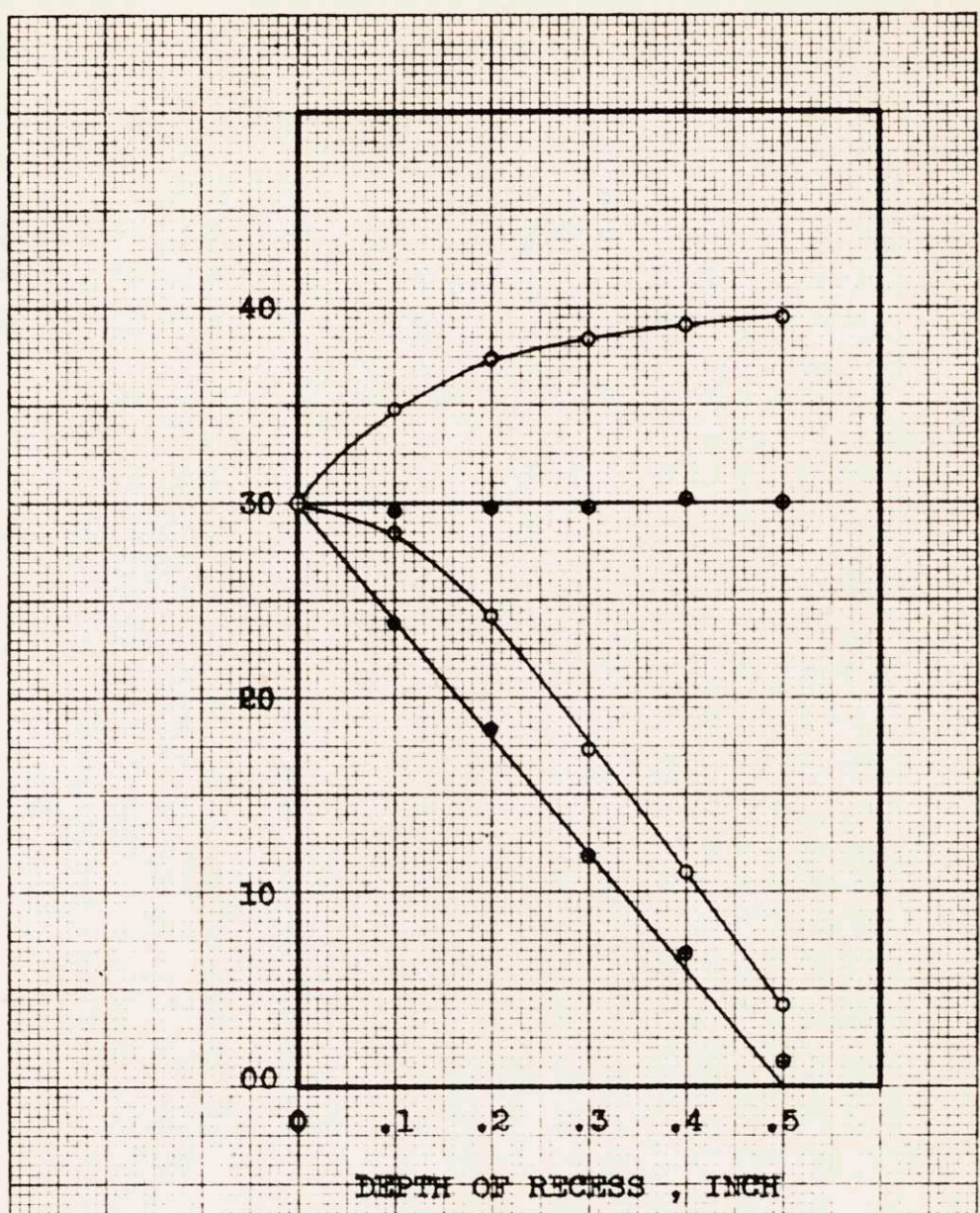


Fig. 60 - Stress Measured in one half of an inch Diameter Recess (open circles) in Tension and in Bending, and the corrected Stresses (crossed circles). Straight Lines represent the Stress Pattern produced in the Specimen.

When the depth of the recess is increased slots one-eighth inch wide are cut in the longitudinal and transverse directions of the plate in order to permit the reflected x-rays to come out of the recess, Figure 65. It will be shown later that the effect of these slots on the stress at the bottom of the recess is not large enough to merit consideration. In Figure 65, the camera is set for the exposure at forty-five degrees in the longitudinal direction of the plate. The rod extending from the camera into the recess is used to adjust the camera, so that x-rays will strike at the center of the recess at an angle of forty-five degrees. The results obtained in measuring the apparent stress in recesses of different depths are in Table 57 and in Figure 69.

XV EFFECT OF THE SLOTS ON THE MEASURED APPARENT  
STRESSES IN A RECESS

If the depth of a recess of one-half inch diameter is more than 0.09 inches, the reflected x-rays cannot come out of the recess while shooting at an angle of forty-five degrees at the bottom center of the recess. In order to allow these reflected rays to come out of the recess, a slot one-eighth inch wide is machined in the specimen. After measurement of stresses in the recess of the bent plate is completed, another recess is machined in the plate in order to investigate the effect of the slots in the longitudinal and transverse directions.



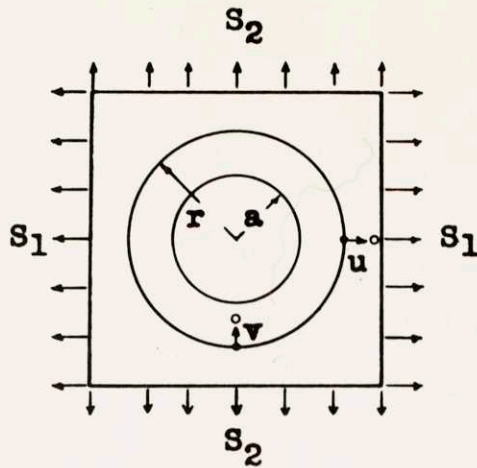


Fig. 61 - Deformation of a circular Hole in a Plate .

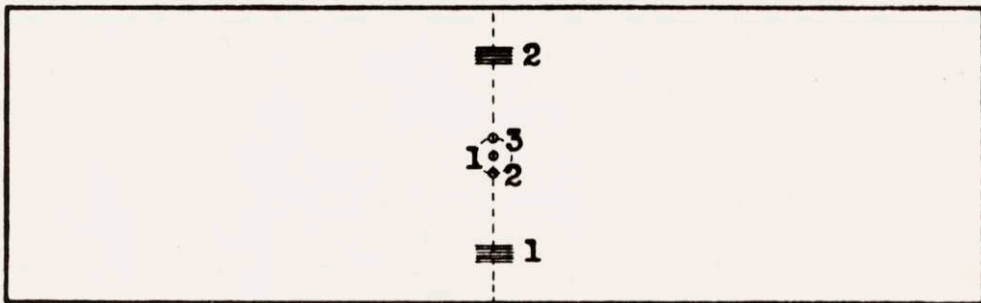


Fig. 62 - The Bent Plate and the Layout of Gages. The three Points at the Center of the Plate show where Stresses are measured before Recessing. The dotted Circle is the Recess.

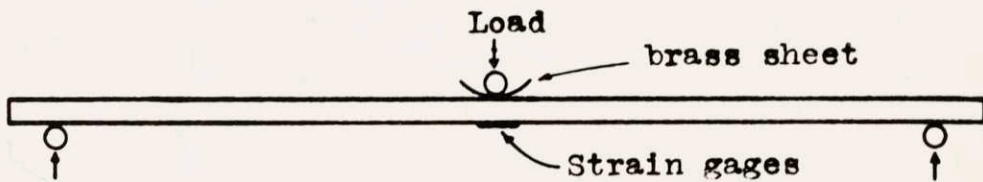


Fig. 63 - The Bending of the Plate



Table 57

Stresses measured in recesses in the longitudinal and  
transverse direction in psi

<u>Recess Number</u>	<u>Depth of Recess in Inches</u>	<u>Apparent Stress in Longitudinal Direction S'<sub>x</sub></u>	<u>Apparent Stress in Transverse Direction S'<sub>y</sub></u>
0	0	-29,200	+13,200
1	0.068	-22,500	+12,600
2	0.125	-11,400	- 5,930
3	0.210	- 4,560	+13,200
4	0.347	+11,400	+ 9,600
5	0.480	+10,500	+ 8,200

#### A. Machining of Slots and Results of the Tests

The second recess is machined beside the first one, Figure 67. The recess is 0.354 inches deep. This depth was chosen because the stress in the longitudinal direction and the variation of stress in the specimen are at their maximum at this depth, Figure 69. An electrical resistance strain gage of type A-8 (one-eighth inch long) is cemented at the bottom of the recess in the longitudinal direction, and the gage reading is taken. Then the slot in the longitudinal direction is cut in steps; and, at each step, the gage reading is recorded.

In cutting the slot, an end mill of one-eighth inch diameter is used. Cutting is done in the horizontal direction, starting from the edge of the recess. At each step of the cutting a layer

0.050 inches from the bottom of the recess, Figure 68, to permit the reflected x-rays to come out. The slot in the transverse direction is machined in the same manner as the one in the longitudinal direction. The results are in Table 58.

## XVI DISCUSSION OF RESULTS

### A. Relaxations Caused by the Slots

As is seen in Table 58, the making of the slot in the longitudinal direction is hardly felt by the strain gage in the same direction at the bottom of the recess. The machining of the transverse slot caused a relaxation of  $-32$  micro inches per inch, i.e., a relaxation of stress of  $-960$  pounds per square inch. The second recess in which the effect of the slots was examined is too close to the edge of the specimen. There is another recess at the center of the specimen with another slot in the transverse direction. The area removed in the slot of the second recess is appreciable compared to the remaining section. Actually, if the relaxation caused by the slot in the first recess was measured, a figure lower than  $-960$  psi would be expected because a relatively small area of the cross-section of the plate would be removed, and the area removed would be further away from the edge of the plate than is the case in the second recess, Figure 67.

### B. Stresses Measured in the Recess

Apparent stresses measured in the recess in the longitudinal and transverse directions of the plate are in Table 57. The apparent

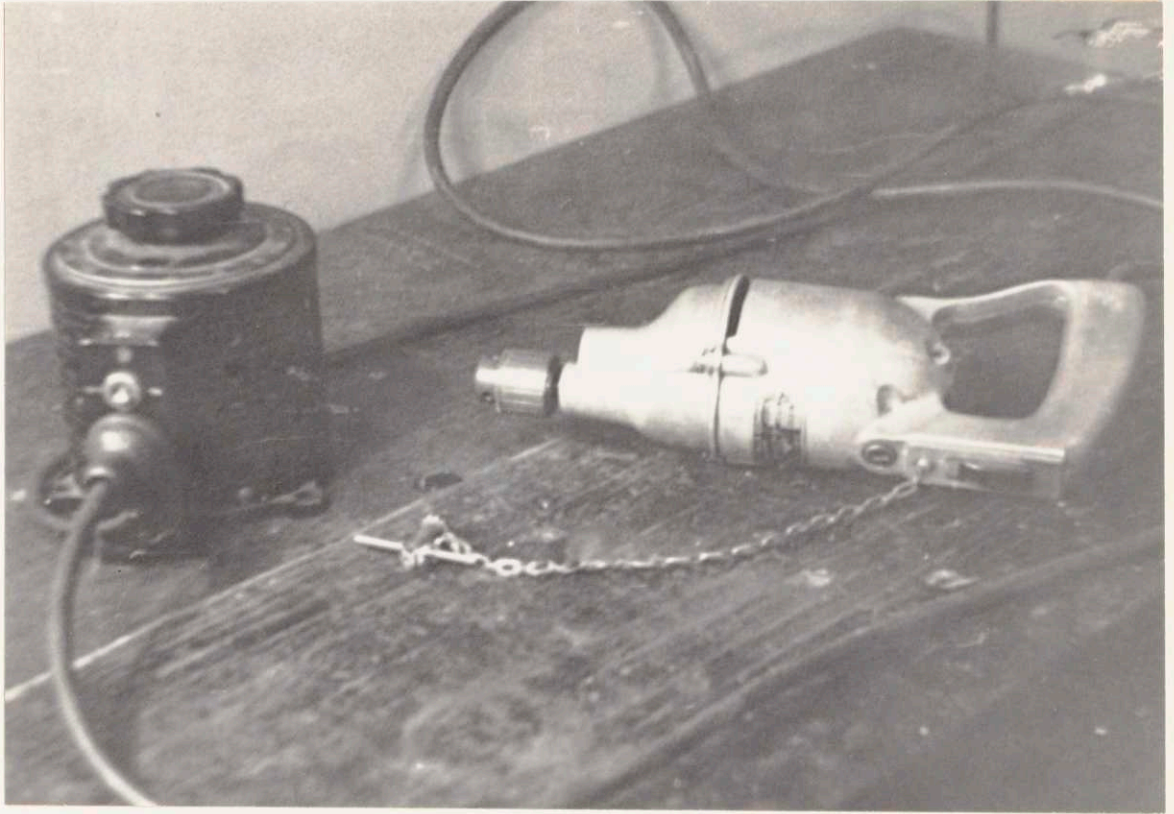


Figure 64. A picture of the hand drill and the Variac transformer.



Table 58

Relaxation recorded in the recess with the machining of  
the slots in the longitudinal and transverse directions

<u>Depth of Longitudinal Slot in Inches</u>	<u>Relaxation in Micro Inches per Inch</u>	<u>Depth of Transverse Slot in Inches</u>	<u>Relaxation in Micro Inches per Inch</u>
0.00	0	0.00	0
0.050	0	0.060	0
0.100	0	0.100	- 5
0.150	0	0.140	-10
0.200	-2	0.160	-15
0.250	-3	0.200	-22
0.270	-8	0.220	-22
		0.240	-27
		0.260	-32
		0.270	-32

stress measured in the transverse direction for recess No. 2 looks out of line as compared with stresses measured in recesses No. 1 and 3. The check of the surface preparation for recess No. 2 showed that all the steps were carried out according to the standard procedure used throughout this thesis. Measurement of the exposed x-ray films were also checked, and they were in order. However, the probability of a sharp change of this kind in the stress pattern in the transverse direction in the specimen is small. It might be caused either by a discontinuity in the structure of the

specimen or an unusual cold working introduced during the machining of the recess, that was not entirely removed in the preparation of the surface for x-rays. Cold working in the metal would cause the x-ray to measure lower stresses. In the calculation of true stresses the stress measured in recess No. 2 is not taken into consideration. However, the calculation was also carried out with the stress in recess No. 2 included, and the change in the result of calculation for the other points was not more than 300 psi.

#### C. Calculation of True Stress from the Apparent Stresses Measured in Recesses

Equation (14) is used to compute the true stress from the apparent stresses in Table 57. The terms appearing in equation (14) for stresses in the longitudinal direction and the results are in Table 59. In Table 60 true stresses in the transverse direction are computed.

The results are shown in Figure 69. Figure 70 contains stresses in the bent plate measured by the recessing method with preliminary results of stresses measured in an identical specimen by the block method of measuring stresses.

#### D. Conclusion

The residual stress pattern, in a one inch thick plate bent to one percent plastic deformation at the surface is shown in Figures 69 and 70. In Figure 70 stresses measured by the recessing method and by the block method are shown together. Stresses measured by the

Table 59

Calculation of true stresses in the longitudinal direction from the apparent  
stress measured in the recess

<u>Recess Number</u>	<u>Depth of Recess z in Inches</u>	<u>9.05z</u>	<u><math>e^{-9.05z}</math></u>	<u><math>e^{+9.05z}</math></u>	<u>Apparent Stress <math>S'_u</math></u>	<u><math>S'_u e^{9.05u}</math></u>	<u><math>\int_0^z S'_u e^{9.05u} du</math></u>	<u>True Stress S</u>
0	0	0	1.	1.	-29,200	- 29,200	0	-29,200
1	0.068	0.615	0.540	1.849	-22,500	- 41,600	- 2,410	-19,580
2	0.125	1.131	0.323	3.0987	-11,400	- 35,300	- 4,605	- 8,090
3	0.210	1.900	0.1495	6.686	- 4,560	- 30,500	- 7,405	- 2,065
4	0.347	3.140	0.0433	23.104	+11,400	+263,500	- 2,895	+11,682
5	0.480	4.344	0.1298	77.015	+10,500	+809,000	+68,605	+ 8,500



Table 60

Calculation of stress in the transverse direction of the bent plate from the apparent stresses measured in the recess

<u>Recess Number</u>	<u>Depth of Recess z in Inches</u>	<u><math>9.05z</math></u>	<u><math>e^{-9.05z}</math></u>	<u><math>e^{+9.05z}</math></u>	<u>Apparent Stress <math>S'_u</math></u>	<u><math>S'_u e^{9.05u}</math></u>	<u><math>\int_0^z S'_u e^{9.05u} du</math></u>	<u>True Stress S</u>
0	0.0	0.	1.	1.	+13,200	13,200	0	+13,200
1	0.068	0.615	0.540	1.849	+12,600	23,300	1,240	+11,090
2	0.125	1.131	0.323	3.0987				
3	0.210	1.900	0.1495	6.686	+13,200	88,200	8,360	+10,380
4	0.347	3.140	0.0433	23.104	+ 9,600	222,000	29,560	+ 6,730
5	0.480	3.344	0.01298	77.015	+ 8,200	631,000	86,260	+ 5,680

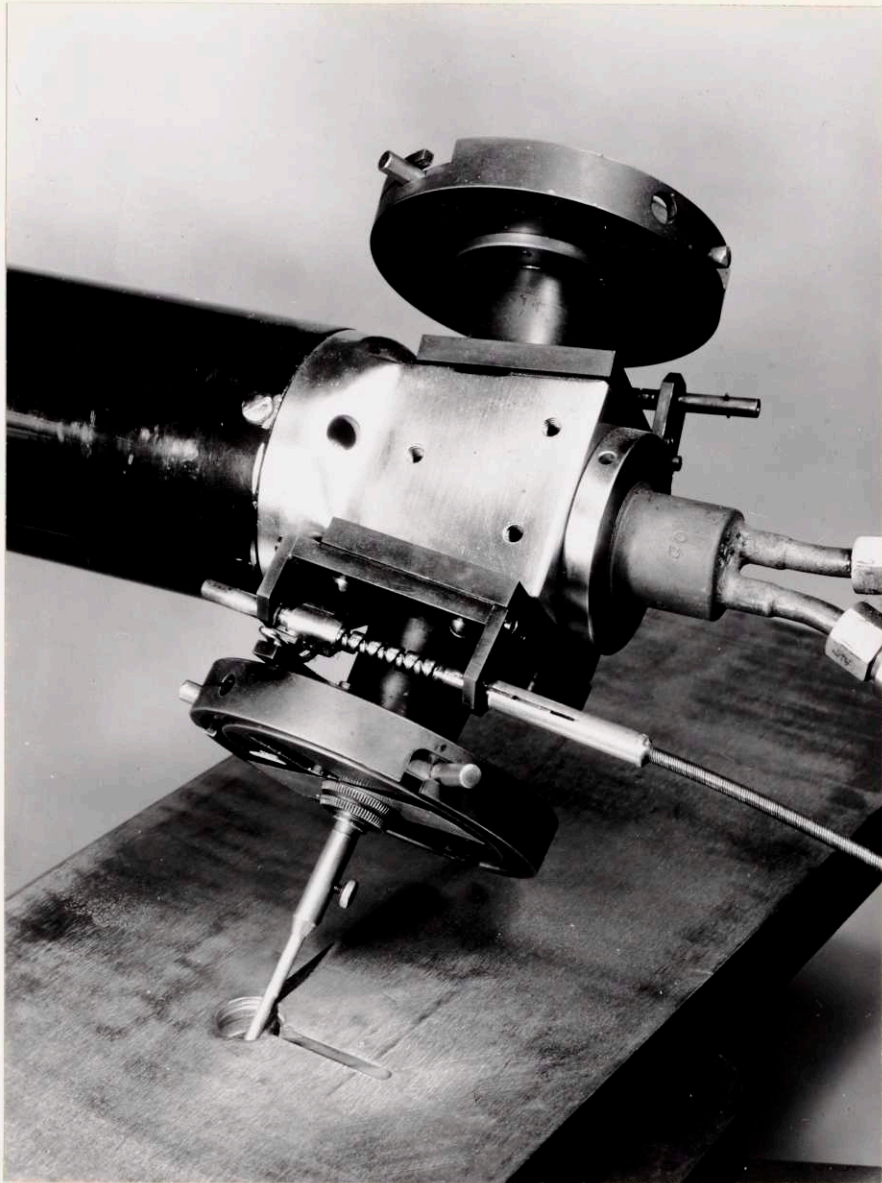
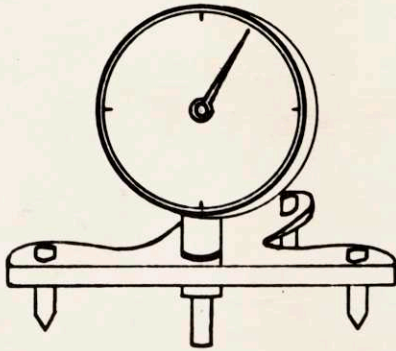
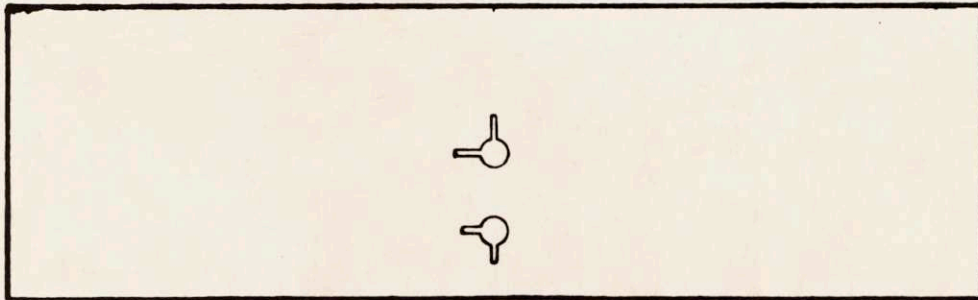


Figure 65. A picture of the bent plate under the x-ray camera.



**Fig. 66 - The Gage to Measure the Depth of the layer Removed in Surface Preparation for Measurement of Stresses by X-Rays**



**Fig. 67 - Recesses and the Slots in the Bent Plate.**

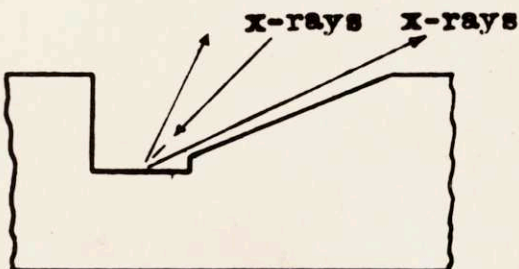


**Fig. 68 - The Cross-section of a Recess and Slot.**



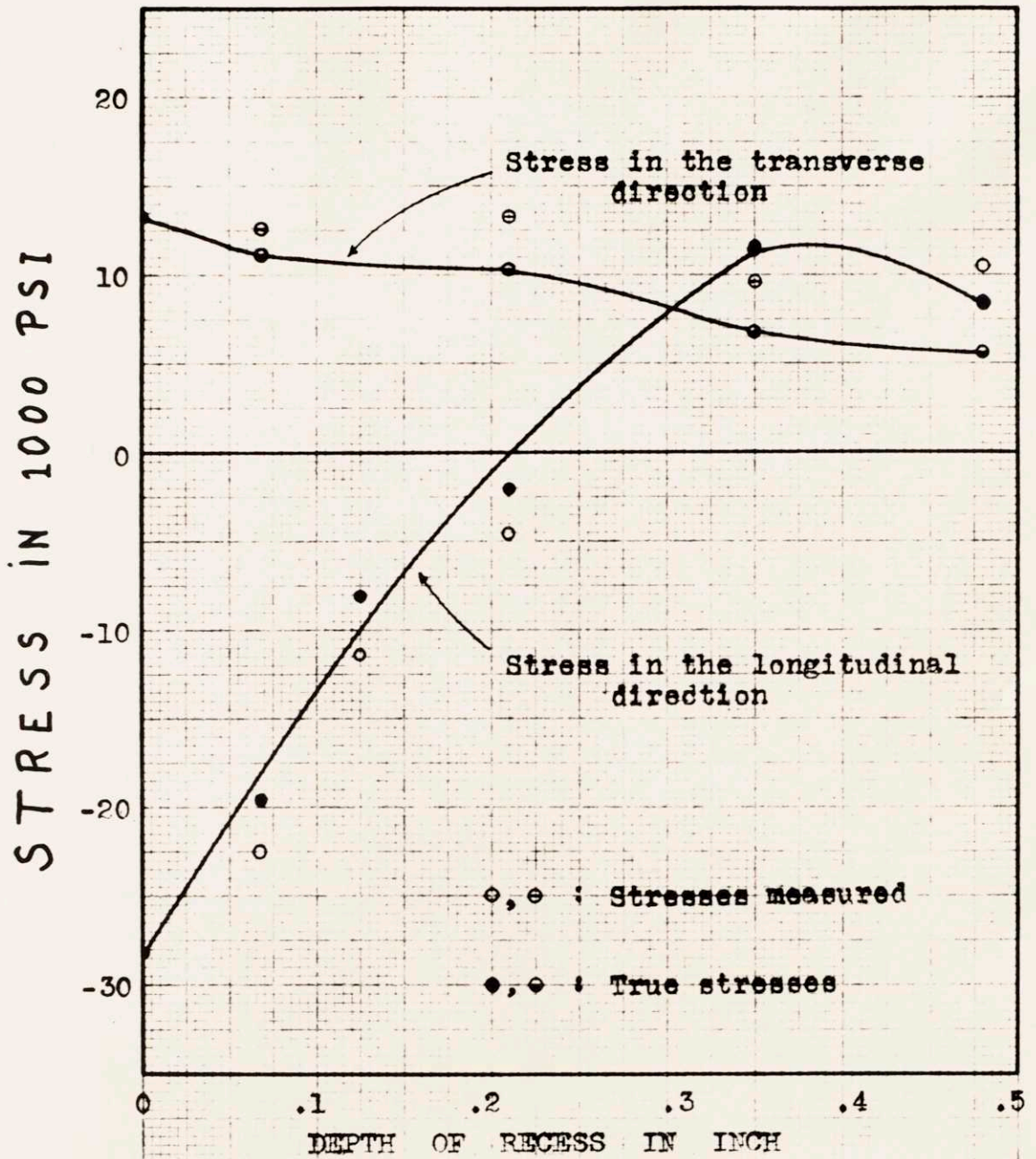


Fig. 69 - Residual Stresses through the thickness of one inch thick bent Plate. Stresses are Measured by X-Rays in a half-inch Diameter Recess and corrected according to the Theory of Recessing

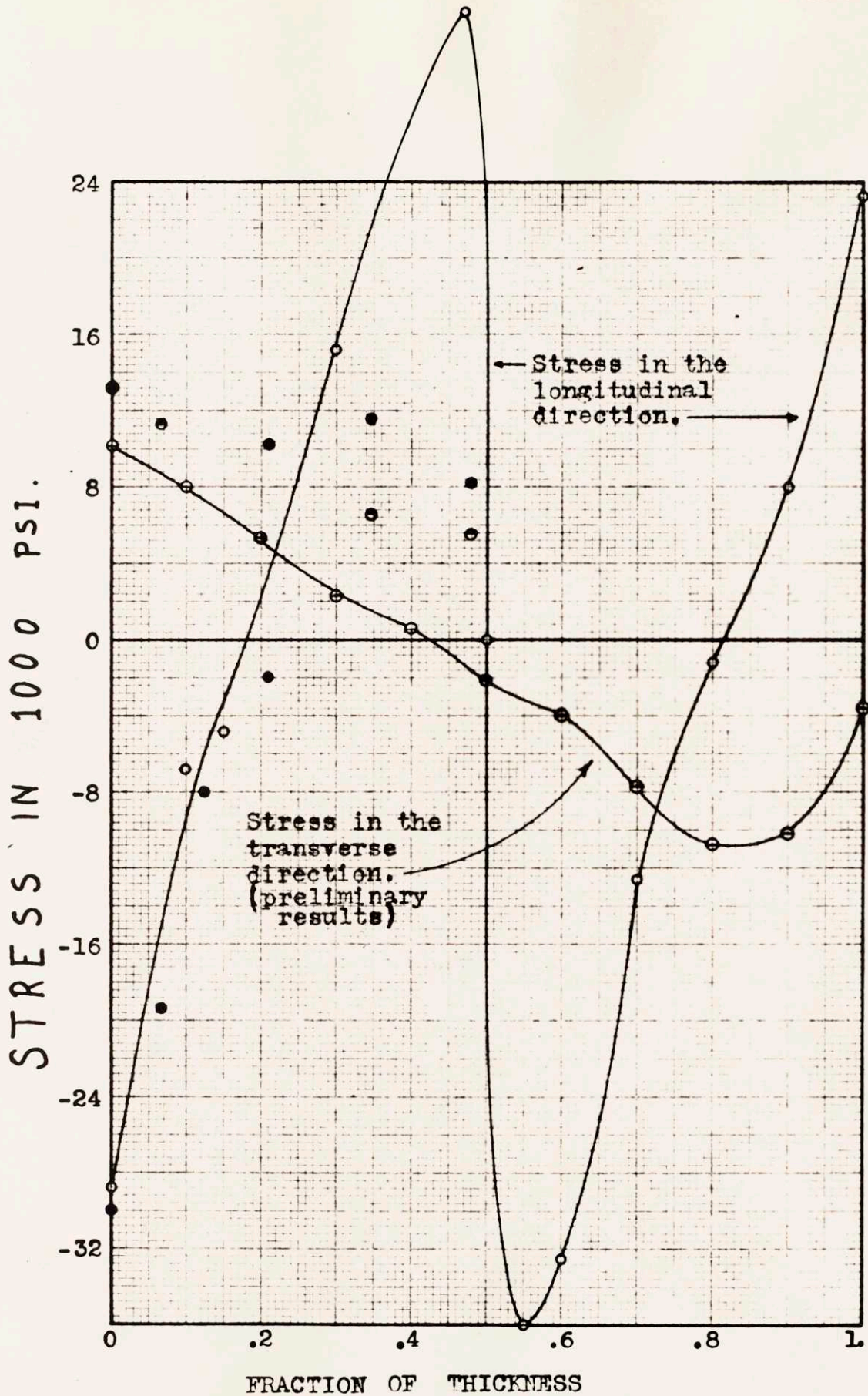


Fig. 70 - Residual Stresses in the one inch thick bent Plate Measured by the Block Method. Black and half black Circles are Stresses measured in the Recess by x-rays.



two methods in the longitudinal direction are in very close agreement while those in the transverse direction are not that close, but, it must be said again that the results of the block method are preliminary and further calculations might reveal a closer agreement.

In comparing the recessing method and the block method, the comparison by direct answers obtained by the former makes it much more attractive than the block method, which involves lots of charts and calculations to obtain the result.



RECOMMENDATIONS FOR FURTHER WORK

From the investigations on the disk and on the plate it is concluded that the thickness of one and one-half inches is too small for a stress in the direction of thickness comparable in size to the stresses in the radial and tangential directions. Investigations of a two and one-half inch thick plate having a circular weld at the center, similar to the disk above, by the recessing method would be very interesting.

In the recessing method the depth of the slot can be decreased if instead of tungsten lines used as reference another material is chosen that gives lines in the x-ray film inside the iron lines. Probably aluminum could be used for this purpose.

BIBLIOGRAPHY

1. J. H. Hollomon. "The Problem of Fracture." Supplement to the Journal of the American Welding Society, September 1946, pp. 534-s - 579-s.
2. D. J. McAdam, Jr. "The Technical Cohesive Strength of Metals in Terms of the Principal Stresses." Metals Technology, December 1944, pp. 5-31.
3. G. Sachs and J. Lubahn. "The Effect of Triaxiality on the Technical Cohesive Strength of Steel." Journal of Applied Mechanics, Vol. 12, No. 4 (1945) pp. A241 - A252.
4. E. Sieben and A. Maier. "Effect of Multiaxial Stress on Ductility". Zeitschrift des Vereines Deutcher Ingenieure, Vol. 77 (1933) pp. 1345 - 1349.
5. John T. Norton and D. Rosenthal. "An Investigation of the Behavior of Residual Stresses Under External Load and Their Effect on Safety." Welding Journal Research Supplement, February 1943.
6. C. S. Barrett. Experimental Stress Analysis. Vol. II, No. 1, (1944) pp. 147 - 156.
7. John Johnston. Trans. A. I. M. E., Vol. 150, (1942) pp.13 - 29.
8. J. E. Howard. Tests of Metals. Watertown Arsenal, (1893) p. 283.
9. E. Heyn. Journal of the Institute of Metals. Vol. 12, No. 2, (1914) pp. 3 - 37.
10. G. Sachs. Zietschrift für Metallkunde. Vol. 19, (1927) pp. 352 - 357

11. G. Sachs and G. Espey. "The Iron Age" Vol. 148, (1941) September 18, pp. 63 - 71; September 25, pp. 36 - 42.
12. D. Rosenthal and J. T. Norton. "A Method of Measuring Tri-axial Residual Stress in Plates." The Welding Journal Research Supplement, May 1945.
13. L. Frommer and E. H. Lloyd. The Journal of the Institute of Metals. Vol. 70, (1944) pp. 91 - 124.
14. W. Spraragen and G. E. Claussen. The Welding Journal, 16 (11), Research Supplement, November 1937.
15. W. Spraragen and M. A. Cordoni. The Welding Journal, Research Supplement, May 1944.
16. D. Rosenthal. Private conversation, (1946).
17. L. R. Jackson. "Some Speculations Regarding the Plastic Flow and Rupture under Complex Stresses." Metals Technology, December 1944, pp. 59 - 79.
18. J. Mathar. Archiv für das Eisenhüttenwesen, Vol. 10, (1936 - 1937) pp. 59 - 63.



BIOGRAPHICAL NOTE

The author was born on January 2, 1920 in the Camidagi Köyu, Rize, Turkey. He started the elementary school in his village and finished it in Samsun, Turkey where he attended the high school (Lise) graduating in 1938 from the Lise of Kastamonu, Kastamonu, Turkey. He attended the Universitee de Liege in Liege, Belgium for the school year 1939-40. In September 1941 he entered the Massachusetts Institute of Technology and received his S.B. degree at the end of 1943.

In January 1947 he submitted the thesis entitled "Contribution to the Methods of Measuring Stresses Below the Surface" in partial fulfillment of the requirements for the degree of Doctor of Science.